THE UNIVERSITY OF MICHIGAN

COLLEGE OF ENGINEERING
Department of Meteorology and Oceanography

Technical Report

THE MAINTENANCE OF THE TIME-AVERAGED STATE OF THE ATMOSPHERE

Jacques F. Derome

Aksel C. Wiin-Nielsen
Project Director

ORA Project 08759

NATIONAL SCIENCE FOUNDATION
GRANT NO. GA-841
WASHINGTON, D.C.

administered through:

OFFICE OF RESEARCH ADMINISTRATION ANN ARBOR

July 1968

This report was also a dissertation submitted in partial fulfillment of the requirements for the degree of Doctor of Philosophy in The University of Michigan, 1968.

TABLE OF CONTENTS

TABLE OF CONTENTS (Concluded)

LIST OF FIGURES

LIST OF TABLES

LIST OF FIGURES (Concluded)

LIST OF SYMBOLS

a = mean radius of the earth (6371 km) except in section 4.3 where it is a constant determined from observations

c_p = specific heat of air at constant pressure, 1004 kj t^{-1} deg^{-1}

f = Coriolis parameter, $2\Omega \sin \phi$

f_o = Coriolis parameter f evaluated at 45°N

g = acceleration of gravity, 9.8 $msec^{-2}$

h = $a \cos \phi_o$, a being the mean radius of the earth

$\vec{i}$ = unit horizontal vector pointing to the east

$\vec{j}$ = unit horizontal vector pointing to the north

$\vec{k}$ = unit vertical vector pointing upward

m = $qa^2 f_o^2 / ARSp$

n = zonal wave number in Chapters 2 and 3

n = degree of the Legendre polynomial in Chapter 4

p = pressure

p_g = standard pressure at the ground

q = heating or cooling coefficient

q' = $c_p q$

t = time

u = component of speed along the x axis

v = component of speed along the y axis

w = vertical component of speed

x = distance coordinate increasing to the east

y = distance coordinate increasing to the north

z = height above mean sea level

A = the ratio of the amplitude of $\hat{\psi}_1$ to that of $\hat{\psi}_3$ in Chapter 2

A = $g^2K/R^2\bar{T}^2$ in Chapter 4

A_n^* = coefficient in the Fourier expansion of $\hat{\psi}_*$

B_n^* = coefficient in the Fourier expansion of $\hat{\psi}_*$

A_n^T = coefficient in the Fourier expansion of $\hat{\psi}_T$

B_n^T = coefficient in the Fourier expansion of $\hat{\psi}_T$

C_n^* = amplitude of the nth Fourier component of $\hat{\psi}_*$

C_n^T = amplitude of the nth Fourier component of $\hat{\psi}_T$

C_d = drag coefficient

F = friction coefficient in Chapter 2 and 3

F = friction force per unit mass in Chapter 4

F_o = value of the friction coefficient over the oceans

F_c = value of the friction coefficient over the continents

G = part of a forcing function, see (4.18b)

H = diabatic heating per unit mass and unit time, except on pp. 14 and 61 where it is a scale height

I = $\int_o^p M\, dp$

K = coefficient of eddy viscosity

L = characteristic horizontal scale

L_y = effective meridional wavelength

M = $(\overline{u_E v_E})_z$

N = $(v_E T_E)_z$

P_n = Legendre polynomial of degree n

Q_n = coefficient in the Fourier expansion of $\hat{H}$

R = gas constant for air

R_n = coefficient in the Fourier expansion of $\hat{p}_g$

S = a measure of the static stability

S_n = coefficient in the Fourier expansion of $\hat{p}_g$

T = temperature

$\tilde{T}$ = a representative value of the temperature

T_n = coefficient in the Fourier expansion of $\hat{H}$

T_R = convective-radiative equilibrium temperature

T_s = temperature in a reference standard atmosphere

U = velocity component (in the basic state) along the x axis

V = characteristic horizontal wind speed

$\vec{V}$ = horizontal wind vector

W = characteristic vertical wind speed

Z_g = the height of the ground above mean sea level

α = specific volume

α_n^* = phase angle of the nth Fourier component of $\hat{\psi}_*$ in Chapter 2

α_n^T = phase angle of the nth Fourier component of $\hat{\psi}_T$ in Chapter 2

α_n = coefficient in (3.13), defined by (3.14) in Chapter 3

β = df/dy, the Rossby parameter

γ_n = coefficient first appearing in (3.13), defined by (3.15)

δ^2 = $8f_o^2/\sigma_2 p_4^2$

ζ = vertical component of relative vorticity

θ = potential temperature

λ = longitude

μ = $2\pi/L_y$, an effective meridional wave number in Chapters 2 and 3

μ = ρK in Chapter 4

ρ = density

σ = $-\alpha\partial \ell n\theta/\partial p$ (where α is the specific volume), a measure of the static stability

τ = zonal component of the frictional stress acting across a horizontal surface

ϕ = latitude

ϕ_o = 45°N

ψ = perturbation stream function for the horizontal flow in Chapters 2 and 3; stream function for the mean meridional circulation in Chapter 4

ω = dp/dt

ω_{4F} = that part of ω_4 which is due to the boundary layer friction

ω_{4M} = that part of ω_4 which is due to the mountains

Φ = gz, the geopotential

Ψ = stream function for the horizontal flow (perturbations plus basic state)

Ω = angular velocity of the earth

$( )_Z$ = the zonal average of ( )

$( )_E$ = $( ) - ( )_Z$ = the eddy component of $( )$

$( )_i$ = the value of $( )$ at p = 0, 25, 50, 75 and 100 cb for i = 0, 1,2,3 and 4, respectively

$( )_* = \frac{1}{2}[( )_1 + ( )_3]$

$( )_T = \frac{1}{2}[( )_1 - ( )_3]$

$( )_H$ = that part of $( )$ which is due to the heat sources and sinks

$( )_M$ = that part of $( )$ which is due to the mountains

$( )_g$ = the value of $( )$ at the ground

$(\hat{})$ = that part of $( )$ which depends on the longitude only

$\overline{( )}$ = the time average of $( )$

$\nabla = \vec{i}\,\partial/\partial x + \vec{j}\,\partial/\partial y$

$\nabla^2 = \partial^2/\partial x^2 + \partial^2/\partial y^2$

ABSTRACT

The problem of modelling the main processes which maintain the time-averaged state of the atmosphere is divided into a first part dealing with the maintenance of the standing eddies and a second part dealing with the maintenance of the axisymmetric regime.

The maintenance of the standing eddies is studied by means of a quasi-geostrophic, linear, steady state model of the atmosphere in which the zonal current is perturbed by the lower boundary topography and by a distribution of heat sources and sinks. Initially all the perturbations are assumed to have a single effective meridional wavelength and the frictionally induced vertical motion at the top of the boundary layer is related to the vorticity through a constant "friction coefficient."

After investigating some basic properties of the model atmosphere, some computations are made to determine its response to the combined forcing by the topography as obtained from Berkofsky and Bertoni (1955) and by the diabatic heating obtained from Brown (1964) for January 1962. The resulting perturbations are found to be in rather good agreement with the observed standing waves. The results also indicate that the standing waves forced by the topography are in about the same position as those forced by the diabatic heating and that the former have somewhat larger amplitudes than the latter.

The effect of allowing the friction coefficient to have one constant value F_c over the continents and another value F_o over the oceans is examined and found to be important if $F_c/F_o = 6$ but small (although bringing the computed and observed eddies into closer agreement than in the case $F_c/F_o = 1$) if $F_c/F_o = 2$.

The assumption concerning the existence of a single effective meridional wavelength is relaxed somewhat by considering an atmosphere bounded by walls at 30°N and 60°N. The most important effect of the additional degrees of freedom is to permit the forced perturbations to exhibit a tilt from the north-east to the south-west as found most noticeably in the observed trough near the east coast of North America.

The maintenance of the axisymmetric regime is also studied by means of a steady state, quasi-geostrophic formulation of the hydrodynamic equations. The diabatic heating is assumed to be Newtonian and the eddy heat and momentum transports are assumed known from observations. It is then shown that the meridional variations in the time-averaged axisymmetric temperature are forced by functions depending on the eddy heat and momentum transports and on the convective-radiative equilibrium temperature (also assumed known). It is shown, in particular, that the combined effect of the eddy heat and momentum transports is to raise

(lower) the temperature of the high (low) latitudes, with the maximum effect being found near 70 cb. One advantage of the formulation is that it gives the effects of the eddies on the temperature field in degrees Kelvin rather than in the form of heating rates as in previous studies.

The importance of the eddies in determining the zonal wind distribution is also investigated. It is shown that the combined effect of the eddy heat and momentum transports is to create easterlies in the low and high latitudes and weak westerlies in the middle latitudes. The complete solution for the zonal wind shows strong westerlies in the middle latitudes and weak easterlies in the low and high latitudes. It is believed that some differences between the computed and observed zonal winds are due mainly to the simple distribution of the equilibrium temperature used in the model, or to the type of momentum transport data used, or to a combination of both factors.

CHAPTER 1

INTRODUCTION

1.1 THE PURPOSE AND SCOPE OF THE STUDY

The first attempt at a classification of the earth's climates was based on astronomical considerations only and resulted in the concept of five climatic zones encircling the earth in the east-west direction. This classification was, of course, an oversimplification and naturally with the advent of a greater number of meteorological observations new and more elaborate schemes were developed to categorize climatic regions. There is no doubt that the classification of climates can serve useful purposes but clearly it should be supplemented by a general theory capable of describing how the earth-ocean-atmosphere system makes use of the solar energy to maintain the observed distribution of climates.

It is the purpose of the present study to treat a few of the problems encountered in the development of a general theory of climates. More precisely, the maintenance of the quasi-permanent zonal asymmetries in the atmospheric variables is investigated by considering a model in which the zonal current is perturbed by the earth's topography and by a distribution of heat sources and sinks obtained from Brown (1964). The maintenance of the zonally symmetric part of the atmospheric variables is also investigated. The annual mean conditions in the axisymmetric regime are deduced by considering a steady state quasi-geostrophic model in which the horizontal eddy

heat and momentum transports are taken from observations and the diabatic heating is taken to be Newtonian in form.

1.2 A BRIEF REVIEW OF PREVIOUS WORK

The progress in the development of a theory of climates has been made so far along two main fronts which differ primarily in their mathematical formulation. In the first approach the mathematical problem is formulated as an initial value problem. The procedure consists in starting with some initial state of the earth-ocean-atmosphere system and in predicting its evolution over a long period of time by means of a mathematical model based on the hydrodynamical equations. In view of the complexity of these equations the long-term time integration is accomplished by replacing the differential equations by their finite difference analogs. Considering the time-averaged solution as the climate of the model, it is then possible to examine how the various physical mechanisms included in the model contribute to bring about the computed climate. A greater understanding of the maintenance of the earth's climate can thus be achieved provided, of course, that the climate of the model resembles that of the earth.

Models based on the above approach have been developed by Phillips (1956), Smagorinsky (1963), Mintz (1964), Leith (1965), Smagorinsky, Manabe and Holloway (1965), Manabe, Smagorinsky and Strickler (1965), Kasahara and Washington (1967). The results of these studies are encouraging but in view of the complexity of the problem it is useful to supplement the above approach with a second one.

The second approach used in developing the theory of climates also makes use of the hydrodynamic equations but in a different way. The procedure here consists in first separating each dependent variable appearing in the model into two parts, one being the time average of the variable over a chosen time period and the other being the instantaneous departure from the time average, that is, the transient part of the variable. After averaging the model equations over the time period of concern it is found that the terms remaining in the integrated equations fall into two main categories, namely, those consisting exclusively of time-averaged variables and those consisting exclusively of time-integrated products of the transient parts of the variables (see, for example, Saltzman (1961)). A considerable simplification would be achieved if we could parameterize the time-averaged effects of the transient eddies in terms of the properties of the time-averaged variables. Alternately we can consider the terms depending on the transient eddies as known from previous computations or we can neglect them if they are sufficiently small.

The integrals of the form $\frac{1}{\tau}\int_{t}^{t+\tau}\frac{\partial f}{\partial t}\,dt$, where f is any dependent variable, are in general nonzero but if τ is sufficiently large they can be safely neglected. When this is done the equations for the time-averaged variables become steady state equations so that given the appropriate boundary conditions around the spacial domain of interest the time-averaged state of the system can be obtained by solving a boundary value problem. This, then, is the main difference from the mathematical stand point between this second approach to the problem and the first one where a mixed initial and boundary value problem must be solved.

We recall that in the second approach described above the dependent variables were divided in two part, one of which, the time-averaged part, became the unknown. It is convenient to use this technique again, this time subdividing each unknown time-averaged variable into a first part consisting of its zonal average and a second part being the deviation from the zonal average. In the subsequent discussion the first and second components will be called the zonal mean component and the standing eddy component, respectively. This decomposition is particularly useful because it is observed that the standing eddy components are small compared to their respective zonal mean components. This means that the nonlinear differential equations governing the maintenance of the eddy components can be thrown into the form of linear perturbation equations using the zonal mean values as the basic undisturbed state and thus a major mathematical simplification is achieved. In the following we shall review briefly the most important investigations of the standing eddies using perturbation equations.

In 1939 Rossby showed that the linearized form of the equation expressing the conservation of absolute vorticity in a Cartesian coordinate system possesses solutions representing free waves with phase speeds depending on their zonal wavelength (the meridional wavelength having been assumed infinite for all waves) and on the speed of the basic zonal current. The waves were found to travel westward with respect to the basic current so that for a given speed in the undisturbed current one wavelength was found stationary with respect to the earth. Using these results Rossby then discussed qualitatively the displacements of the "semi-permanent" eddies in the atmosphere, as observed

on five-day mean charts, in relation to the change in the speed of the zonal current.

Rossby's analysis of the free travelling and stationary (Rossby) waves was later reformulated by Haurwitz (1940) within the framework of spherical coordinates. Haurwitz also stressed the fact that in addition to the free waves the atmosphere could also have forced modes in response to the external forces, but his discussion of the latter was only a qualitative one.

It appears that Blinova (1943) was the first author to study the relation between two atmospheric variables in the standing eddies. Just as Haurwitz (loc. cit.) had done, she assumed the flow to be purely horizontal and non-divergent, but contrary to Haurwitz she retained the longitudinal variation of the temperature in the solenoidal term of the perturbation vorticity equation. With the steady state version of the latter equation she was then able to relate the stationary stream function pattern to the stationary temperature distribution. Similarly, from the linearized steady state form of the first equation of motion she obtained a relation between the stationary pressure and stream function distributions.

In her formulation Blinova did not include any forcing mechanism and therefore did not seek an explanation for the maintenance of the standing forced waves. The purpose of the study was simply to show that if the temperature distribution in the standing waves is given, some information can be obtained about the position and phase of the stream function and pressure in the standing eddies.

Six years later Charney and Eliassen (1949) published the first paper dealing with one possible mechanism capable of maintaining standing eddies in the atmosphere. Using an equivalent barotropic model, they were able to show that the mountain barriers near 45°N could deflect the basic zonal current in such a way as to produce stationary waves of about the same amplitude and in about the same position as those observed on the mean monthly pressure maps in January. It was clear that these standing waves were "forced" modes and the possibility of pure resonance with the "free" stationary modes described by Rossby (1939) was eliminated by the inclusion of friction.

Bolin (1950) also studied the effects of the earth's topography on the zonal current by considering the perturbed flow in the vicinity of a single axisymmetric mountain. He showed that a mountain of sufficiently large horizontal dimension could cause standing perturbations in two ways; firstly, by forcing some of the air to flow <u>over</u> the mountain, and secondly, by forcing some of the air to flow <u>around</u> it. The most interesting feature of this study was the demonstration that the first type of flow creates disturbances far away as well as near the mountain whereas the second type of flow results in perturbations which decay rapidly with the distance away from the mountain.

Another way in which the continents can participate in the maintenance of the standing eddies is through the difference between their thermal and radiative properties and those of the oceans. It is well known that in the winter the surface layer of the oceans is on the average warmer than that of the continents and that the reverse holds in summer. Thus in the winter, for

example, the continents and oceans may be expected to play the roles of heat sinks and sources, respectively, for the atmosphere thereby providing a second possible mechanism for the maintenance of standing waves. Since these heat sources and sinks change both in strength and position from winter to summer it seems that their effects on the atmosphere should be studied on a monthly or seasonal basis rather than on a yearly basis.

Smagorinsky (1953) made a study of the heat sources and sinks as possible contributors to the maintenance of the standing eddies, neglecting the effects of the earth's topography. Lacking adequate knowledge about the true distribution of heat sources and sinks in the atmosphere, he assumed a simple distribution and derived the effects that it would have on the atmospheric flow. In a qualitative discussion based on his theoretical study he then showed that diabatic heating was probably one of the main mechanisms responsible for the standing waves, at least in the low levels of the atmosphere. This paper did not resolve the controversy as to the relative importance of the topography and diabatic heating in explaining the presence of the standing eddies but served as an incentive to carry further the study of the two mechanisms.

A series of theoretical papers followed dealing with the response of model atmospheres to the forcing by the bottom topography (for example, Wiin-Nielsen (1961), Murakami (1963), Sankar-Rao (1965a,b, 1966)) or by the diabatic heating (for example, Gilchrist (1954), Döös (1962), Sankar-Rao (1965c)) or by both mountains and heating (Saltzman (1965)). Again these studies could not determine whether the topography and the diabatic heating are of

about equal importance in maintaining the standing eddies or whether one effect dominates the other since only hypothetical distributions of heat sources and sinks were used.

Although we still know relatively little about the true distribution of heat sources and sinks, some information has been published on this subject by Wiin-Nielsen and Brown (1960) and Brown (1964) for a layer near 50 cb. It is one of the main purposes of the present study to investigate how a steady state model atmosphere responds to the forcing by Brown's computed distribution of heat sources and sinks and then to make a direct comparison of the standing waves thus obtained with those forced by the bottom topography. Just as in the above investigations the model equations are linearized and lead to a steady state boundary value problem.

In the linearized models dealing with the maintenance of the standing waves it is assumed that the basic zonal state of the atmosphere is known from observations. It is an interesting and fundamental problem, on the other hand, to determine how the basic state itself is being maintained against the dissipative forces.

It has been shown by Houghton (1954) and London (1957), for example, that if the radiative processes were the only ones determining the temperature of any vertical column in the atmosphere, the equatorial regions would be much warmer and the polar regions much colder than they are observed to be. To reach the observed zonal mean state, therefore, the atmosphere must transport the excess energy northward, thereby acting as a heat engine between a warm source and a cold sink.

Attempts have been made, for example by Adem (1962), at studying the maintenance of the axisymmetric regime of the atmosphere. Adem considered the heat budget of the vertically integrated troposphere as influenced by the radiation processes, the turbulent heat transfer between the troposphere and the underlying surface and the horizontal heat transfer by the large-scale eddies. The mean toroidal motion in the atmosphere was neglected and the meridional heat transport by the eddies was parameterized in terms of the axisymmetric temperature using a constant Austausch coefficient. The model presented by Williams and Davies (1965), on the other hand, took the mean toroidal motion into account but here again the effects of the eddies were parameterized through the use of Austausch processes. A further contribution was made by Saltzman (1967), a fundamental difference between his model and the previous ones being that the Austausch coefficient was permitted to be a free variable, thus adding another degree of freedom to the system. The mean toroidal motion of the atmosphere, however, was neglected.

The basic difficulty in the above studies clearly resides in adequately parameterizing the various physical processes affecting the axisymmetric regime in terms of the axisymmetric variables. It is no small task, for example, to parameterize the meridional eddy heat transport in terms of the axisymmetric temperature field knowing that on the average the eddies transport heat from warm to cold temperatures in the troposphere whereas the reverse holds in the lower stratosphere (Oort (1964), White (1954), Wiin-Nielsen (1967)). While further progress in this respect may be forthcoming, it would seem important to examine how the large-scale eddies in the atmos-

phere actually affect the axisymmetric regime. This is done in the present study by using a model in which the terms representing the heat and momentum transports by the eddies take the form of forcing functions and are taken to be known from previous computations.

1.3 AN OUTLINE OF THE STUDY

The central problem of studying the maintenance of the time-averaged state of the atmosphere is divided into two major sections, the first one dealing with the maintenance of the standing eddies and the second one dealing with the maintenance of the axisymmetric regime. The first topic is treated in Chapters 2 and 3; a treatment of the second topic is given in Chapter 4.

In Chapter 2 the basic equations to be used in studying the maintenance of the standing waves are presented. It is assumed that the flow is steady and that the amplitudes of the standing waves are sufficiently small to permit the use of the linearized equations. The standing perturbations appear as modes that are forced by the topography and the heat sources and modified by friction at the earth's surface. The frictionally induced vertical motion at the top of the boundary layer is related to the 100 cb vorticity through a friction coefficient which at first is assumed to be a constant. To gain some insight into the basic properties of the equations, the response of the model to a series of hypothetical distributions of mountains and heat sources is computed.

The model is then used in Chapter 3 to compute the amplitude and phase of the mid-latitude perturbations forced by the distribution of heat sources

and sinks computed by Brown (1964) from meteorological observations for January 1962 and by the distribution of mountains obtained from Berkofsky and Bertoni (1955). The calculations are restricted to two basic levels in the vertical direction and at first to variations along a single latitude circle. The remainder of the chapter is devoted to studying the effects of varying the friction coefficient from ocean to continental areas. With the method of solution that is presented, an arbitrary variation of the friction coefficient can be specified but the actual solution of the model is computed only for simple cases where the friction coefficient has one value (relatively large) over the continents and another value (relatively small) over the oceans.

An attempt is also made at improving the north-south resolution in the model. In the previous sections it had been possible to focus the attention on the east-west variations in the perturbations by assuming that a single "effective" meridional wave number could be assigned to all perturbation quantities and by considering the basic zonal wind speed to be independent of the meridional coordinate. In trying to relax these restrictions, the approach is to start with the same basic set of equations as previously without making use of the assumption of an effective meridional scale for the perturbations and to solve the system of equations over a rectangular region bounded by the latitudes 30°N and 60°N. The solution then contains several meridional modes and, furthermore, since the equations are solved numerically it is possible to use a basic state in which the zonal wind speed varies with latitude.

Chapter 4 deals with the maintenance of the axisymmetric regime in the atmosphere. The model used is based on the quasi-geostrophic formulation of the hydrodynamic equations in spherical coordinates. The factors influencing the axisymmetric regime in the model are the heat and momentum transports by the eddies (standing and transient), the radiative heating and cooling and friction. The eddy transports of heat and momentum are taken to be known from previous computations based on meteorological observations and the diabatic heating is taken to be of the Newtonian type. With the above formulation it is possible to examine the extent to which the quasi-geostrophic eddy motions participate in maintaining the north-south variations in the axisymmetric regime.

The results of the study are reviewed in Chapter 5 and some suggestions for future improvements are offered.

CHAPTER 2

SOME BASIC PROPERTIES OF THE STEADY STATE TWO LEVEL MODEL

2.1 PRELIMINARY REMARKS

In the present study the atmospheric standing waves are considered to be maintained by the effects of the bottom topography and permanent heat sources and sinks on a steady zonal current. It is realized that this approach cannot yield a perfectly satisfactory solution to the standing wave problem since the effects of the transient disturbances are completely ignored. Future research may show that the nonlinear effects resulting from the presence of transient waves produce important modifications in the standing eddies resulting from linear processes, but before embarking on a study of nonlinear effects it would be advisable to improve our understanding of the basic linear mechanisms. This is the underlying purpose of the treatment given in this study.

In the present chapter we shall present the equations defining the two level model of the atmosphere and investigate in some detail a number of its properties. This well-known model has proven to be extremely useful both in the field of numerical weather prediction and in theoretical research but it appears that no one, as yet, has used it to investigate the problem of the standing eddies as forced by both the bottom topography and the diabatic heating. It is true that the model has only a crude vertical resolution but on the other hand it has the distinct advantage of being consistent with the model used by Brown (1964) to compute the diabatic heating field which is

going to be a basic input to the present investigation. Furthermore, since the structure of the standing eddies changes rather slowly with height (Saltzman and Rao (1963)) the limited vertical resolution should not be too serious a handicap in the present context.

The large-scale flow in the atmosphere is observed to be quasi-nondivergent, quasi-horizontal and quasi-hydrostatic. A description of the scale analysis based on the above observations leading to the quasi-geostrophic model used in this chapter was given by Young (1966) so that only a few comments on this topic need be made here.

If we let $V \simeq 15$ msec^{-1} denote the characteristic horizontal speed, $W \leq 0.1V$ the characteristic vertical speed, $L \simeq 10^6$ m the characteristic horizontal length and $H \simeq 10^4$ m the characteristic vertical scale, we observe that $VW/Lg < V^2/Lg < V^2/Hg \ll 1$, where $g = 9.8$ msec^{-2} is the acceleration of gravity. The equation for the vertical component of velocity can then be approximated by the hydrostatic relation, in which case it is convenient to use the pressure instead of the height as the vertical coordinate. For the large-scale flow it is also true that the Rossby number is small compared to unity whereas the reverse holds for the Richardson number. The horizontal pressure and Coriolis forces therefore nearly balance each other so that the horizontal accelerations are small and the vertical stratification is sufficiently stable to prevent large vertical velocities. In this case the quasi-geostrophic formulation provides a useful approximation to the complete set of hydrodynamic equations.

2.2 THE STEADY STATE QUASI-GEOSTROPHIC MODEL

We shall assume that the motion is on a β plane centered at 45°N so that we can use a Cartesian coordinate system in which the x and y coordinates increase to the east and north, respectively. The vorticity and thermodynamic equations for the quasi-geostrophic model then take the form

$$\vec{V}\cdot\nabla(\zeta+f) = f_o \frac{\partial\omega}{\partial p} \tag{2.1}$$

and

$$\vec{V}\cdot\nabla\left(\frac{\partial\Phi}{\partial p}\right) + \sigma\omega = \frac{RH}{c_p p} \tag{2.2}$$

respectively. In the above $\vec{V}$ is the nondivergent part of the horizontal velocity vector, with components u and v along the x and y axes, respectively; $\zeta = \partial v/\partial x - \partial u/\partial y = \partial^2\Psi/\partial x^2 + \partial^2\Psi/\partial y^2$ where Ψ is the stream function; f is the Coriolis parameter, f_o being its value at 45°N; ω is the "vertical velocity" dp/dt, where p is the pressure and t the time; $g = 9.8$ msec^{-2} is the acceleration of gravity; $\nabla = \vec{i}\partial/\partial x + \vec{j}\partial/\partial y$, where $\vec{i}$ and $\vec{j}$ are unit vectors pointing to the east and north, respectively; $\Phi = gz$, where z is the height above the mean sea level; $\sigma = -\alpha\partial\ell n\theta/\partial p$, where α is the specific volume and θ the potential temperature; $R = 287$ kj t^{-1} deg^{-1} is the gas constant for air; $c_p = 1004$ kj t^{-1} deg^{-1} is the specific heat at constant pressure; H is the diabatic heating per unit time and unit mass. In the quasi-geostrophic formulation the static stability parameter σ is independent of the horizontal coordinates (see, for example, Phillips (1963)). The friction terms do not appear explicitly in (2.1) but the effect of friction will be taken into account through the lower boundary condition on ω, in the manner suggested by

Charney and Eliassen (1949), that is, by considering that friction in the boundary layer introduces some vertical motion at the bottom of the free atmosphere. No internal friction mechanism will be included in order to have a formulation which is consistent with the model (including only boundary layer friction) used by Brown (1964) to compute the diabatic heating values which will constitute a basic input for the present study.

In (2.1) we have neglected the vertical advection of vorticity and the terms expressing the turning of the vortex tubes, which is equivalent to neglecting the vertical advection of momentum ($\omega\partial u/\partial p$, $\omega\partial v/\partial p$) in the two equations of motion from which (2.1) is derived. In the first term on the right-hand side of (2.1) we have also neglected the relative vorticity on the grounds that it is small compared to f and, for consistency (Wiin-Nielsen (1959a)), we have adopted a constant value of f. In (2.2) we shall introduce the further approximation

$$\Phi = f_o \Psi \ . \tag{2.3}$$

The nature of this approximation has been discussed by Phillips (1958).

For convenience we divide the atmosphere into horizontal layers as shown in Fig. 1. The boundary conditions at the top and bottom of the free atmosphere are

$$\omega = 0 \quad \text{at} \quad p = 0 \tag{2.4}$$

and

$$\omega = \omega_4 = \omega_{4M} + \omega_{4F} \quad \text{at} \quad p = p_4 \tag{2.5a}$$

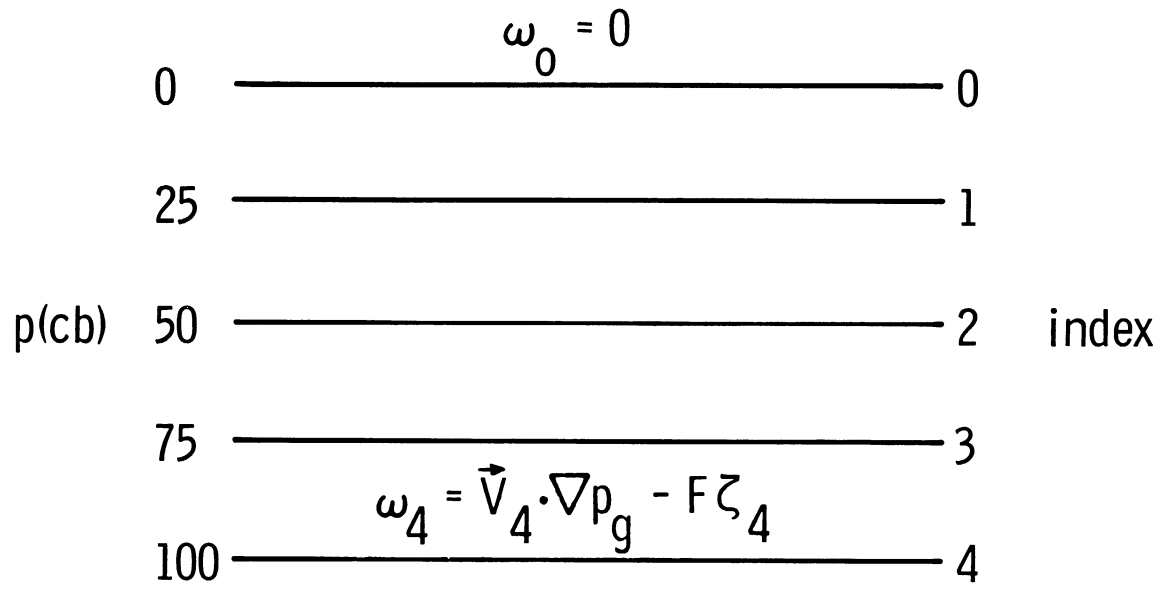

Fig. 1. Schematic representation of the two level model.

where

$$\omega_{4M} = \vec{V}_4 \cdot \nabla p_g \qquad (2.5b)$$

and

$$\omega_{4F} = -F\zeta_4 \ . \qquad (2.5c)$$

ω_{4M} is the expression for that part of ω_4 which is due to the flow of air over the uneven terrain where the standard pressure is $p_g(x,y)$. The expression for ω_{4M} follows from the relation

$$w_{4M} = \vec{V}_4 \cdot \nabla z_g$$

where w_4 is the vertical component of speed (in a coordinate system with height as the vertical coordinate) at level 4 due to the flow of air over a terrain with height $z_g(x,y)$ above mean sea level ($z = 0$). By integrating the hydrostatic relation from $z = 0$ where p = constant to $z = z_g$ where $p = p_g$, assuming a constant density, we find that the above expression for w_{4M} can be written as

$$w_{4M} = -\frac{1}{g\rho} \vec{V} \cdot \nabla p_g \ .$$

In the steady state quasi-geostrophic formulation, on the other hand, we have

$$w_{4M} = \left(\frac{dz}{dt}\right)_{4M} = \omega_{4M}\left(\frac{\partial z}{\partial p}\right)_4 = -\frac{1}{g\rho}\,\omega_{4M} \ .$$

By combinding the above two equations we obtain (2.5b).

ω_{4F} is defined as the vertical motion at the top of the boundary layer produced by friction and is approximated by

$$\omega_{4F} = -F\zeta_4$$

as was done, for example, by Charney and Eliassen (1949), Phillips (1956), Saltzman (1961), Smagorinsky (1953), and Wiin-Nielsen (1961). In this chapter F, the coefficient of friction, will be taken to be a constant (4×10^{-6} sec^{-1}, the value used by Phillips (1956)) but in the next chapter some computations will be made using a larger value of F over the continents than over the oceans.

In developing the usual two level model of the atmosphere, the procedure consists in applying the vorticity equation (2.1) at 25 cb and 75 cb, expressing the derivatives with respect to pressure as finite differences. For convenience the resulting two equations are then added and subtracted to yield the following two equivalent equations:

$$\vec{V}_* \cdot \nabla(\zeta_* + f) + \vec{V}_T \cdot \nabla\zeta_T = \frac{f_o}{p_4}\omega_4 \tag{2.6}$$

$$\vec{V}_* \cdot \nabla\zeta_T + \vec{V}_T \cdot \nabla(\zeta_* + f) = \frac{f_o}{p_2}\omega_2 - \frac{f_o}{p_4}\omega_4 \tag{2.7}$$

where the subscripts "$*$" and "T" are defined by

$$(\ )_* = \frac{1}{2}[(\ )_1 + (\ )_3] \tag{2.8a}$$

$$(\ )_T = \frac{1}{2}[(\ )_1 - (\ )_3]\ . \tag{2.8b}$$

The vector $\vec{V}_4$ appearing in (2.5b) is expressed in terms of the stream function Ψ_4 through the relation

$$\vec{V}_4 = \vec{k} \times \nabla\Psi_4 \tag{2.9}$$

where $\vec{k}$ is the unit vertical vector. If we assume that the vertical temperature lapse rate is a constant, it is then possible, by integrating the hydrostatic equation, to express Ψ_4 as a linear combination of Ψ_* and Ψ_T. In fact, with a temperature lapse rate of $6.5°C\ km^{-1}$ we obtain

$$\Psi_4 = \Psi_* - 1.6\Psi_T \tag{2.10a}$$

which leads to the relation

$$\vec{V}_4 = \vec{V}_* - 1.6\vec{V}_T \tag{2.10b}$$

since $\vec{V}_*$ and $\vec{V}_T$ are nondivergent.

By using (2.5) and (2.10) we can now rewrite (2.6) and (2.7) as

$$\vec{V}_*\cdot\nabla(\zeta_*+f) + \vec{V}_T\cdot\nabla\zeta_T = \frac{f_o}{p_4}(\vec{V}_*-1.6\vec{V}_T)\cdot\nabla p_g - F(\zeta_*-1.6\zeta_T) \tag{2.11}$$

$$\vec{V}_*\cdot\nabla\zeta_T + \vec{V}_T\cdot\nabla(\zeta_*+f) = \frac{f_o}{p_2}\omega_2 - \frac{f_o}{p_4}(\vec{V}_*-1.6\vec{V}_T)\cdot\nabla p_g + F(\zeta_*-1.6\zeta_T)\ . \tag{2.12}$$

To complete the system of equations we apply the thermodynamic equation at 50 cb (level 2), again expressing the derivative with respect to pressure in finite difference form. The resulting equation is then

$$2f_o\vec{V}_2\cdot\nabla\Psi_T + \sigma_2 p_2\omega_2 = \frac{R}{c_p}H. \tag{2.13}$$

Just as for Ψ_4, we can express Ψ_2, and hence $\vec{V}_2$, in terms of Ψ_* and Ψ_T. Using the same temperature lapse rate as above we obtain

$$\Psi_2 = \Psi_* - 0.2\Psi_T \ . \tag{2.14}$$

With this expression for Ψ_2 it follows that

$$\vec{V}_2 \cdot \nabla\Psi_T \equiv \vec{V}_* \cdot \nabla\Psi_T$$

so that (2.13) can be written as

$$2f_o \vec{V}_* \cdot \nabla\Psi_T + \sigma_2 p_2 \omega_2 = \frac{R}{c_p} H \ . \tag{2.15}$$

We note that since $\vec{V}_*$ and ζ_* are functions of Ψ_*, and similarly $\vec{V}_T$ and Ψ_T are functions of Ψ_T, (2.11), (2.12), and (2.15) comprise a system of three equations in three unknown, namely, Ψ_*, Ψ_T, and ω_2 provided that p_g and H are known functions of x and y.

In the following we shall assume that the flow consists of small perturbations superimposed on a basic zonal current. The perturbations will be taken to be periodic in both x and y while the speed of the basic zonal current, U, will be assumed to be a function of pressure alone. It is then possible to write Ψ_* and Ψ_T in the form

$$\Psi_* = -U_* y + \psi_*(x,y) \tag{2.16a}$$

$$\Psi_T = -U_T y + \psi_T(x,y) \tag{2.16b}$$

where U_* and U_T are the (constant) speeds of the mean and thermal zonal winds of the basic flow while ψ_* and ψ_T are the mean and thermal perturbation stream

functions. In this context the diabatic heating H and the standard pressure at the ground must also be considered as perturbation quantities.

When (2.11), (2.12), and (2.15) are linearized using (2.16) and the vertical velocity is eliminated among the resulting equations, the following linear system in ψ_* and ψ_T is then obtained:

$$U_* \frac{\partial}{\partial x} \nabla^2\psi_* + \frac{F}{2} \nabla^2\psi_* + \beta \frac{\partial \psi_*}{\partial x} + U_T \frac{\partial}{\partial x} \nabla^2\psi_T - 0.8F\nabla^2\psi_T = \frac{f_o}{p_4} (U_*-1.6U_T) \frac{\partial p_g}{\partial x} \tag{2.17a}$$

$$U_T \frac{\partial}{\partial x} \nabla^2\psi_* - \frac{F}{2} \nabla^2\psi_* + \delta^2 U_T \frac{\partial \psi_*}{\partial x} + U_* \frac{\partial}{\partial x} \nabla^2\psi_T + 0.8F\nabla^2\psi_T + (\beta-U_*\delta^2) \frac{\partial \psi_T}{\partial x}$$

$$= - \frac{4Rf_o}{c_p\sigma_2 p_4^2} H - \frac{f_o}{p_4} (U_*-1.6U_T) \frac{\partial p_g}{\partial x} \tag{2.17b}$$

where

$$\delta^2 = \frac{8f_o^2}{\sigma_2 p_4^2}$$

and $\beta = df/dy$ = constant (16×10^{-12} m^{-1} sec^{-1} at 45°N).

We note that since all the derivatives with respect to y in (2.17) are of the second order and since all the coefficients are independent of y it follows that if p_g and H have the form[1]

$$p_g = \hat{p}_g(x) \cos(\mu y) \tag{2.18a}$$

$$H = \hat{H}(x) \cos(\mu y) \tag{2.18b}$$

---

[1] In the sequel we shall use a circumflex over a symbol, as in (2.18), to designate that part of the variable which depends on the longitude only.

then ψ_* and ψ_T must have the form

$$\psi_* = \hat{\psi}_*(x) \cos(\mu y) \tag{2.18c}$$

$$\psi_T = \hat{\psi}_T(x) \cos(\mu y) . \tag{2.18d}$$

In this and the following chapter we shall assume that p_g, H, ψ_*, and ψ_T are given by (2.18). This means that if we put the origin of the coordinate system at 45°N the above functions have a maximum absolute value at 45°N and a meridional wavelength given by $L_y = 2\pi/\mu$. Charney and Eliassen (1949) evaluated, from an inspection of the main mountain barriers, that L_y should be approximately 50 degrees of latitude. They found, on the other hand, that their model for the standing waves forced by the topography yielded standing waves which closely approximated the observed ones when the meridional wavelength was assumed to be 66 degrees of latitude. Wiin-Nielsen (1961) computed the effective meridional wavelength of the observed standing waves for various latitude circles using the formula

$$\frac{\partial^2 Z}{\partial y^2} = -\mu^2 Z$$

where Z is the height of a pressure surface, and obtained values for μ which are relatively close to the one used by Charney and Eliassen (1949). In the present study the meridional wavelength will be taken to be 60 degrees of latitude or 6666 km so that $\mu = 0.95 \times 10^{-6}\ m^{-1}$.

Since the perturbation quantities in the model are periodic in x we can expand them in Fourier series. For convenience we replace the coordinate x by $a\lambda \cos \phi_o$ where a is the radius of the earth, ϕ_o is 45° and λ is the

longitude in radians. We can then write

$$\hat{p}_g(\lambda) = \sum_{n=1}^{N} (R_n \cos(n\lambda) + S_n \sin(n\lambda)) \tag{2.19a}$$

$$\hat{H}(\lambda) = \sum_{n=1}^{N} (Q_n \cos(n\lambda) + T_n \sin(n\lambda)) \tag{2.19b}$$

$$\hat{\psi}_*(\lambda) = \sum_{n=1}^{N} (A_n^* \cos(n\lambda) + B_n^* \sin(n\lambda)) \tag{2.19c}$$

$$\hat{\psi}_T(\lambda) = \sum_{n=1}^{N} (A_n^T \cos(n\lambda) + B_n^T \sin(n\lambda)). \tag{2.19d}$$

When (2.18) and (2.19) are substituted in (2.17) the following system of linear algebraic equations for A_n^*, B_n^*, A_n^T, and B_n^T is obtained:

$$a_1 A_n^* - a_2 B_n^* - 1.6a_1 A_n^T + a_3 B_n^T = -bS_n \tag{2.20a}$$

$$a_2 A_n^* + a_1 B_n^* - a_3 A_n^T - 1.6a_1 B_n^T = bR_n \tag{2.20b}$$

$$a_1 A_n^* + a_4 B_1^* - 1.6a_1 A_n^T + a_5 B_n^T = -bS_n - qQ_n \tag{2.20c}$$

$$a_4 A_n^* - a_1 B_n^* + a_5 A_n^T + 1.6a_1 B_n^T = -bR_n + qT_n \tag{2.20d}$$

where the coefficients are defined as follows:

$$a_1 = Fh(n^2 + \mu^2 h^2)/(2U_*)$$

$$a_2 = n[(\frac{\beta}{U_*} - \mu^2)h^2 - n^2]$$

$$a_3 = \frac{nU_T}{U_*} (n^2 + \mu^2 h^2)$$

$$a_4 = \frac{nU_T}{U_*}\,[(\delta^2-\mu^2)h^2 - n^2]$$

$$a_5 = n[(\frac{\beta}{U_*} - \mu^2 - \delta^2)h^2 - n^2]$$

$$b = \frac{nf_o h^2}{p_4}\,(1 - \frac{1.6U_T}{U_*})$$

$$q = \frac{4Rf_o h^3}{\sigma_2 c_p p_4^2 U_*}$$

and $h = a\cos\phi_o$.

If S_n, R_n, Q_n, and T_n can be obtained from observations the problem then consists in solving the algebraic system (2.20) for A_n^*, B_n^*, A_n^T, and B_n^T. When this is done for $1 \leq n \leq N$ and the results are substituted in (2.19c,d) the solutions for $\hat{\psi}_*$ and $\hat{\psi}_T$ are obtained. It is then a simple matter to obtain $\hat{\psi}_1$ and $\hat{\psi}_3$ along 45°N by means of the relations

$$\hat{\psi}_1(\lambda) = \hat{\psi}_*(\lambda) + \hat{\psi}_T(\lambda) \qquad (2.21a)$$

$$\hat{\psi}_3(\lambda) = \hat{\psi}_*(\lambda) - \hat{\psi}_T(\lambda) \qquad (2.21b)$$

which follow from the definition of the subscripts "*" and "T" given after (2.5). Similarly $\hat{\psi}_2$ can be obtained from $\hat{\psi}_*$ and $\hat{\psi}_T$ by means of (2.14).

We observe from either (2.17), or (2.19) together with (2.20), that the solution $\hat{\psi}_*$ can be written as

$$\hat{\psi}_*(\lambda) = \hat{\psi}_{*M}(\lambda) + \hat{\psi}_{*H}(\lambda)\ ,$$

where $\hat{\psi}_{*M}$ is that part of $\hat{\psi}_*$ which arises from the presence of the mountains and $\hat{\psi}_{*H}$ is that part which is due to the diabatic heating. Similar remarks apply to $\hat{\psi}_T$ so that we can write

$$\hat{\psi}_T(\lambda) = \hat{\psi}_{TM}(\lambda) + \hat{\psi}_{TH}(\lambda).$$

Clearly $\hat{\psi}_{*M}$ and $\hat{\psi}_{TM}$ can be obtained by solving the model equations with $\hat{H} \equiv 0$ while $\hat{\psi}_{*H}$ and $\hat{\psi}_{TH}$ are the solutions in the case $\hat{p}_g = 0$.

To get some insight into the basic properties of the two level model we shall compute the response of the model to forcing by <u>either</u> the bottom topography <u>or</u> by the diabatic heating. The attention will be focussed, in the following sections, on the changes in the model properties with the zonal wavelength of the disturbance.

2.3 THE RESPONSE OF THE MODEL TO AIR FLOW OVER IDEALIZED TOPOGRAPHY

We shall obtain some useful information about the two level model by solving (2.20) with $S_n = Q_n = T_n = 0$ for <u>all</u> n, $R_n = 1$ for <u>some</u> n and $R_m = 0$ for $m \neq n$. In other words, we consider the adiabatic flow of the model atmosphere over a surface where the standard pressure is

$$\hat{p}_g(\lambda) = \cos(n\lambda) \tag{2.22}$$

and solve (2.20) first with n = 1, then with n = 2, and so on. The solution for the mean stream function has the form

$$\hat{\psi}_*(\lambda) = \hat{\psi}_{*M}(\lambda) = A_n^* \cos(n\lambda) + B_n^* \sin(n\lambda)$$
$$= C_n^* \cos(n\lambda - \alpha_n^*) \tag{2.23a}$$

where

$$C_n^* = [A_n^{*2} + B_n^{*2}]^{1/2} \tag{2.23b}$$

and

$$\alpha_n^* = \tan^{-1}(B_n^*/A_n^*) \ . \tag{2.23c}$$

The solution for the thermal stream function has also the form (2.23) except that the asterisks are replaced by the letter "T".

The solutions for ψ_* and ψ_T were obtained under the above conditions for the integral values of n in the range $1 \leq n \leq 18$. From these results the amplitudes C_n^* and C_n^T and the phase angles α_n^* and α_n^T were computed for the same values of n. In all the computations the parameters were assigned the following values:

$$F = 4 \times 10^{-6} \text{ sec}^{-1}, \quad U_* = 15 \text{ m sec}^{-1}, \quad \sigma_2 = 3 \text{ m}^4 \text{ sec}^2 \text{ t}^{-2},$$
$$\mu = 0.95 \times 10^{-6} \text{ m}^{-1}, \quad U_T = 5 \text{ m sec}^{-1}.$$

The plot of C_n^*, the amplitude of the mean stream function, appears in Fig. 2 as a function of n, the number of waves in the interval $0 \leq \lambda \leq 2\pi$. We note that the amplitude of the ψ_* wave is largest for n = 2 and decreases rather rapidly as n increases. This means that the model atmosphere is more easily excited on the scale of the wave with n = 2 than on any other scale. For example, we see that the amplitude of the wave is approximately 15 times larger for n = 2 than for n = 10. The model is therefore relatively insensitive to the presence of the high wave number components in the expansion (2.19a) for $\hat{p}_g$.

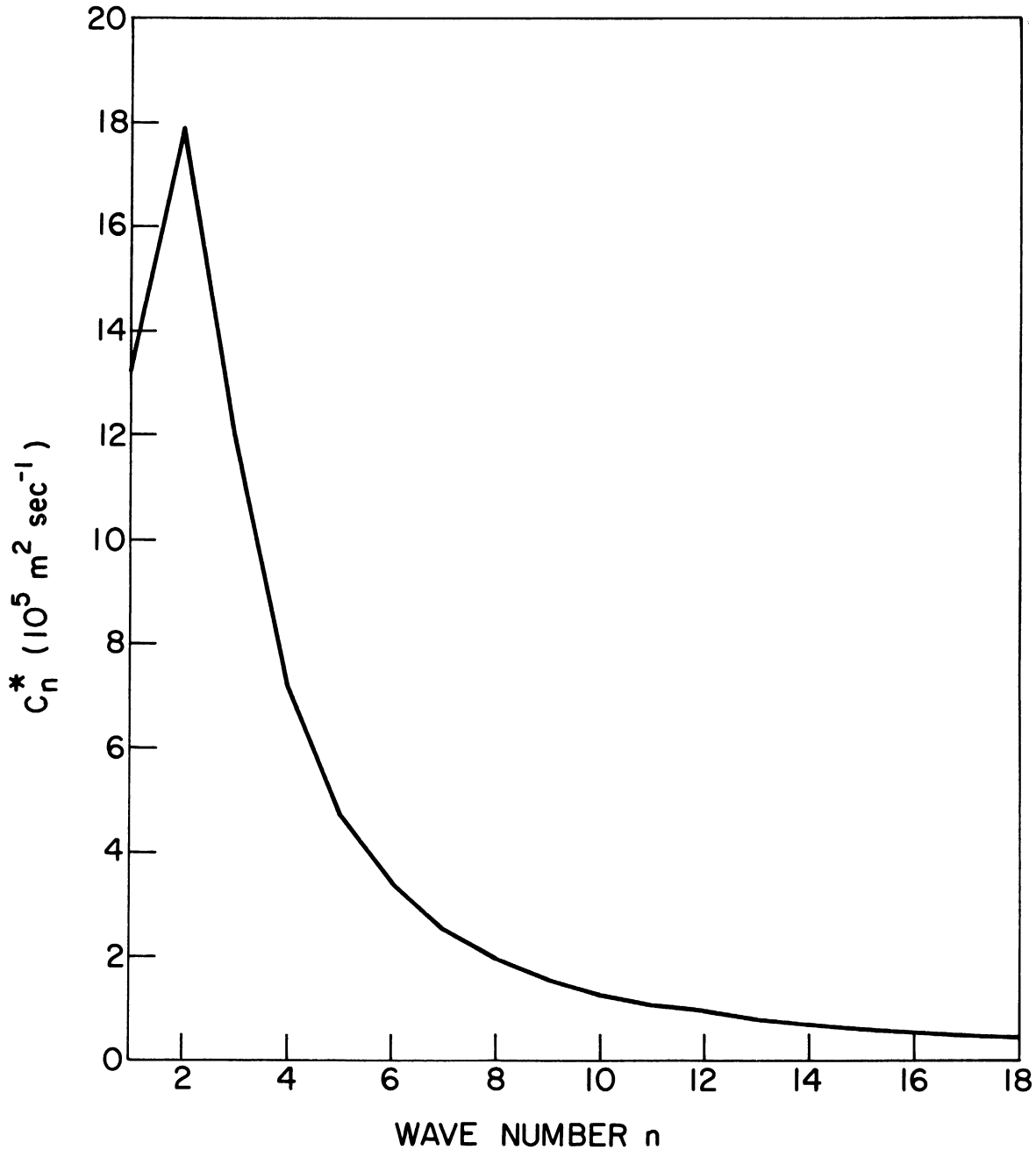

Fig. 2. The amplitude of the mean stream function forced by a sinusoidal distribution of $\hat{p}_g$ with unit amplitude and zonal wave number n. Parameters: $\mu = 0.95 \times 10^{-6}$ m^{-1}, $U_* = 15$ m sec^{-1}, $U_T = 5$ m sec^{-1}, $F = 4 \times 10^{-6}$ sec^{-1}.

In order to determine the position of the $\hat{\psi}_*$ wave in relation to the $\hat{p}_g$ wave given in (2.22), the phase angle α_n, defined by (2.23c), was computed for $1 \leq n \leq 18$. It was found that for each value of n the ridge in the $\hat{\psi}_*$ wave was positioned somewhat upstream from the trough in the $\hat{p}_g$ wave. If we think of the trough in the $\hat{p}_g$ wave as representing a ridge in the $\hat{Z}_g$ wave, where $\hat{Z}_g$ is the height of the ground above mean sea level, we can conclude from the results that the crest in the $\hat{\psi}_*$ wave is somewhat to the west of the crest in the $\hat{Z}_g$ wave.

Figure 3 shows the phase difference, as a fraction of one wavelength, between the trough in the $\hat{p}_g$ wave and the upstream ridge in the $\hat{\psi}_*$ wave. We see, for example, that for zonal wave number 2 the phase lag is about one fifth of one wavelength so that the ridge in the $\hat{\psi}_*$ wave is about 0.2 x 14,000 km = 2800 km upstream from the trough in the $\hat{p}_g$ wave. For zonal wave number 14, on the other hand, the ridge in the $\hat{\psi}_*$ wave is only 0.05 of one wavelength, or about 0.05 x 2000 km = 100 km, upstream from the trough in the $\hat{p}_g$ wave. The conclusion to be drawn from the computations, therefore, is that for small zonal wave numbers the ridge in the $\hat{\psi}_*$ wave is relatively far upstream from the trough in the $\hat{p}_g$ wave (or ridge in the $\hat{Z}_g$ wave) whereas for large zonal wave numbers the ridge in the $\hat{\psi}_*$ wave is only slightly to the west of the trough in the $\hat{p}_g$ wave.

The amplitude and phase of the $\hat{\psi}_T$ waves were also computed for the distribution of $\hat{p}_g$ given by (2.22) and for the zonal wave numbers 1 through 18. Since the difference between the geostrophic stream functions at 25 cb and 75 cb is proportional to the mean temperature between these levels, we

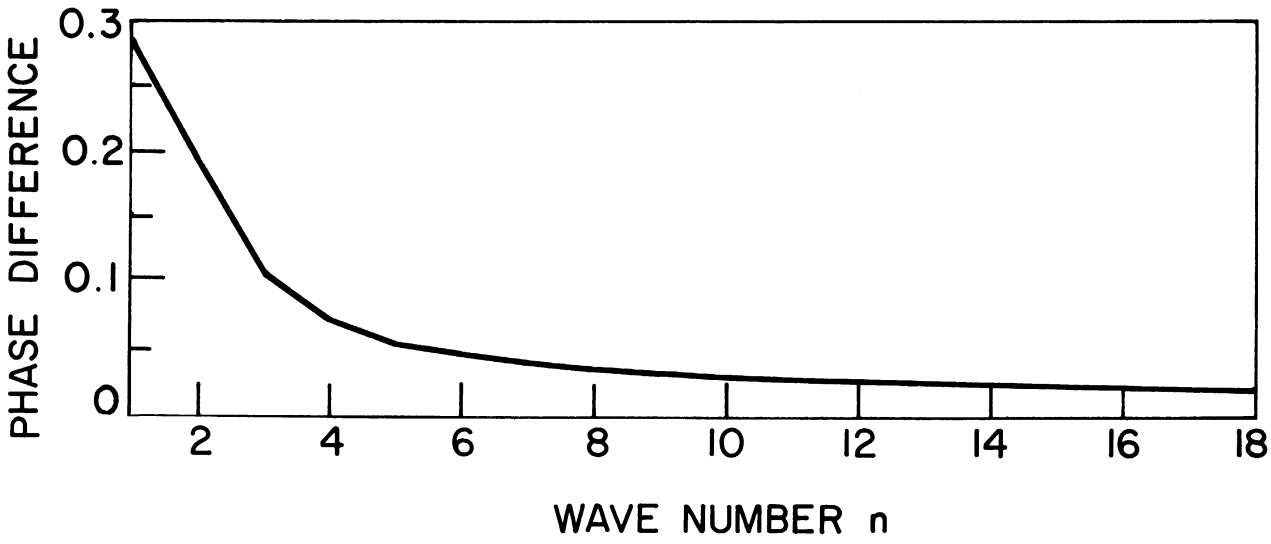

Fig. 3. The phase difference between the nth zonal harmonic in the mean stream function and the same harmonic in the function $-\hat{p}_g$. The mean stream function wave is to the west of the $-\hat{p}_g$ wave by the fraction of the zonal wavelength indicated on the ordinate. Parameters: same as Fig. 2.

can think of $\hat{\psi}_T$ as representing the temperature near 50 cb. The amplitude of the $\hat{\psi}_T$ wave is given as a function of the zonal wave number in Fig. 4. We see that a $\hat{p}_g$ wave of unit amplitude forces a temperature disturbance with the largest amplitude when n = 1. The relative minimum in the amplitude of the thermal wave near wave numbers 3 and 4 coincides with the region of the spectrum where a radical change in the phase relationship between the $\hat{\psi}_*$ and $\hat{\psi}_T$ waves occur. In fact, when α_n^* and α_n^T are compared, we find that the thermal and mean stream functions are exactly in phase for n = 1, 2, and 3 and out of phase by exactly half a wavelength for $n \geq 4$.

It follows from (2.21) that if, for a given zonal wave number n, the $\hat{\psi}_*$ and $\hat{\psi}_T$ waves are exactly in phase then the $\hat{\psi}_1$ and $\hat{\psi}_3$ wave are also exactly in

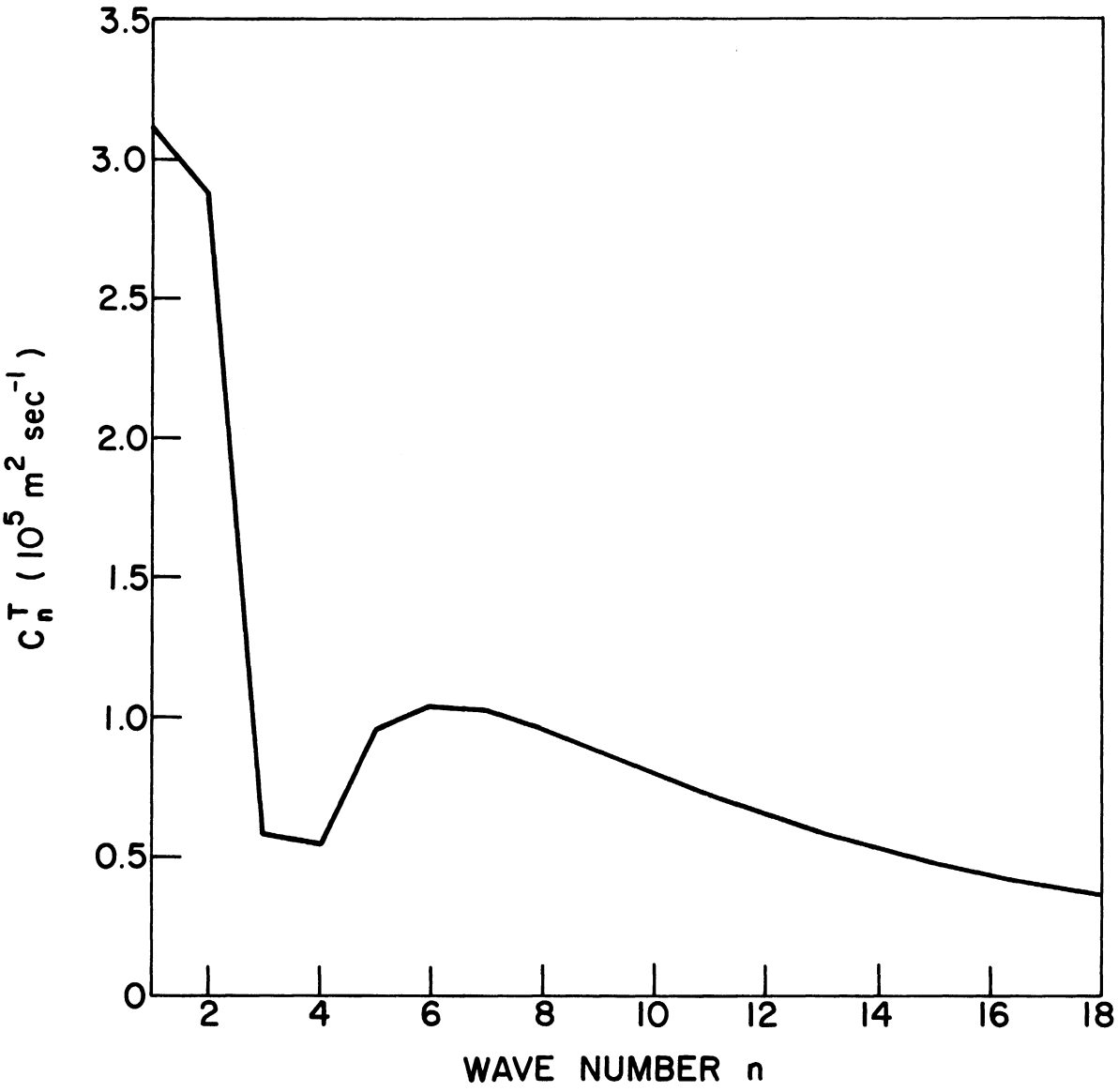

Fig. 4. The amplitude of the thermal stream function forced by a sinusoidal distribution of $\hat{p}_g$ with unit amplitude and zonal wave number n. Parameters: same as in Fig. 2.

phase and the amplitude of the former is larger than that of the latter. The $\hat{\psi}$ wave has therefore no tilt in the vertical and amplifies with height. We note that this is the case for the zonal wave numbers 1, 2, and 3. On the other hand, if the $\hat{\psi}_*$ and $\hat{\psi}_T$ waves are precisely half a wavelength out of phase and the amplitude of the $\hat{\psi}_*$ wave is larger than that of the $\hat{\psi}_T$ wave, the $\hat{\psi}$ wave has again no tilt in the vertical and the $\hat{\psi}_1$ wave has a smaller amplitude than the $\hat{\psi}_3$ wave so that the stream function wave is damped with height. This wave structure applies for zonal wave numbers $4 \leq n \leq 18$.

We conclude from the above discussion that when the zonal wave numbers are considered individually the bottom topography forces standing waves which have no tilt in the vertical, a result also obtained by Saltzman (1965). We saw also that the forced harmonics of the stream function either amplify or damp with height depending on their zonal wave number. As a convenient measure of the amplification or damping with height we can use the ratio of the amplitude of the $\hat{\psi}_1$ wave to that of the $\hat{\psi}_3$ wave. This ratio, denoted by A, appears in Fig. 5 as a function of the zonal wave number. Clearly, for $A > 1$ we have amplification and for $A < 1$ we have damping with height. Just as observed earlier, those components with n = 1,2, and 3 amplify while the others damp with height. For example, we see that the amplitude of the wave component n = 1 is about 1.6 times larger at 25 cb than at 75 cb whereas that of wave component n = 16 is about 10 times smaller at 25 cb than at 75 cb.

2.4 THE RESPONSE OF THE MODEL TO IDEALIZED HEAT SOURCES AND SINKS

The discussion presented in this section is similar to that of the previous one except that here the standing waves are produced by the diabatic

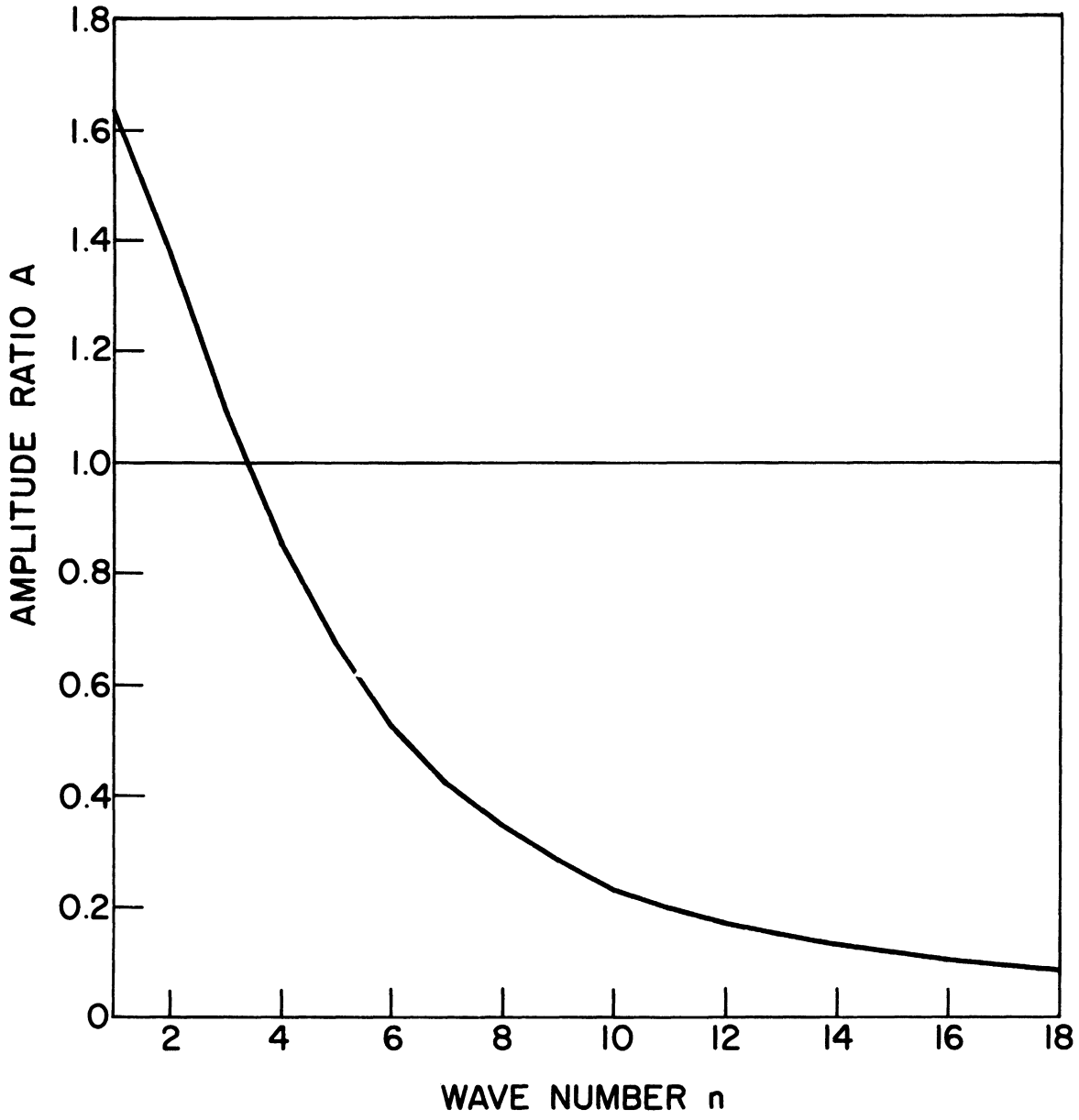

Fig. 5. The amplitude ratio of the stream function forced by a sinusoidal distribution of $\hat{p}_g$ with zonal wave number n. Parameters: same as in Fig. 2.

heating instead of by the topography. After setting $R_n = S_n = T_n = 0$ for all values of n, $Q_n = 1$ for some n and $Q_m = 0$ for $m \neq n$, we solve (2.20) first with n = 1, then n = 2, and so on. Since in each case the heating function has the form

$$\hat{H}(\lambda) = Q_n \cos(n\lambda) \tag{2.24}$$

the solution for the mean stream function can be written as

$$\hat{\psi}_*(\lambda) = \hat{\psi}_{*H}(\lambda) = A_n^* \cos(n\lambda) + B_n^* \sin(n\lambda) \tag{2.25a}$$

$$= C_n^* \cos(n\lambda - \alpha_n^*) \tag{2.25b}$$

where

$$C_n^* = [A_n^{*2} + B_n^{*2}] \tag{2.25c}$$

and

$$\alpha_n^* = \tan^{-1}(B_n^*/A_n^*) , \tag{2.25d}$$

with similar expressions holding true for the $\hat{\psi}_T$ solution.

The amplitude C_n^* of the mean stream function appears as a function of the zonal wave number in Fig. 6. We see that contrary to the case where the perturbations result from the presence of the topography (Fig. 2) the most easily excited mode here is zonal wave number one. The decrease in C_n^* as n increases is seen to be quite rapid; in fact, C_4^* is less than 10% of C_1^* and C_{10}^* is again less than 10% of C_4^*.

The amplitude C_n^T of the thermal stream function can be seen in Fig. 7 as a function of the zonal wave number. Just as in the case of the mean stream function, zonal wave number 1 is found to be the most easily excited mode.

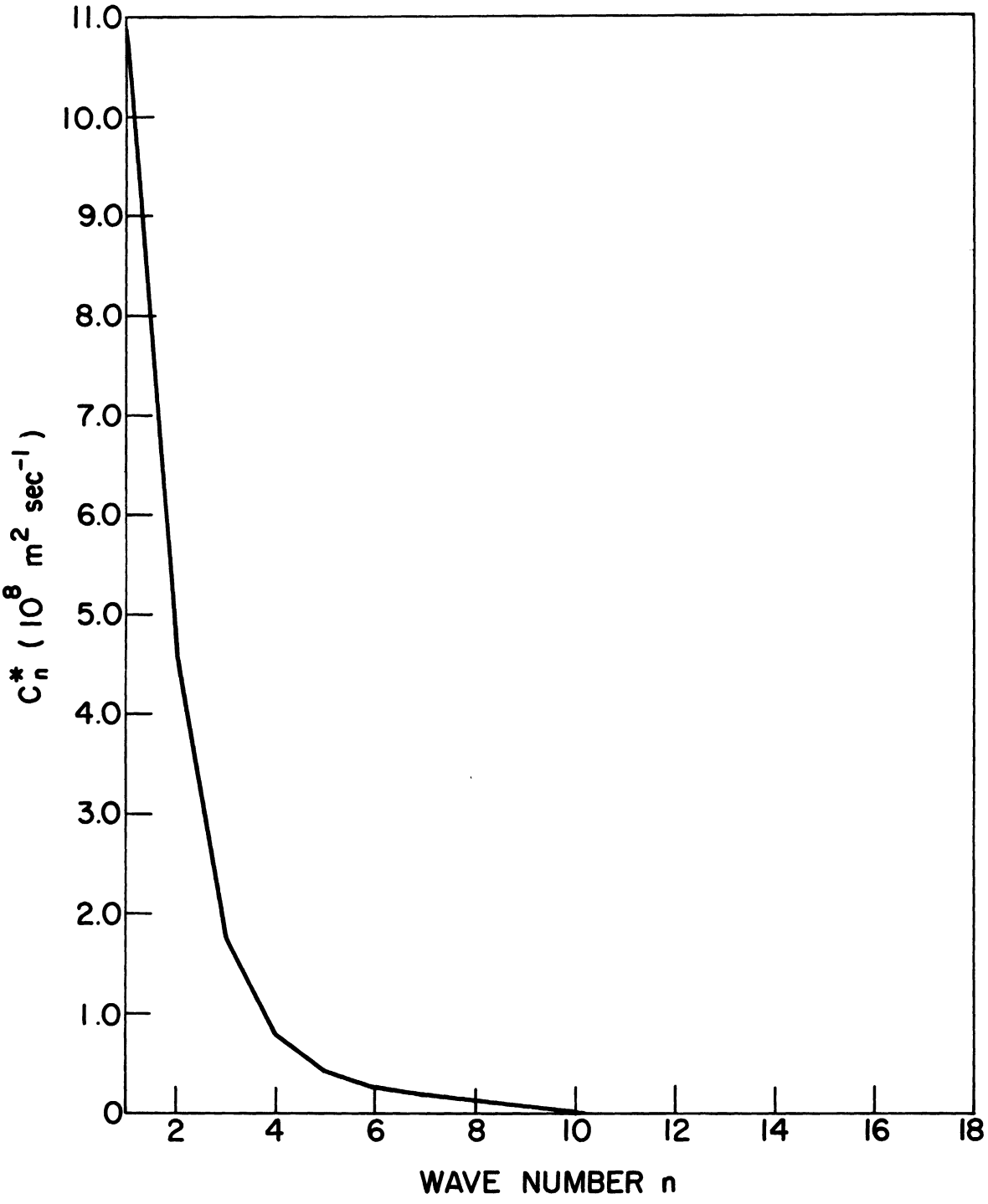

Fig. 6. The amplitude of the mean stream function forced by a sinusoidal distribution of $\hat{H}$ with unit amplitude and zonal wave number n. Parameters: same as in Fig. 2.

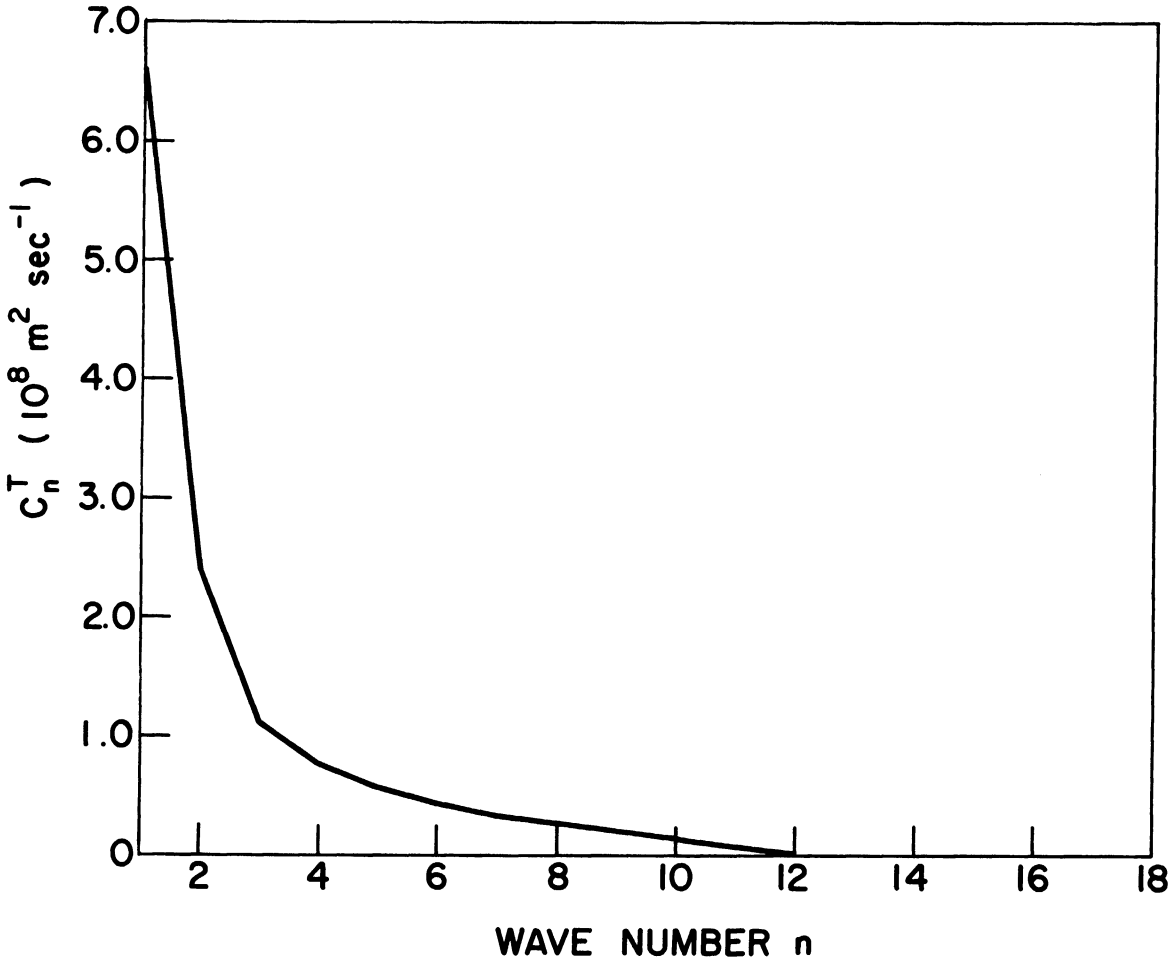

Fig. 7. The amplitude of the thermal stream function forced by a sinusoidal distribution of $\hat{H}$ with unit amplitude and zonal wave number n. Parameters: same as in Fig. 2.

The phase lag between the individual Fourier components ($1 \leq n \leq 18$) of the heating function $\hat{H}$ and the corresponding components in $\hat{\psi}_*$ and $\hat{\psi}_T$ can be seen as the upper and lower curves, respectively, of Fig. 8. The phase lag is defined here as the distance, in units of the zonal wavelength determined by n, between a ridge in the forcing function, $\hat{H}$, and the first ridge downstream in the response, that is, $\hat{\psi}_*$ or $\hat{\psi}_T$. Thus we observe that for zonal wave number two the ridge in the mean stream function $\hat{\psi}_*$ is about 0.42 of one wavelength downstream from the ridge in the heating function. For this wave number, therefore, the ridges (troughs) in the mean stream function occur only slightly to the west of the longitudes of maximum cooling (heating). This is in close agreement with the results obtained by Smagorinsky (1953) using a zonal wavelength of 160 degrees of longitude and a meridional wavelength of 53.9 degrees of latitude (ours is 60 degrees of latitude).

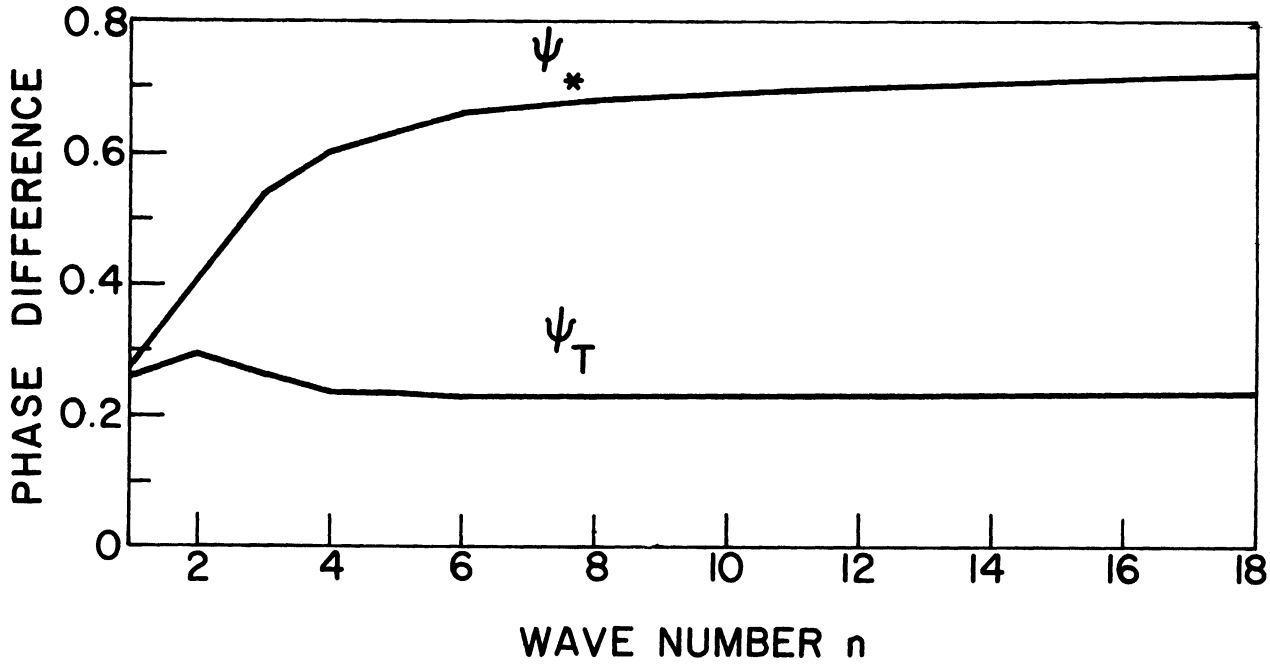

Fig. 8. The phase difference between the nth zonal harmonic in the function $\hat{H}$ and the same harmonic in the mean stream function (upper curve) or thermal stream function (lower curve). The mean and thermal stream function waves are to the east of the $\hat{H}$ wave by the fraction of the zonal wavelength indicated on the ordinate. Parameters: same as in Fig. 2.

For zonal wave number 2, the thermal stream function is displaced about 0.29 of one wavelength to the east of the heating wave and is therefore about 0.13 of one wavelength to the west of the $\hat{\psi}_*$ wave. This, together with (2.21), means that the stream function wave slopes to the west with height, a result also obtained by Smagorinsky (loc. cit.). We note that as the zonal wave number increases so does the phase difference between the mean and thermal stream functions. In fact for n = 18 the $\hat{\psi}_*$ and $\hat{\psi}_T$ waves are displaced from each other by 0.49 of a wavelength so that the crests of the thermal stream function nearly coincides with the troughs of the mean stream function. From (2.21) we find that in this case the stream function wave is nearly vertical and that its amplitude decreases with height.

The amplitude ratio A, defined as the ratio of the amplitude of the $\hat{\psi}_1$ wave to that of the $\hat{\psi}_3$ wave appears in Fig. 9. We see that wave components 1 and 2 amplify with height whereas the others damp with height. It is interesting to compare these results with those shown in Fig. 5 where the standing waves are maintained by the topography. We note, for example that the amplitude of the stream function for n = 1 increases by a factor of about 3.9 between 75 cb and 25 cb when the wave is created by the diabatic heating (Fig. 9) whereas it increases by only a factor of about 1.6 when the wave is due to topographical effects (Fig. 5).

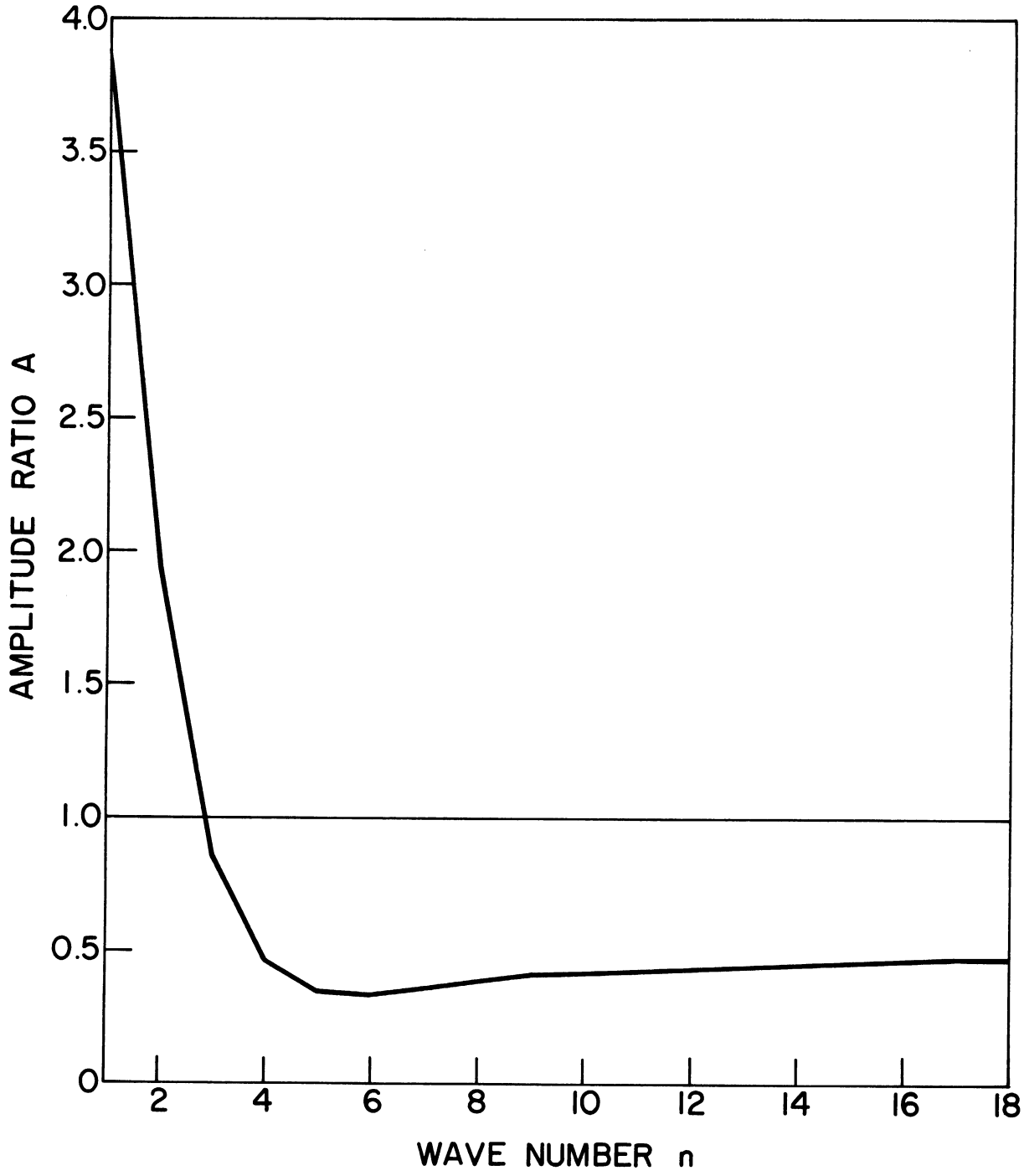

Fig. 9. The amplitude ratio of the stream function forced by a sinusoidal distribution of $\hat{H}$ with zonal wave number n. Parameters: same as in Fig. 2.

CHAPTER 3

THE RESPONSE OF THE TWO LEVEL MODEL TO THE TOPOGRAPHY AND DIABATIC HEATING NEAR 45°N

3.1 THE RESPONSE IN THE CASE OF A CONSTANT FRICTION COEFFICIENT

In an attempt to see whether or not the model presented in Chapter 2 is capable of reproducing the main features of the observed standing waves, we shall determine the solution that it yields when p_g is obtained (using a standard atmosphere) from the ground height values published by Berkofsky and Bertoni (1955) and H is taken from the computations by Brown (1964) for January 1962. Since the system (2.17) is linear we can compute the response of the model atmosphere to the topography and to the diabatic heating separately and then obtain the complete solution by adding the separate constributions.

In solving the model equations we shall use the same values for the parameters as in Chapter 2, namely, $F = 4 \times 10^{-6}$ sec^{-1}, $U_* = 5$ m sec^{-1}, $U_T = 5$ m sec^{-1}, and $\mu = 0.95 \times 10^{-6}$ m^{-1}. The values of U_* and U_T were chosen to be representative of the middle latitude conditions in January, the month for which the values of the diabatic heating apply. We shall also present the response to the topography and heating for the case $F = 6 \times 10^{-6}$ sec^{-1} to show how an increase in the friction coefficient affects the standing waves. By assuming that the value of F is independent of longitude, as we have done in Chapter 2 and are doing in the present section, we are effectively assuming that we can neglect the variation of the friction coefficient from land to ocean. This assumption will be tested in Section 3.2. Sim-

ilarly the assumption that we can use an effective meridional wave number μ will be discussed in Section 3.3.

Since we write the expressions for the pressure at the ground and for the diabatic heating as

$$p_g = \hat{p}_g(\lambda) \cos(\mu y) \tag{3.1a}$$

and

$$H = \hat{H}(\lambda) \cos(\mu y) \tag{3.1b}$$

we require, strickly speaking, to know only $\hat{p}_g$ and $\hat{H}$ along one latitude circle, say 45°N. To introduce some smoothing, on the other hand, $\hat{p}_g(\lambda)$ and $\hat{H}(\lambda)$ were taken to be the meridional averages of p_g and H, respectively, between 30°N and 60°N. The Fourier coefficients R_n and S_n appearing in the expansions (2.19a) for $\hat{p}_g(\lambda)$ were then computed from the relations

$$R_n = \frac{1}{\pi} \int_0^{2\pi} \hat{p}_g(\lambda) \cos(n\lambda) d\lambda \tag{3.2a}$$

$$S_n = \frac{1}{\pi} \int_0^{2\pi} \hat{p}_g(\lambda) \sin(n\lambda) d\lambda. \tag{3.2b}$$

The coefficients Q_n and T_n in the Fourier expansion (2.19b) for $\hat{H}(\lambda)$ were obtained by means of analogous relations. The integrals in (3.2) were evaluated numerically using intervals of 5 degrees of longitude and the integral values of n in the range $1 \leq n \leq 18$.

As a check on the computations, the functions $\hat{p}_g(\lambda)$ and $\hat{H}(\lambda)$ were reconstructed using (2.19a,b) and N = 18. The results are reproduced in Figs. 10(a) and 10(b) to facilitate the forthcoming discussion of the forced waves.

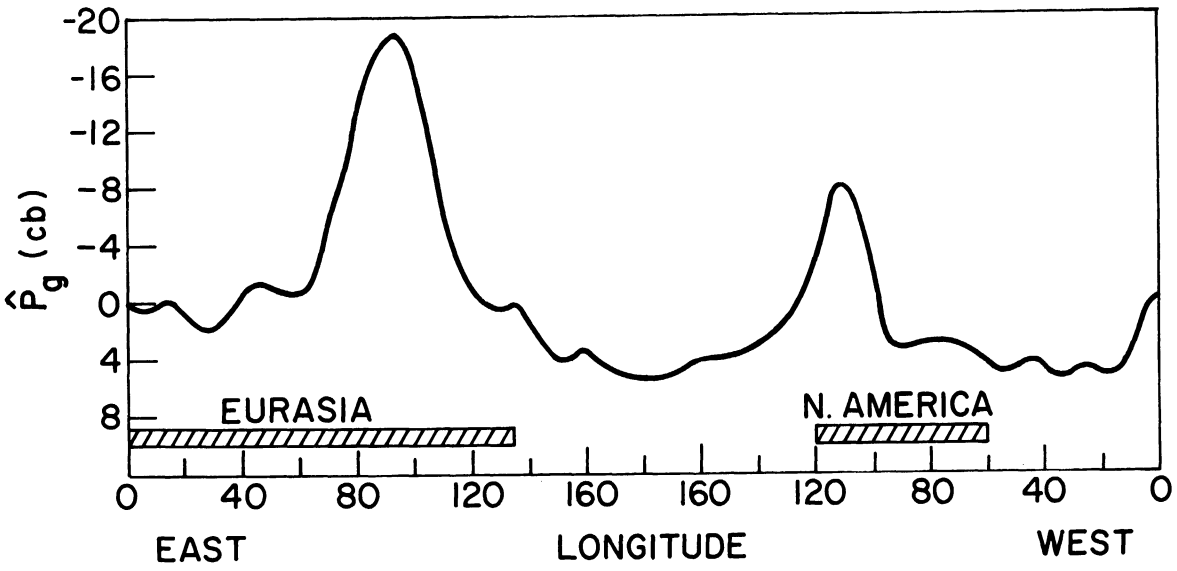

Fig. 10(a). The function $\hat{p}_g$ as obtained from the first 18 zonal harmonics (except n = 0) of the mean standard pressure at the ground between 30°N and 60°N. The position of the continents is shown schematically.

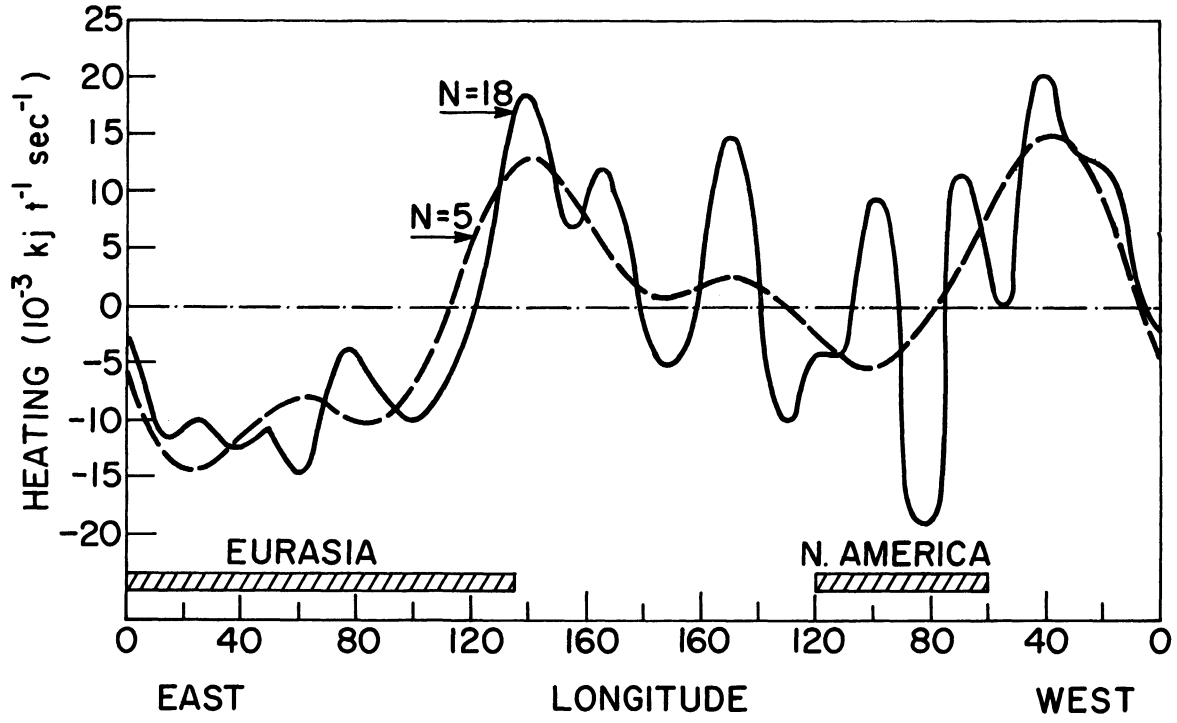

Fig. 10(b). The diabatic heating function $\hat{H}$ as reconstructed from the first 5 and 18 zonal components (except n = 0) of Brown's (1964) diabatic heating values between 30°N and 60°N for January 1962. The position of the continents is shown schematically.

In Fig. 10(b) the function $\hat{H}(\lambda)$ reconstructed from (2.19b) with N = 5 is also presented as the dashed curve to show that the smoothed version of Brown's (1964) heating has the tendency to be positive over the oceans and negative over the continents, as expected for the month of January.

To determine the importance of the topography in creating standing eddies in our model atmosphere, we first considered the case $H \equiv 0$. The system (2.20) was solved for $1 \leq n \leq 18$ and the result substituted into (2.19c,d) to obtain $\hat{\Psi}_*$ and $\hat{\Psi}_T$. The stream functions at 25, 50, and 75 cb were obtained by means of (2.14) and (2.21) and finally the perturbation height Z was obtained from (2.3). The results appear in Fig. 11. At the three levels the forced pattern consists of a major trough near 140°E, a ridge near 120°W and a trough near 70°W. If we refer to Fig. 10(a) we observe that the major trough at 140°E in Fig. 11 occurs in the lee of the Himalayas and nearly coincides with the eastern coast of Asia. We note also that the trough deepens by about 55 m and shifts by 5 degrees to the east from 75 cb to 25 cb. Near the west coast of North America we find a ridge which slopes from 120°W at 75 cb to 125°W at 25 cb. The second major trough in Fig. 11 appears near 65°W at the three pressure levels, that is, near the eastern coast of North America (see Fig. 10(a)), about 45° downstream from the peak of the Rockies.

The response of the model atmosphere to the diabatic heating alone (solid curve, Fig. 10(b)) appears in Fig. 12. Again we find that the most prominent feature in the response is a trough near the eastern edge of Asia. The trough is about three times deeper at 25 cb than at 75 cb and shifts to the west by 20° from 75 to 25 cb. A second trough can be seen over the Atlantic, sloping

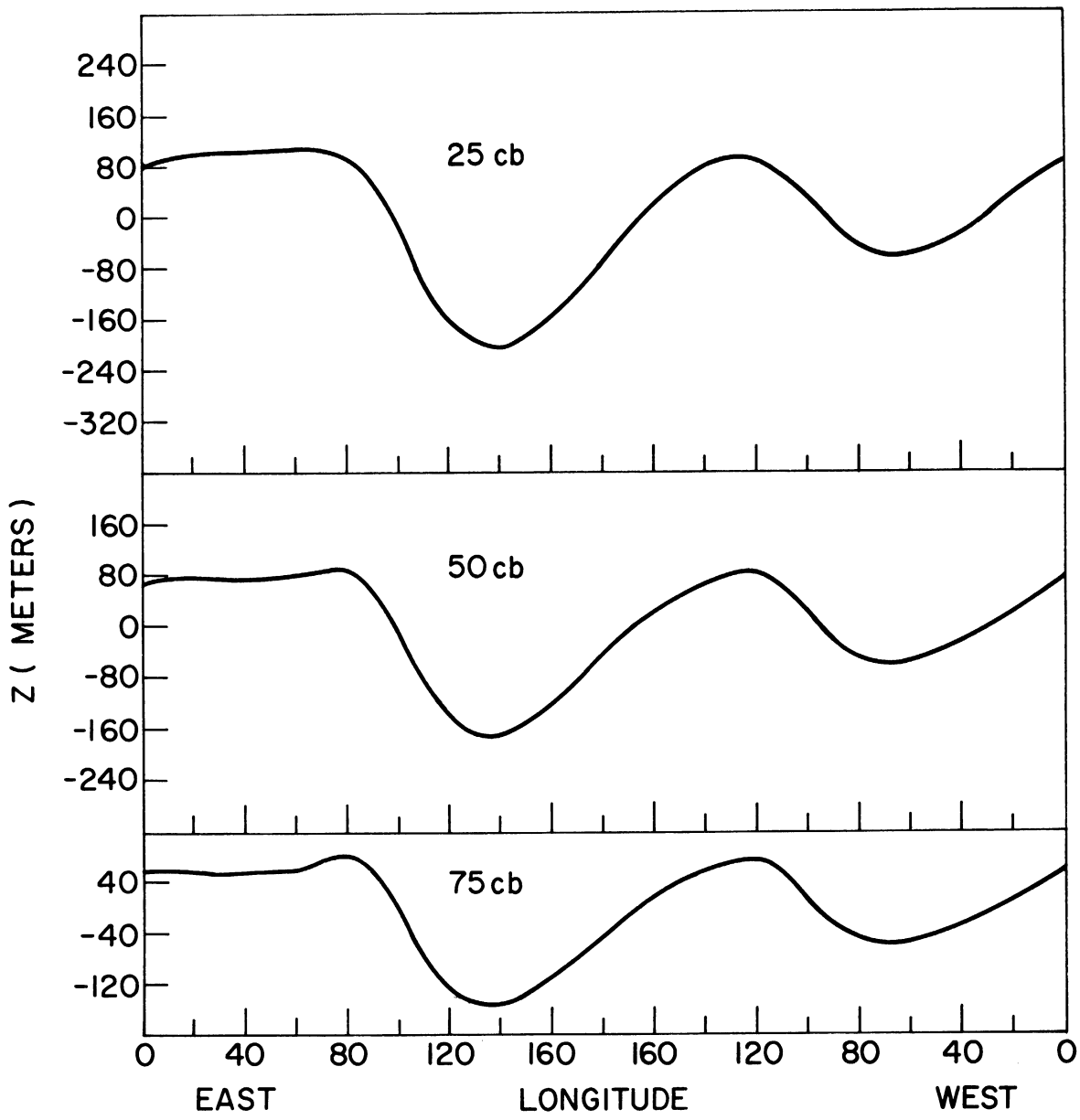

Fig. 11. The perturbation heights of the 25, 50, and 75 cb surfaces produced by the interaction of the zonal current with the distribution of standard pressure at the ground shown in Fig. 10(a). Parameters: same as in Fig. 2.

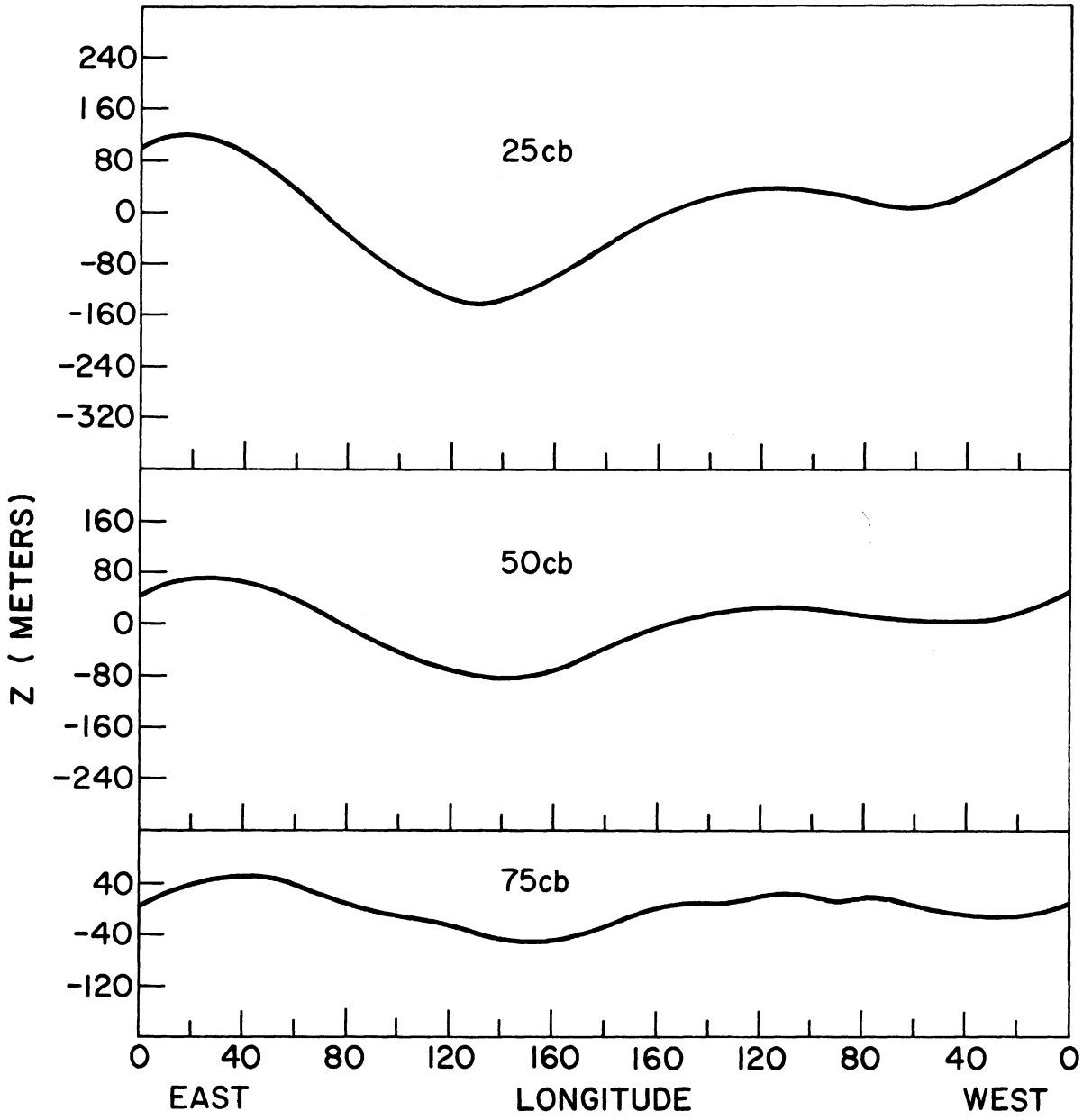

Fig. 12. The perturbation heights of the 25, 50, and 75 cb surfaces produced by the distribution of diabatic heating and cooling given by the solid curve in Fig. 10(b). Parameters: same as in Fig. 2.

from 30°W at 75 cb to 65°W at 25 cb. By comparing with Fig. 11 we find that this trough, just as the previous one, is in the vicinity of a terrain-induced trough and therefore will tend to reinforce it. It is worth noting also that according to our model the standing eddies created by the diabatic heating are somewhat weaker than those produced by the topography.

It is apparent from a comparison of the response in Fig. 12 with the diabatic heating given by the solid curve in Fig. 10(b), that the small scale fluctuations in the heating have very little effect on the standing eddy pattern, just as was indicated in Figs. 6 and 7. It follows that if we want to relate qualitatively the position of the standing eddies to the heating we can, as a first approximation, relate the forced pattern in Fig. 12 to the smoothed heating given by the dashed curve in Fig. 10(b). By doing this we find that the troughs tend to occur near the regions of large-scale heating and the ridges near the regions of large-scale cooling. These results agree qualitatively with those obtained by Smagorinsky (1953) and Gilchrist (1954), for winter conditions, using a single zonal wave number.

The response of the model atmosphere to the forcing by both the topography and the diabatic heating appears in Fig. 13 as the dashed curve at each of the three levels. The solid lines show how the observed heights of the pressure surfaces, averaged between 30°N and 60°N, vary with longitude. We see that the model atmosphere is reasonably successful, especially at 75 cb, in reproducing the main features of the observed pressure surfaces. The dot-dashed curve in the figure is analogous to the dashed one except that it has been computed with $F = 6 \times 10^{-6}$ sec^{-1} instead of $F = 4 \times 10^{-6}$ sec^{-1}. The

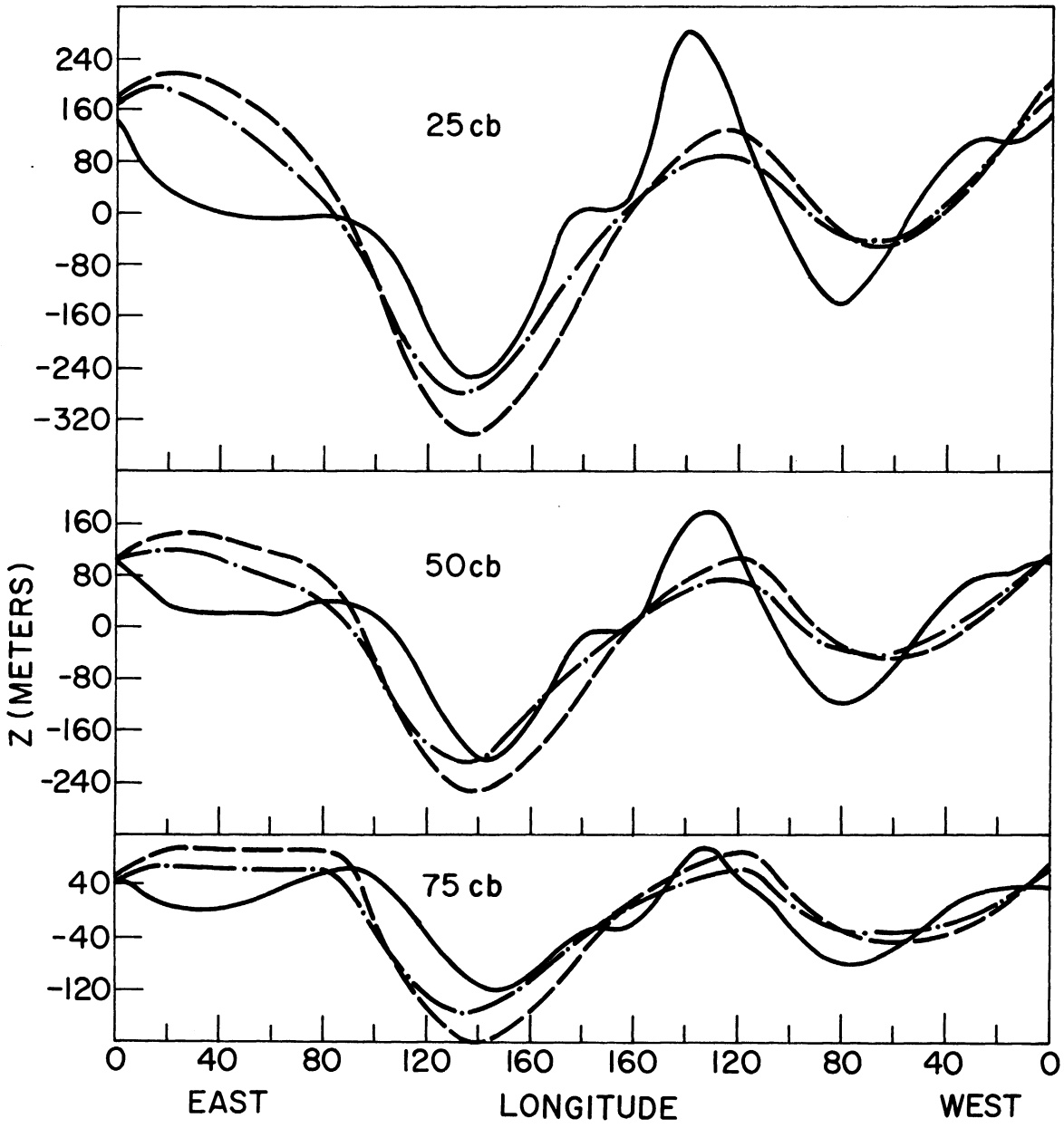

Fig. 13. The perturbation heights of the 25, 50, and 75 cb surfaces. The solid curves give the observed distribution for January 1962, as averaged between 30°N and 60°N. The dashed and dot-dashed curves show the response of the model to the combined forcing by the topography and diabatic heating (with N = 18) using $F = 4 \times 10^{-6}$ sec^{-1} and $F = 6 \times 10^{-6}$ sec^{-1}, respectively. The other parameters are the same as in Fig. 2.

larger friction coefficient reduces the amplitude of the eddies but the effect is not drastic. The change in the value of the friction coefficient also affects the position and vertical slope of the forced waves to some extent. For the smaller value of F we find, at 75 cb, a major trough at 140°E, a ridge at 120°W and a trough at 60°W, all of which slope to the west by 5° from 75 to 25 cb. Between 10°E and 80°E the computed height at 75 cb shows little change with longitude but at the upper levels a ridge is found sloping from 25°E at 50 cb to 20°E at 25 cb. For the greater value of F we find that at 75 cb the major systems are a trough at 135°E, a ridge at 120°W and a trough at 60°W. These systems slope to the west by 5, 10, and 15 degrees of longitude, respectively, from 75 to 25 cb. The ridge over Europe is again rather flat at 75 cb but more distinct in the upper levels, extending from 15°E at 50 cb to 10°E at 25 cb.

It is important to note that for both values of F the troughs and ridges slope to the west with height and share this feature with the observed standing waves. The westward slope with height in the observed standing eddies is not a peculiarity of January 1962 but rather seems to be the usual structure observed in January (see, for example, Gilchrist (1953), Wiin-Nielsen (1961), Saltzman and Sankar Rao (1963)) and is therefore one feature which a model of the standing waves for January should be able to reproduce. We note that with the present model the systematic westward tilt was not present in the topographically induced perturbations (Fig. 11) since of the three major systems one was sloping to the west, another was vertical and the third was sloping to the east with height. The westward tilt of the eddies in Fig. 13

is therefore due to the superposition of the thermally generated perturbations on those produced by the topography.

We can conclude from the results presented so far that our model atmosphere can reproduce the main features of the observed standing waves at 25, 50, and 75 cb. We have seen also that the computed standing waves forced by the topography and diabatic heating tend to be similar in the sense that they are nearly in phase, but different in the sense that the response to the topography is somewhat larger than the response to the heating. When considered alone, neither the response to the topography nor that to the diabatic heating can adequately explain both the amplitude and structure of the observed standing waves since the vertical slope of the former is not in good agreement with observations and the amplitudes of the thermally produced waves are too small. By adding the waves created by the diabatic heating to those produced by the topography, on the other hand, we obtain standing eddies which compare rather well with the observed ones in that they are in about the right position, have about the right amplitude and slope to the west with height.

We recall that in the above model it was assumed that the friction coefficient F could be taken to be a constant and that a single meridional wave number could be assigned to all the perturbations. In the following we shall relax these assumptions somewhat and see how the results are modified.

3.2 THE RESPONSE IN THE CASE OF A VARIABLE FRICTION COEFFICIENT

The oceans and continents have been taken into account in our model insofar as they (a) affect the distribution of heat sources and sinks in the

atmosphere and (b) produce a zonally asymmetric distribution of vertical velocity at the lower boundary of the free atmosphere through the ascending or descending motion of the air along the mountain slopes. There is a third way, however, in which the distribution of continents and oceans can have a bearing on the standing wave problem, namely, by causing a zonal asymmetry in the distribution of the friction coefficient F. Unlike the topography and the distribution of heat sources and sinks, the zonal variation in F cannot, at least in the present formulation, interact directly with the zonal current to produce standing eddies, but it can modify those created by the other two mechanisms. It is our purpose in this section to investigate the extent to which the standing eddies produced by the topography and diabatic heating are modified when F is allowed to vary with longitude. The variation of F with latitude will be neglected.

The basic system of equations for ψ_* and ψ_T in the case where F is a given function of longitude is still (2.17). We can again let p_g, H, ψ_*, and ψ_T be given by (2.18) so that after substituting (2.18) into (2.17) we obtain

$$\frac{d^3\hat{\psi}_*}{d\lambda^3} + \frac{Fh}{2U_*}\frac{d^2\hat{\psi}_*}{d\lambda^2} + \left(\frac{\beta}{U_*} - \mu^2\right)h^2\frac{d\hat{\psi}_*}{d\lambda} - \frac{F\mu^2h^3}{2U_*}\hat{\psi}_* + \frac{U_T}{U_*}\frac{d^3\hat{\psi}_T}{d\lambda^3} - \frac{0.8Fh}{U_*}\frac{d^2\hat{\psi}_T}{d\lambda^2}$$
$$- \frac{U_T\mu^2h^2}{U_*}\frac{d\hat{\psi}_T}{d\lambda} + \frac{F\mu^2h^3}{U_*}\hat{\psi}_T = \frac{f_oh}{p_4}\left(1 - \frac{1.6U_T}{U_*}\right)\frac{d\hat{p}_g}{d\lambda} \qquad (3.3a)$$

and

$$\frac{U_T}{U_*}\frac{d^3\hat{\psi}_*}{d\lambda^3} - \frac{Fh}{2U_*}\frac{d^2\hat{\psi}_*}{d\lambda^2} + \frac{U_T}{U_*}(\delta^2-\mu^2)h^2\frac{d\hat{\psi}_*}{d\lambda} + \frac{F\mu^2h^3}{2U_*}\hat{\psi}_* + \frac{d^3\hat{\psi}_T}{d\lambda^3} + \frac{0.8Fh}{U_*}\frac{d^2\hat{\psi}_T}{d\lambda^2}$$
$$+ \left(\frac{\beta}{U_*} - \mu^2 - \delta^2\right)h^2\frac{d\hat{\psi}_T}{d\lambda} - \frac{F\mu^2h^3}{U_*}\hat{\psi}_T = -\frac{f_oh^2}{p_4}\left(1 - \frac{1.6U_T}{U_*}\right)\frac{d\hat{p}_g}{d\lambda} - \frac{4Rf_oh^3}{c_p\sigma_2p_4^2U_*}\hat{H} \qquad (3.3b)$$

where $\delta^2 = (8f_o^2)/(\sigma_2 p_4^2)$ and $h = a \cos \phi_o$. To solve these equations for $\hat{\psi}_*$ and $\hat{\psi}_T$ we expand $\hat{\psi}_*$, $\hat{\psi}_T$, $\hat{p}_g$, and $\hat{H}$ in Fourier series as in (2.19). The sinusoidal functions are not the eigenfunctions of the differential operators in (3.3) but they are convenient here since they satisfy the periodicity condition in λ.

When the expansions (2.19) are substituted into (3.3) no difficulty arises until the terms containing $F(\lambda)$ are encountered. These terms are treated as described in the following example. Consider the term $\frac{F\mu^2 h^3}{2U_*}\psi_*$ in (3.3a). Let

$$F(\lambda)\hat{\psi}_*(\lambda) = \sum_{n=1}^{N} (g_n \cos(n\lambda) + h_n \sin(n\lambda)) \tag{3.4}$$

where

$$g_n = \frac{1}{\pi}\int_0^{2\pi} F(\lambda)\hat{\psi}_*(\lambda) \cos(n\lambda)d\lambda \tag{3.5a}$$

and

$$h_n = \frac{1}{\pi}\int_0^{2\pi} F(\lambda)\hat{\psi}_*(\lambda) \sin(n\lambda)d\lambda. \tag{3.5b}$$

We recall from (2.19c) that

$$\psi_*(\lambda) = \sum_{k=1}^{N} (A_k^* \cos(k\lambda) + B_k^* \sin(k\lambda)) \tag{3.6}$$

in which, for convenience, we have replaced the dummy index of summation n by the index k. Substituting (3.6) into (3.5a) and interchanging the summation over k and the integral over λ, we obtain

$$g_n = \frac{1}{\pi} \sum_{k=1}^{N} A_k^* \int_0^{2\pi} F \cos(k\lambda) \cos(n\lambda) d\lambda + \frac{1}{\pi} \sum_{k=1}^{N} B_k^* \int_0^{2\pi} F \sin(k\lambda) \cos(n\lambda) d\lambda \tag{3.7}$$

or

$$g_n = \sum_{k=1}^{N} c_{k,n} A_k^* + \sum_{k=1}^{N} e_{k,n} B_k^* \tag{3.8}$$

where

$$c_{k,n} = \frac{1}{\pi} \int_0^{2\pi} F(\lambda) \cos(k\lambda) \cos(n\lambda) d\lambda \tag{3.9a}$$

and

$$e_{k,n} = \frac{1}{\pi} \int_0^{2\pi} F(\lambda) \sin(k\lambda) \cos(n\lambda) d\lambda \, . \tag{3.9b}$$

Similarly, we find that

$$h_n = \sum_{k=1}^{N} j_{k,n} A_k^* + \sum_{k=1}^{N} q_{k,n} B_k^* \tag{3.10}$$

where

$$j_{k,n} = \frac{1}{\pi} \int_0^{2\pi} F(\lambda) \cos(k\lambda) \sin(n\lambda) d\lambda \tag{3.11a}$$

and

$$q_{k,n} = \frac{1}{\pi} \int_0^{2\pi} F(\lambda) \sin(k\lambda) \sin(n\lambda) d\lambda \, . \tag{3.11b}$$

We note that once $F(\lambda)$ is specified the integrals in (3.9) and (3.11) can be evaluated, at least numerically, and hence the factors $c_{k,n}$, $e_{k,n}$, $j_{k,n}$, and $q_{k,n}$ appearing in (3.8) and (3.10) can be considered known. If we now substitute (3.8) and (3.10) into (3.4) we find that the product $F(\lambda)\psi_*(\lambda)$

can be written in terms of the basic unknowns A_1^*, $A_2^*,\ldots,A_N^*$ and B_1^*, $B_2^*,\ldots,B_N^*$ as follows:

$$F(\lambda)\hat{\psi}_*(\lambda) = \sum_{n=1}^{N}\left\{\left[\sum_{k=1}^{N} c_{k,n}A_k^* + \sum_{k=1}^{N} e_{k,n}B_k^*\right]\cos(n\lambda) + \left[\sum_{k=1}^{N} j_{k,n}A_k^* + \sum_{k=1}^{N} q_{k,n}B_k^*\right]\sin(n\lambda)\right\}. \tag{3.12}$$

The terms of the form $F(\lambda)d^2\hat{\psi}_*/d\lambda^2$ appearing in (3.3) can be treated in a similar manner without added difficulty.

If we treat the terms containing $F(\lambda)$ in (3.3) by the method described above and substitute for $\hat{\psi}_*$, $\hat{\psi}_T$, $\hat{p}_g$, and $\hat{H}$ from (2.19) in the terms with constant coefficients, we obtain, after some manipulation,

$$\alpha_n A_n^* + \gamma_n A_n^T = -JT_n \tag{3.13a}$$

$$\alpha_n B_n^* + \gamma_n B_n^T = JQ_n \tag{3.13b}$$

$$\sum_{k=1}^{N}\alpha_n X_{k,n}A_k^* + \sum_{k=1}^{N}\alpha_n Y_{k,n}B_k^* + \sum_{k=1}^{N}(\xi_{k,n}-1.6\alpha_n X_{k,n})A_k^T - \sum_{k=1}^{N}1.6\alpha_n Y_{k,n}B_n^T = \alpha_n nKR_n - a_n JT_n \tag{3.13c}$$

$$\sum_{k=1}^{N}\alpha_n Z_{k,n}A_k^* + \sum_{k=1}^{N}\alpha_n W_{k,n}B_k^* - \sum_{k=1}^{N}1.6\alpha_n Z_{k,n}A_k^T - \sum_{k=1}^{N}(\xi_{k,n}-1.6\alpha_n W_{k,n})B_k^T = -\alpha_n nKS_n - a_n JQ_n \tag{3.13d}$$

for $1 \le n \le N$, where

$$\alpha_n = n^3\left(1 + \frac{U_T}{U_*}\right) - nh^2\left[\frac{\beta}{U_*} - \mu^2 + \frac{U_T}{U_*}(\delta^2-\mu^2)\right] \tag{3.14}$$

$$\gamma_n = n^3\left(1 + \frac{U_T}{U_*}\right) - nh^2\left[\frac{\beta}{U_*} - \delta^2 - \mu^2\left(1 + \frac{U_T}{U_*}\right)\right] \tag{3.15}$$

$$h = a \cos \phi_o$$

$$J = \frac{4Rf_o h^3}{c_p \sigma_2 p_4^2 U_*} \tag{3.16}$$

$$K = \frac{f_o h^2}{p_4}\left(1 - \frac{1.6U_T}{U_*}\right) \tag{3.17}$$

$$\xi_{k,n} = n^2\left\{\left[n^2 - \left(\frac{\beta}{U_*} - \mu^2\right)h^2\right]\left[n^2 - \left(\frac{\beta}{U_*} - \mu^2 - \delta^2\right)h^2\right] - \left(\frac{U_T}{U_*}\right)^2 (x)\left[n^2 - (\delta^2 - \mu^2)h^2\right]\left[n^2 + \mu^2 h^2\right]\right\} \tag{3.18a}$$

if $k = n$, or

$$\xi_{k,n} = 0 \quad \text{if} \quad k \neq n \tag{3.18b}$$

$$W_{k,n} = r_k e_{k,n} \tag{3.19}$$

$$X_{k,n} = r_k j_{k,n} \tag{3.20}$$

$$Y_{k,n} = r_k q_{k,n} \tag{3.21}$$

$$Z_{k,n} = r_k c_{k,n} \tag{3.22}$$

$$r_k = \frac{h}{2U_*}\left(k^2 + \mu^2 h^2\right). \tag{3.23}$$

We note that there are $4N$ unknowns in (3.13), namely, A_n^*, B_n^*, A_n^T, and B_n^T for the integral values of n in the range $1 \leq n \leq N$. Contrary to the case where F is a constant, the $4N$ unknowns here can be obtained only by solving the system of $4N$ algebraic equations implied in (3.13) since both (3.13c) and (3.13d) contain all the unknowns. Of course, in the special case where F is a constant the system (3.13) reduces to the system (2.20), in which case the procedure consists in solving N systems of four equations in four unknowns rather than one system of $4N$ equations in $4N$ unknowns.

In spite of the rather complex nature of (3.13) it is possible to deduce at least two properties of the eddies forced by the topography without solving the system of $4N$ equations explicitly. The first property relates to the phase relationship between the $\hat{\psi}_*(\lambda)$ and $\hat{\psi}_T(\lambda)$ waves. It follows from (3.13a) and (3.13b) with $T_n = Q_n = 0$ that

$$\frac{B_n^*}{A_n^*} = \frac{B_n^T}{A_n^T} \tag{3.24}$$

The nth component of $\hat{\psi}_*$ is therefore either (a) exactly in phase or (b) exactly half a wavelength out of phase with the nth component of $\hat{\psi}_T$ (see (2.23)). Furthermore, since the eddy heat transport across a latitude circle is proportional to the integral

$$I = \int_0^{2\pi} \hat{\psi}_T \frac{\partial \hat{\psi}_*}{\partial \lambda} \, d\lambda$$

which here is equal to zero whether the alternative (a) or (b) holds true, we conclude that the topographically induced standing waves in our model do not transport heat in the meridional direction. This conclusion, we empha-

size, is valid for any distribution of the friction coefficient.

We can also show from (3.13a) and (3.13b) that the various Fourier components of the topographically induced stream function amplify or damp with height in a manner which is independent of the function $F(\lambda)$. Since the nth components of $\hat{\psi}_*$ and $\hat{\psi}_T$ have the form

$$\hat{\psi}_{*n} = A_n^* \cos(n\lambda) + B_n^* \sin(n\lambda)$$

and

$$\hat{\psi}_{Tn} = A_n^T \cos(n\lambda) + B_n^T \sin(n\lambda)$$

it follows from (2.21) that the amplitude ratio A, defined as in Chapter 2, is given by

$$A_n = \left[\frac{(A_n^* + A_n^T)^2 + (B_n^* + B_n^T)^2}{(A_n^* - A_n^T)^2 + (B_n^* - B_n^T)^2} \right]^{1/2} . \qquad (3.25)$$

Using (3.24) and the relation

$$A_n^{*2} + B_n^{*2} = \left(\frac{\gamma_n}{\alpha_n}\right)^2 (A_n^{T2} + B_n^{T2})$$

which also follows from (3.13a) and (3.13b), it is easy to rewrite (3.25) as

$$A_n = \frac{\alpha_n - \gamma_n}{\alpha_n + \gamma_n} . \qquad (3.26)$$

Since both α_n and γ_n are independent of $F(\lambda)$ we conclude that in the case of topographically induced perturbations in our model each Fourier component of the stream function has an amplitude ratio which does not depend on the distribution of the friction coefficient. Figure 5 is therefore valid whether or not F is constant.

In the following we shall prescribe a distribution of the friction coefficient and seek the solution to (3.13) using the same surface topography and diabatic heating as in the previous section.

Since the friction coefficient $F(\lambda)$ enters the computations only through the integrals in (3.9) and (3.11) we can solve the standing wave problem with a simple or complicated function $F(\lambda)$ without added difficulty provided that we evaluate the integrals numerically. In view of our limited knowledge about $F(\lambda)$ we consider only simple cases in which $F = F_o$, a constant, over the oceans and $F = F_c$, another constant, over the continents. Thus we assume that the distribution

$$F = F_c \text{ for } 0 \leq \lambda \leq 145°E$$

$$F = F_o \text{ for } 145°E < \lambda \leq 120°W$$

$$F = F_c \text{ for } 120°W < \lambda \leq 60°W$$

$$F = F_o \text{ for } 60°W < \lambda < 0$$

is sufficiently realistic for our purposes.

We consider the response of the model atmosphere to the combined effect of the diabatic heating and the topography using three separate pairs F_o and F_c. First we solve (3.13) with $F_o = F_c = 4 \times 10^{-6}$ sec^{-1}, as in the previous section, to provide a basis of comparison for the other cases where $F_o \neq F_c$. We then obtain the solution to (3.13) with $F_c/F_o = 2$, choosing F_c and F_o in such a way as to keep the zonal average of F equal to 4×10^{-6} sec^{-1}. Finally we use the ratio $F_c/F_o = 6$, again selecting F_c and F_o so that the zonal average of F is 4×10^{-6} sec^{-1}. In all cases the computations are made with

N = 10, although tests have shown that N could have been set equal to five without appreciable effects on the results. Except for F and N, the parameters were assigned the same values as in the previous section, that is, $U_* = 15$ m sec^{-1}, $U_T = 5$ m sec^{-1}, $\mu = 0.95 \times 10^{-6}$ m^{-1}, $\sigma_2 = 3$ m^4 sec^2 t^{-2}.

Figure 14 shows the heights of the 25, 50, and 75 cb surfaces as functions of longitude for the cases $F_c/F_o = 2$ (thin solid lines), F = constant (dashed lines) together with the observed heights averaged between 30°N and 60°N. Changing the distribution of the friction coefficient from F = constant to $F_c/F_o = 2$ has similar effects at all levels, namely, raising the height values from about 100°E eastward to 80°W and decreasing them over the rest of the domain. Thus the trough near 140°E becomes somewhat less deep while the ridge near 120°W and the trough near 60°W become more pronounced. The change in F by a factor of two from oceans to continents does not produce radical changes in the solution for the standing waves but on the other hand it should be noticed that the small changes are such as to bring the computed and observed standing waves into somewhat better agreement than in the case of a constant friction coefficient.

Figure 15 differs from Figure 14 only in that its thin solid curves show the standing eddies computed with $F_c/F_o = 6$ instead of $F_c/F_o = 2$. The effects of the variations in F on the standing eddies are of the same general nature as those discussed above, but appreciably stronger. Again the effects of the variable F are felt predominantly on the scale of wave number one since the height values are raised from about 100°E eastward to 80°W (i.e., 180 degrees of longitude) and lowered from about 80°W eastward to 100°E.

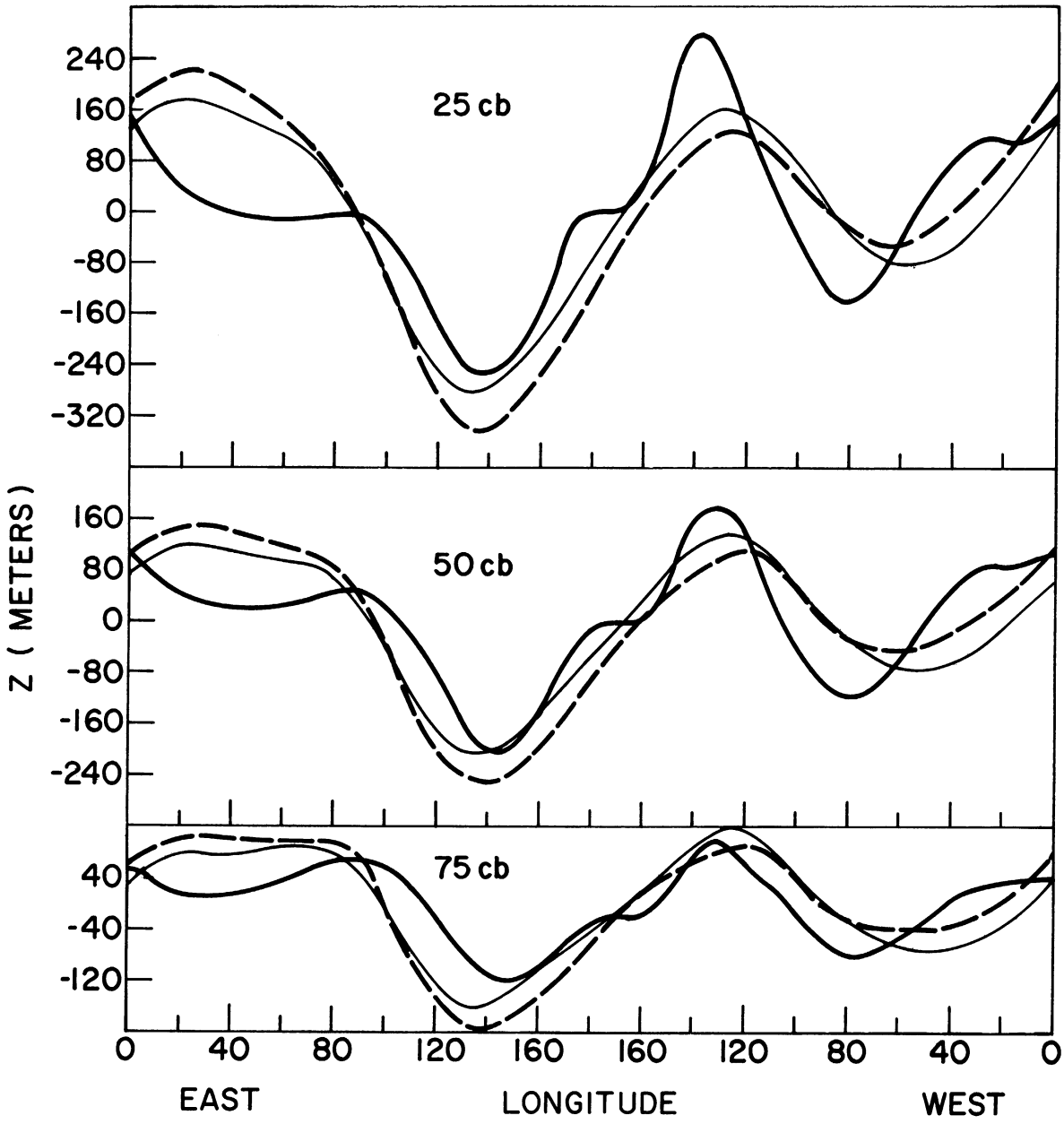

Fig. 14. The perturbation heights of the 25, 50, and 75 cb surfaces as they are (a) observed (thick solid curve), (b) computed as a response to the forcing by the topography and diabatic heating with $F_C/F_O = 1$ (dashed curve) and (c) computed as in (b) but with $F_C/F_O = 2$. The other parameters are as in Fig. 2.

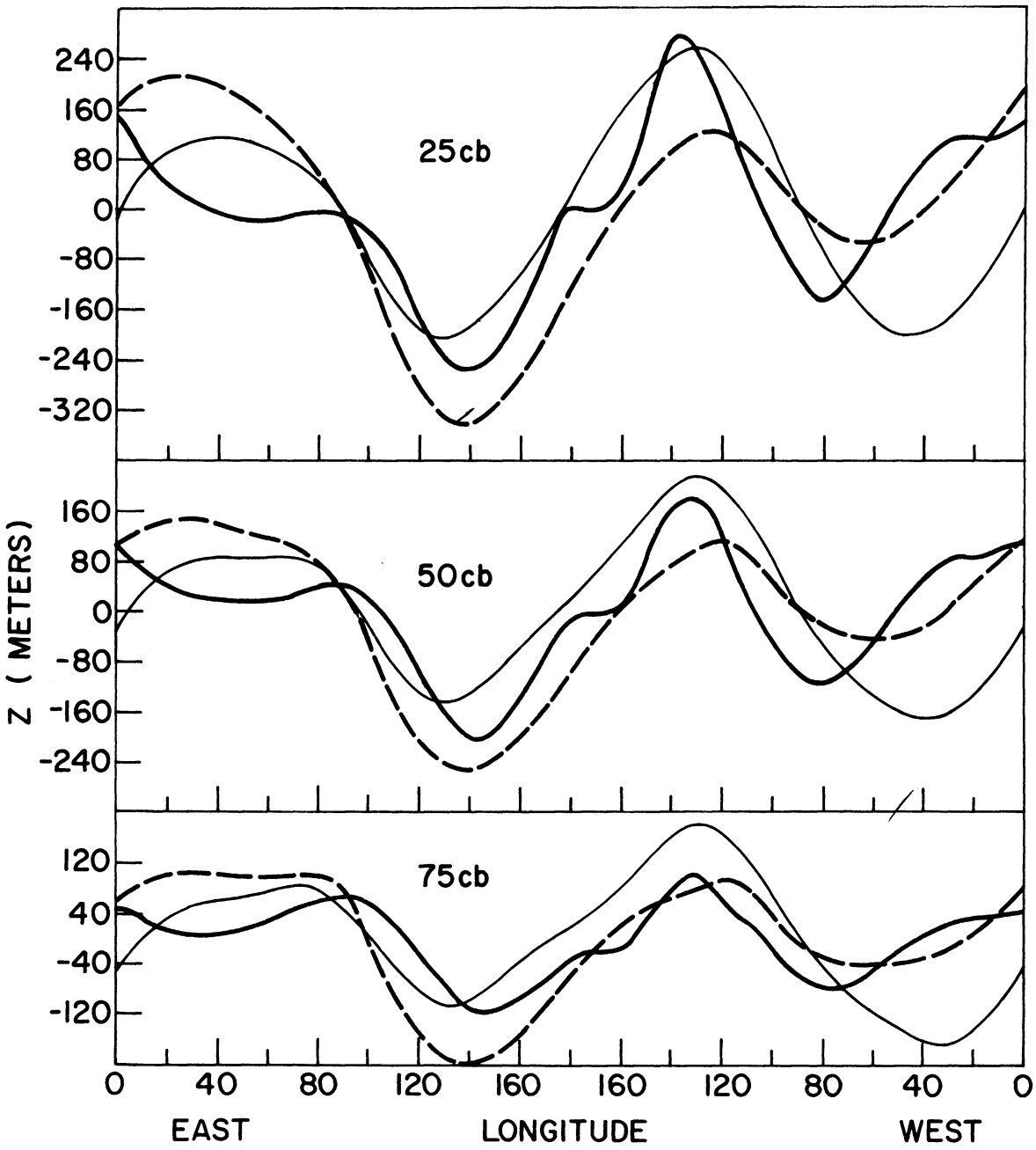

Fig. 15. Same as in Fig. 14 except that for the thin solid curve $F_C/F_O = 6$.

We conclude from the results of this section that if the ratio $F_c/F_o = 2$ is more nearly valid than the ratio $F_c/F_o = 6$ the modifications effected by the variable F can be neglected in the standing wave problem; if the latter ratio is more appropriate than the former, however, the variations in F must be included.

It is helpful at this point to consider the formulation of the friction coefficient F as given by Charney and Eliassen (1949) and to investigate what a given ratio F_c/F_o implies about the flow in the boundary layer over the oceans as compared to that over the continents. Charney and Eliassen (loc. cit.) have shown that F is given by

$$F = \frac{\sin(2\alpha)}{H}\left[\frac{Kf}{2}\right]^{1/2} \tag{3.27}$$

where α is the angle between the isobars and the surface wind, K is the coefficient of eddy viscosity and H is the height of the homogeneous atmosphere. On the average during the winter the air in the boundary layer over the oceans has a somewhat lower static stability than that over the continents since the oceans tend to warm the lower layers of the atmosphere while the continents cool them. This effect tends to make K larger over the oceans than over the continents but on the other hand the greater roughness of the continents tends to have the opposite effect. As a first approximation it appears reasonable, then, to neglect the variations of K with longitude. With this assumption we find that the typical angles $\alpha = \alpha_c$ over the continents and $\alpha = \alpha_o$ over the oceans are related as follows:

$$\frac{F_o}{F_c} = \frac{\sin(2\alpha_o)}{\sin(2\alpha_c)} \quad . \tag{3.28}$$

According to Sutton (1953), α_c has an average value of about 20°. If we were to assume that $F_c/F_o = 6$ we would find that $\alpha_o = 3°$, which is far lower than the observed average value of about 13° (Sutton (1953), pp. 245-246). On the other hand, with a ratio of $F_c/F_o = 2$ we obtain a value of $\alpha_o = 9°$ which is more nearly in agreement with observations. According to the above argument it appears that for January the ratio $F_c/F_o = 2$ is more appropriate than the ratio $F_c/F_o = 6$ so that as a first approximation the variations of F with longitude can be neglected in the standing wave problem.

3.3 SOME EFFECTS OF TRUNCATION IN THE MERIDIONAL PLANE

We have so far assumed that the speed of the basic zonal current is independent of the y coordinate and that all the perturbation quantities have a single meridional wavelength. In this section we shall generalize the model somewhat to allow the basic zonal wind to vary with latitude. In this case the differential equations governing the forced perturbations have coefficients which depend on y so that we cannot assume a simple periodicity in y for both the forcing functions and the dependent variables. For simplicity we shall again make use of the β-plane approximation and replace the periodic boundary conditions in y by the requirement that the perturbation stream function be identically zero along two given latitude circles; this is equivalent to the assumption that the β plane is bounded in the north and south by

solid vertical walls. We shall assume that the walls are located at 30°N and 60°N so that the width of the channel is equal to the half wavelength of the single effective meridional mode previously used.

The perturbation equations for the case where U_* and U_T are functions of y can be obtained by simply subtracting the expressions

$$\left(\frac{d^2U_*}{dy^2}\frac{\partial\psi_*}{\partial x} + \frac{d^2U_T}{dy^2}\frac{\partial\psi_T}{\partial x}\right)$$

and

$$\left(\frac{d^2U_T}{dy^2}\frac{\partial\psi_*}{\partial x} + \frac{d^2U_*}{dy^2}\frac{\partial\psi_T}{\partial x}\right)$$

from the left-hand sides of (2.17a) and (2.17b), respectively. When the expansions (2.19) are generalized so that the left-hand sides are $p_g(\lambda,y)$, $H(\lambda,y)$, $\psi_*(\lambda,y)$, $\psi_T(\lambda,y)$ and the coefficients on the right-hand sides are functions of y, we find that the differential equations for the coefficients $A_n^*(y)$, $B_n^*(y)$, $A_n^T(y)$, and $B_n^T(y)$ take the form

$$\left(q_1\frac{d^2}{dy^2} - q_2 + \xi_3\right)A_n^* + \left(\xi_3 - \xi_4\frac{d^2}{dy^2}\right)B_n^* + \left(q_3\frac{d^2}{dy^2} - q_4\right)A_n^T + 1.6\left(\xi_4\frac{d^2}{dy^2} - \xi_5\right)B_n^T = bR_n(y) \qquad (3.29a)$$

$$\left(\xi_4\frac{d^2}{dy^2} - \xi_5\right)A_n^* + \left(q_1\frac{d^2}{dy^2} - q_2 + \xi_3\right)B_n^* + 1.6\left(\xi_5 - \xi_4\frac{d^2}{dy^2}\right)A_n^T + \left(q_3\frac{d^2}{dy^2} - q_4\right)B_n^T = bS_n(y) \qquad (3.29b)$$

$$(q_3 \frac{d^2}{dy^2} - q_5)A_n^* + (\xi_4 \frac{d^2}{dy^2} - \xi_5)B_n^* + (q_1 \frac{d^2}{dy^2} - q_6 + \xi_3)A_n^T - 1.6(\xi_4 \frac{d^2}{dy^2} - \xi_5)B_n^T$$

$$= -bR_n(y) + \xi_2 T_n(y) \qquad (3.29c)$$

$$(\xi_4 \frac{d^2}{dy^2} - \xi_5)A_n^* - (q_3 \frac{d^2}{dy^2} + q_5)B_n^* - 1.6(\xi_4 \frac{d^2}{dy^2} - \xi_5)A_n^T - (q_1 \frac{d^2}{dy^2} - q_6 + \xi_3)B_n^T$$

$$= bS_n(y) + \xi_2 Q_n(y) \qquad (3.29d)$$

where

$$q_1 = U_* h^2 n$$

$$q_2 = n(U_* n^2 + h^2 \frac{d^2 U_*}{dy^2})$$

$$q_3 = U_T h^2 n$$

$$q_4 = n(U_T n^2 + h^2 \frac{d^2 U_*}{dy^2})$$

$$q_5 = n\left[U_T(n^2 - h^2\xi_1) + h^2 \frac{d^2 U_T}{dy^2}\right]$$

$$q_6 = n\left[U_*(n^2 + h^2\xi_1) + h^2 \frac{d^2 U_*}{dy^2}\right]$$

$$\xi_1 = (8f_o^2)/(\sigma_2 p_4^2)$$

$$\xi_2 = (4f_o R h^3)/(c_p \sigma_2 p_4^2)$$

$$\xi_3 = \beta h^2 n$$

$$\xi_4 = Fh^3/2$$

$$\xi_5 = Fh^2 n^2/2$$

$$b = \frac{f_o h^2 n}{p_4}(U_* - 1.6U_T)$$

The Fourier coefficients $R_n(y)$, $S_n(y)$, $Q_n(y)$, and $T_n(y)$ appearing in (3.29) were evaluated at intervals of five degrees of latitude between 30°N and 60°N for $1 \leq n \leq 5$. The system (3.29) was then solved numerically using intervals of five degrees of latitude and the boundary conditions $A_n^* = B_n^* = A_n^T = B_n^T = 0$ at 30°N and 60°N. The mean and thermal stream functions were then obtained from the generalized form of (2.19) and the 50 cb perturbation height field was computed from (2.3), (2.14), and (2.21).

The computations were first performed using $U_* = 15$ m sec^{-1} and $U_T = 5$ m sec^{-1} between 30°N and 60°N and then repeated using the observed geostrophic winds U_* and U_T shown in Table 1. The results for these cases appear in Figs. 16 and 17, respectively; the observed distribution of the perturbation height is shown in Fig. 18. The results of Fig. 16 are an extension of those in Fig. 13 in the sense that they show the response to several meridional modes in the heating and topography instead of only one. The response in Fig. 16 has most of its relative maxima and minima at 45°N, indicating that the meridional mode with a half wavelength of 30 degrees of latitude is the dominant one.

TABLE 1

THE OBSERVED VALUES OF U_* AND U_T FOR JANUARY 1962

Latitude	30	35	40	45	50	55	60
U_*(m sec^{-1})	21.3	19.6	17.5	16.3	14.8	13.0	11.0
U_T(m sec^{-1})	14.8	12.1	9.6	7.4	6.0	5.4	4.6

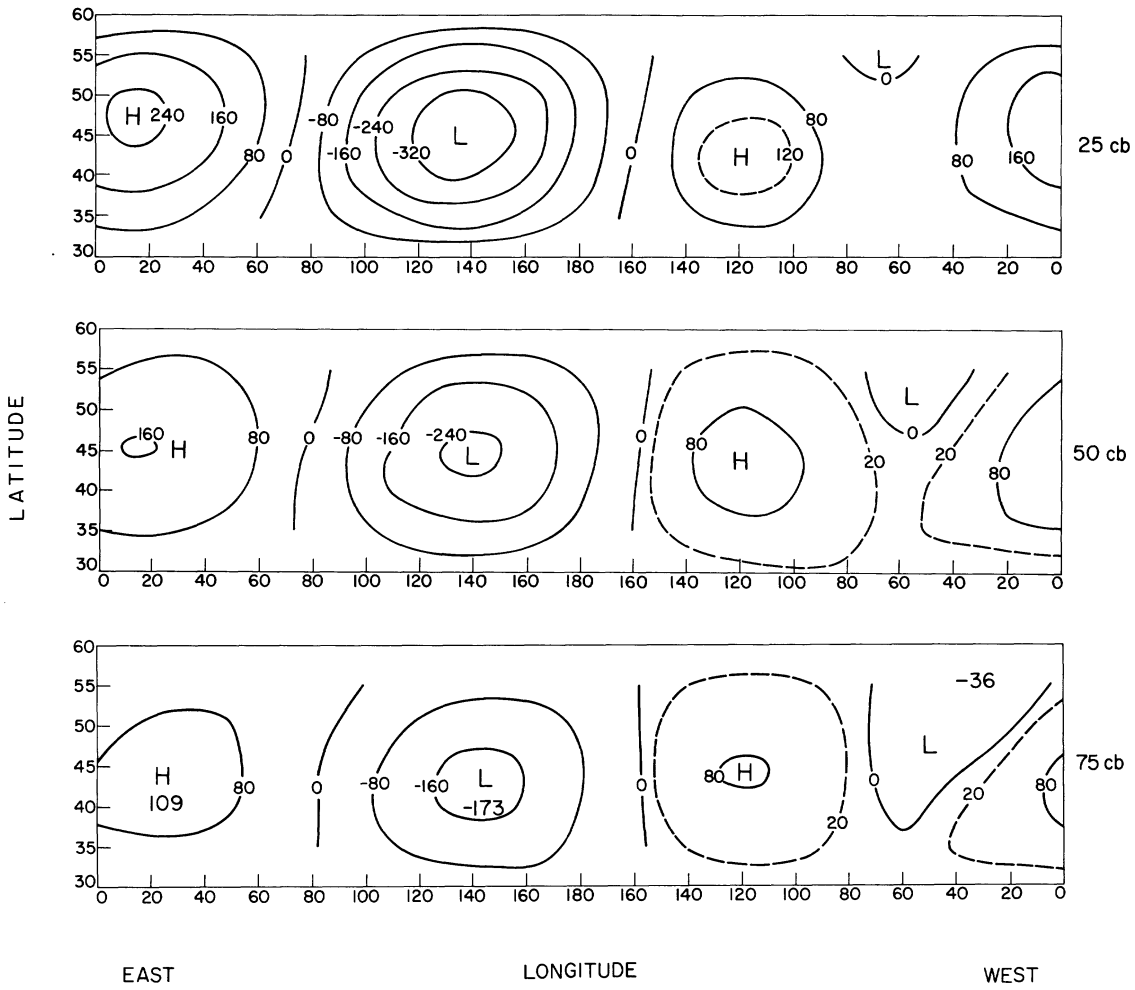

Fig. 16. The perturbation height field in meters computed as a response to the first five zonal Fourier components of the topography and diabatic heating between 30°N and 60°N. Parameters: $U* = 15$ m sec^{-1}, $U_T = 5$ m sec^{-1}, $F = 4 \times 10^{-6}$ sec^{-1}.

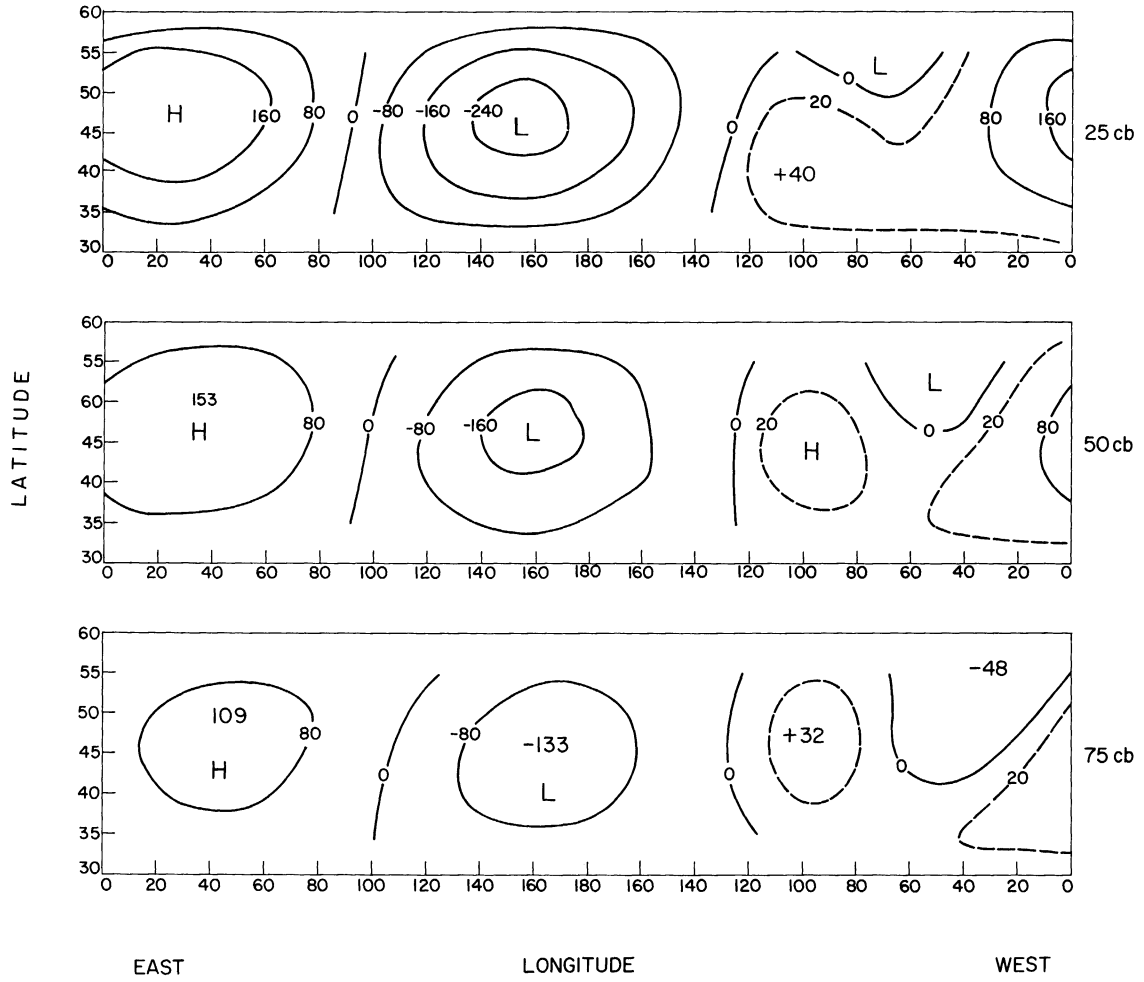

Fig. 17. Same as in Fig. 16 except that U* and U_T are as shown in Table 1.

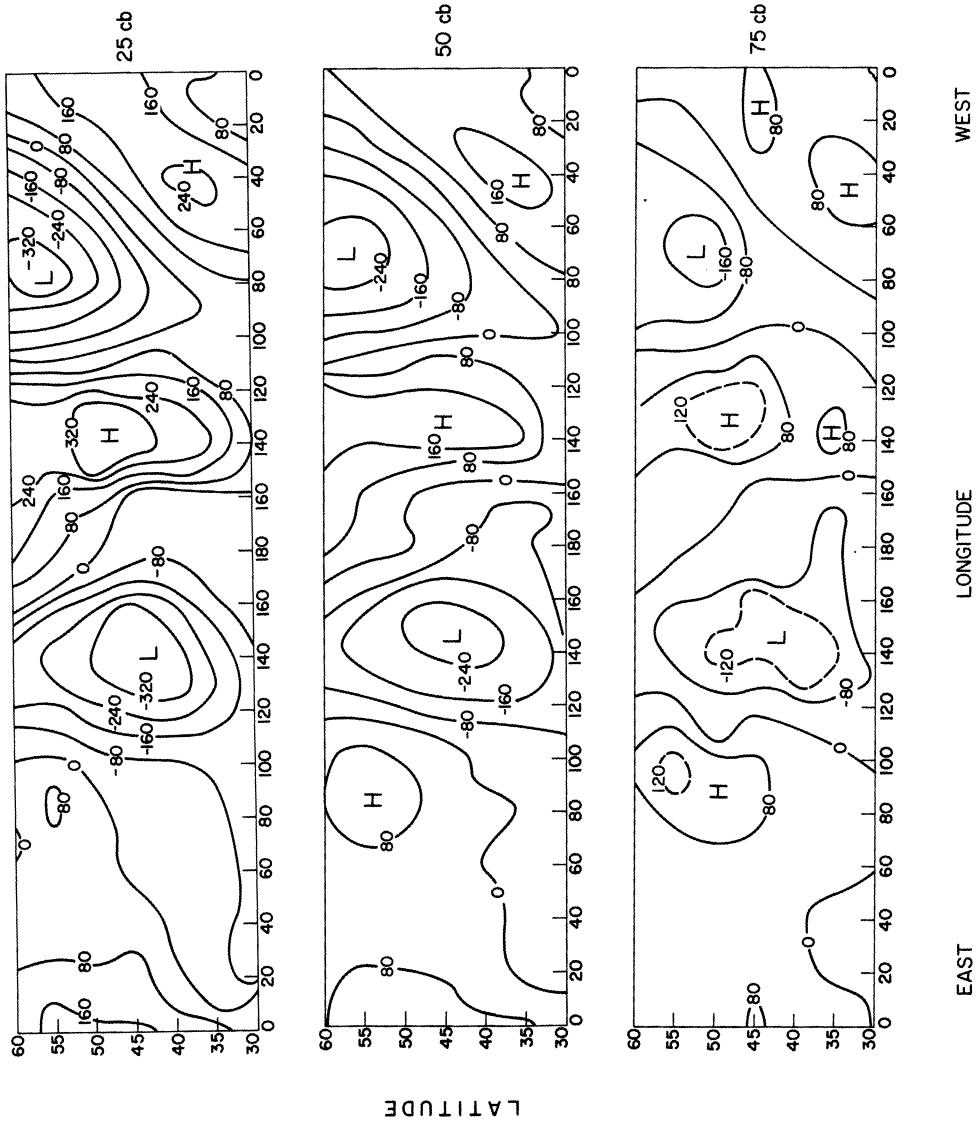

Fig. 18. The observed distribution of the standing eddies in the height field (in meters) for January 1962.

The effect of the higher meridional harmonics is felt most strongly near 60°W where the relative minimum is located at 55°N at all levels. Judging from Fig. 18, this is a desirable effect since the observed trough near 70°W also reaches its deepest value at 55°N at the middle and upper levels and at 50°N at 75 cb. We note also that the trough line near 60°W at both 75 and 50 cb slopes from the north-east to the south-west, just as the observed one at the same levels; this feature could not have been obtained without the superposition of at least two meridional modes. We note also that the computed perturbations slope slightly to the west with height, just as the observed ones.

By comparing Figs. 16 and 17 we see that changing the zonal wind from $U_* = 15$ m sec^{-1} and $U_T = 5$ m sec^{-1} to the values shown in Table 1 results in a general reduction of the perturbation amplitudes and in a slight eastward shift of the perturbations. It appears then that within the framework of the β-plane approximation the observed variation of the zonal wind with latitude does not produce drastic changes in the forced perturbations.

3.4 CRITICAL REMARKS

The model used in Section 3.3 is somewhat more general than the one used in Section 3.1 in the sense that the perturbations are not forced to have a single meridional wave number. On the other hand the model still contains the undesirable feature that the width of the channel is arbitrary. The choice of 30° for the width was made here so that one meridional mode would have the same wavelength as the single meridional mode used previously, thus providing some continuity in the models. Unfortunately some test computa-

tions have shown that the response of the model atmosphere to either the topography or the diabatic heating changes noticeably when the width of the channel is increased to 50 degrees of latitude. It is clear that in the future we should attempt to remove the arbitrariness in the choice of the width of the channel by abandoning the β-plane approximation in favor of a more general formulation in spherical coordinates.

In view of the above remarks the results of this chapter should be considered with some caution. It might be argued, for example, that the results shown in Fig. 13 are reasonably good because the chosen value of μ permits the most easily excited modes ($n = 2$ in Fig. 2 and $n = 1$ in Fig. 6) to be those for which large amplitudes are found in the observed standing waves. This may be the case but it remains a fact that the model places the standing waves in very nearly the same position as the observed ones, a feature which could not have been obtained simply through a fortunate choice of μ.

CHAPTER 4

THE MAINTENANCE OF THE AXISYMMETRIC REGIME

4.1 PRELIMINARY REMARKS

One of the important problems that meteorologists face in developing a theory of climates consists in explaining how the axisymmetric part of the general circulation is maintained against the dissipative forces. It has become clear during the last two decades that while the radiative processes provide the fundamental mechanism through which the atmosphere receives the solar energy, the large-scale eddies play a vital role in redistributing the energy in the north-south direction, thus affecting the axisymmetric component of the flow. Several observational studies (see, for example, Wiin-Nielsen, Brown, and Drake (1963), (1964)) have shown, in particular, that the eddies transport internal energy from the low latitudes, where the radiative processes tend to increase the internal energy of the air, to the high latitudes where the radiative processes tend to decrease the internal energy. It is also observed that the same eddies tend to transport zonal momentum from the low and high latitudes to the middle latitudes, thus helping to maintain the kinetic energy of the jet stream against the dissipative forces and also playing a role in determining the speed of the zonal current in the low and high latitudes.

In the following we shall show that the quasi-geostrophic equations can be written in such a way as to permit a simple analysis of the contribution by the eddies to the maintenance of the time-averaged axisymmetric component

of the flow. The approach differs from that of Adem (1962), Williams and Davies (1965), and Saltzman (1967) mainly in that our treatment of the diabatic heating is simplified compared to theirs and in that we consider the eddy heat and momentum transports to be known from observations rather than try to parameterize them in terms of the axisymmetric variables. It is hoped that the present study can shed additional light on the role of the eddies in the atmosphere and help in future attempts at parameterizing their effects.

4.2 THE MODEL EQUATIONS

Since the large-scale flow in the free atmosphere is observed to be nearly geostrophic, we shall make use of the quasi-geostrophic formulation of the hydrodynamic equations. Also, since we are interested in the meridional, as well as vertical, variations in the axisymmetric regime, we shall write the appropriate equations in terms of a spherical coordinate system where λ, ϕ, and p are the longitude, latitude, and pressure, respectively.

As mentioned in Chapter 1, we shall use the steady state boundary value problem approach. The time dependence will be removed from the equations by averaging them with respect to time over a period of one year and assuming that all yearly averaged quantities are time independent. If we use a bar over a symbol to designate its annual mean value, that is

$$\overline{(\ )} = \frac{1}{\tau} \int_{t_o}^{t_o+\tau} (\ )\,dt \qquad (4.1)$$

where t_o is some fixed time and τ = 1 year, we can write the time-averaged first equation of motion as

$$\overline{\frac{u}{a\cos\phi}\frac{\partial u}{\partial\lambda}} + \overline{\frac{v}{a}\frac{\partial u}{\partial\phi}} - \frac{\overline{uv}\tan\phi}{a} = -\frac{1}{a\cos\phi}\frac{\partial\bar{\Phi}}{\partial\lambda} + f\bar{v} + \bar{F} \qquad (4.2)$$

where F is the friction force per unit mass and the other symbols are defined previously. The vertical advection of momentum, $\omega\partial u/\partial p$, does not appear in (4.2) since we are using the quasi-geostrophic formulation.

Since the wind speed varies much more quickly in the vertical than in the horizontal, we shall neglect those contributions to F which arise from the horizontal variations of the wind speed and write

$$F = g^2\frac{\partial}{\partial p}\left(K\rho^2\frac{\partial u}{\partial p}\right) = \frac{g^2}{R^2}\frac{\partial}{\partial p}\left(\frac{p^2K}{T^2}\frac{\partial u}{\partial p}\right) \qquad (4.3)$$

where K is the coefficient of eddy viscosity, ρ is the density and T is the temperature. If we assume that K is a constant and note that T^2 varies only slowly with pressure, we can approximate (4.3) by

$$F = A\frac{\partial}{\partial p}\left(p^2\frac{\partial u}{\partial p}\right) \qquad (4.4a)$$

where

$$A = \frac{g^2K}{R^2\tilde{T}^2} = \text{constant} \qquad (4.4b)$$

and $\tilde{T}$ is some constant representative value of the temperature. The above formulation of the friction term is the same as that used by Robert (1966) in the time integration of his primitive equations model.

The procedure now consists in substituting (4.4a) into (4.2) and then taking the zonal average of the resulting equation. By making use of the fact that within the quasi-geostrophic theory only the nondivergent part of the wind is retained in the terms on the left-hand side of (4.2), it is then

possible to write the zonally averaged equation in the form

$$\frac{1}{a\cos^2\phi}\frac{\partial(M\cos^2\phi)}{\partial\phi} = f_o\bar{v}_z + A\frac{\partial}{\partial p}\left(p^2\frac{\partial\bar{u}_z}{\partial p}\right) \tag{4.5}$$

where

$$M(p,\phi) = (\overline{u_E v_E})_z \tag{4.6}$$

is assumed known from observations. The subscript z denotes the zonal average of the quantity, that is,

$$(\ )_z = \frac{1}{2\pi}\int_o^{2\pi}(\ )d\lambda \tag{4.7}$$

and the subscript E denotes the deviation from the zonal average, that is, the eddy component,

$$(\ )_E = (\ ) - (\ )_z .$$

Thus M represents the horizontal eddy transport of momentum, averaged with respect to time and longitude.

Within the framework of the quasi-geostrophic theory we can use the thermal wind equation

$$\frac{\partial u_z}{\partial p} = \frac{R}{af_o p}\frac{\partial T_z}{\partial\phi} \tag{4.8}$$

to write (4.5) in the form

$$\frac{1}{a\cos^2\phi}\frac{\partial(M\cos^2\phi)}{\partial\phi} = f_o\bar{v}_z + \frac{AR}{af_o}\frac{\partial}{\partial p}\left(p\frac{\partial\bar{T}_z}{\partial\phi}\right). \tag{4.9}$$

The thermodynamic equation, averaged with respect to time, can be written as

$$\overline{\frac{u}{a\cos\phi}\frac{\partial T}{\partial\lambda}} + \overline{\frac{v}{a}\frac{\partial T}{\partial\phi}} - S\bar{\omega} = \frac{\bar{H}}{c_p} \tag{4.10}$$

where

$$S = S(p) = \frac{R}{c_p}\frac{T_s}{p} - \frac{dT_s}{dp} \tag{4.11}$$

is a measure of the static stability. T_s is the temperature in some standard reference atmosphere and is a function of the pressure only (see Phillips (1963)). For any pressure level p the value of T_s could be obtained, for example, by averaging the observed temperature over the closed surface $0 \le \lambda \le 2\pi$, $-\pi/2 \le \phi \le \pi/2$ and over a long period of time, say one year. This means that we can define $T_s(p)$ as

$$T_s(p) = \frac{1}{2}\int_{-\pi/2}^{\pi/2} \bar{T}_z(p)\cos\phi\, d\phi$$

or

$$T_s(p) = \int_{0}^{\pi/2} \bar{T}_z(p)\cos\phi\, d\phi \tag{4.12}$$

if, as will be done in the following, T_z is assumed to be symmetric about the equator. In a quasi-geostrophic formulation T_s must be specified and therefore with our present model we cannot expect to obtain the area average of T, that is, the average of $\bar{T}_z$ (weighted by $\cos\phi$) between the pole and equator. We shall show, on the other hand, that we can determine how $\bar{T}_z$ changes with latitude at a number of pressure levels.

If we take the zonal average of (4.10) and note that in the quasi-geostrophic formulation the temperature field is advected horizontally by the nondivergent part of the wind only, we find that the resulting equation can be written as

$$\frac{1}{a \cos \phi} \frac{\partial(N \cos \phi)}{\partial \phi} - S\bar{\omega}_z = \frac{\bar{H}_z}{c_p} \tag{4.13}$$

where

$$N(p,\phi) = (\overline{v_E T_E})_z \tag{4.14}$$

is proportional to the meridional eddy transport of sensible heat, averaged with respect to longitude and time. In the following, N will be assumed to be known from observations.

We consider the diabatic heating to be Newtonian in form so that

$$\frac{\bar{H}_z}{c_p} = q(T_R - \bar{T}_z) \tag{4.15}$$

where $T_R(p,\phi)$ is the equilibrium temperature toward which the diabatic processes are driving the atmosphere and q is the heating or cooling coefficient. T_R can be considered to be the temperature that (hypothetically) would be established in the atmosphere in the absence of the large-scale motion but in the presence of radiation and small-scale convection. Charney (1959) has discussed a heating mechanism of the form (4.15) for an atmosphere which was assumed to be isothermal in the vertical, transparent to solar radiation and "gray" to terrestrial radiation. From his discussion we obtain a value of

0.34×10^{-6} sec^{-1} for q whereas Wiin-Nielsen, Vernekar, and Yang (1967) found a value of 0.4×10^{-6} sec^{-1} using the calculated value of the generation of eddy available potential energy from observations. Both of the above determinations of q are based on a two-level representation of the atmosphere with only one temperature value in a vertical column and do not indicate how q varies in the vertical. For lack of more adequate information a constant value of $q = 0.4 \times 10^{-6}$ sec^{-1} is used in the present study. The distribution of $T_R(p,\phi)$, assumed known, will be discussed at a later stage.

For convenience we substitute (4.15) into (4.13) to obtain the thermodynamic equation in the form

$$\frac{1}{a \cos \phi} \frac{\partial(N \cos \phi)}{\partial \phi} - S\bar{\omega}_z = q(T_R - \bar{T}_z) . \qquad (4.16)$$

The equations (4.9) and (4.16) have the unknowns $\bar{T}_z$, $\bar{v}_z$ and $\bar{\omega}_z$; to close the system we introduce the continuity equation which, after being integrated with respect to time and longitude, can be written as

$$\frac{1}{a \cos \phi} \frac{\partial(\bar{v}_z \cos \phi)}{\partial \phi} + \frac{\partial \bar{\omega}_z}{\partial p} = 0 . \qquad (4.17)$$

At this point we eliminate $\bar{v}_z$ and $\bar{\omega}_z$ from (4.9), (4.16), and (4.17) to obtain an equation in the single unknown $\bar{T}_z$. This is done by first multiplying (4.9) throughout by $\cos \phi$, applying the differential operator $\frac{1}{\cos \phi} \frac{\partial}{\partial \phi}$ to the resulting equation and then using (4.17) to eliminate the term containing $\bar{v}_z$. This yields the following equation relating $\bar{\omega}_z$ and T_z:

$$\frac{\partial \bar{\omega}_z}{\partial p} = -\frac{1}{a^2 f_o \cos\phi}\frac{\partial}{\partial\phi}\left(\frac{1}{\cos\phi}\frac{\partial(M\cos^2\phi)}{\partial\phi}\right) + \frac{AR}{a^2 f_o^2}\frac{1}{\cos\phi}\left[\cos\phi\frac{\partial}{\partial p}\left(p\frac{\partial \bar{T}_z}{\partial\phi}\right)\right].$$

We now integrate this equation from p = 0 to an arbitrary p using the boundary conditions

$$\bar{\omega} = 0 \quad \text{at} \quad p = 0$$

and

$$p\frac{\partial \bar{T}_z}{\partial\phi} = 0 \quad \text{at} \quad p = 0$$

the latter of which is equivalent to saying that the frictional stress vanishes at p = 0 (see (4.4a) and (4.8)). We can then eliminate $\bar{\omega}_z$ between the resulting equation and (4.16) to obtain the following differential equation for $\bar{T}_z$:

$$\frac{1}{\cos\phi}\frac{\partial}{\partial\phi}\left(\cos\phi\frac{\partial \bar{T}_z}{\partial\phi}\right) - \frac{qa^2 f_o^2}{ARSp}\bar{T}_z = \frac{a^2 f_o^2}{ARSp}G(p,\phi) \qquad (4.18a)$$

where

$$G(p,\phi) = -qT_R + \frac{1}{a\cos\phi}\frac{\partial(N\cos\phi)}{\partial\phi} + \frac{S}{a^2 f_o \cos\phi}\frac{\partial}{\partial\phi}\left(\frac{1}{\cos\phi}\frac{\partial(I\cos^2\phi)}{\partial\phi}\right) \qquad (4.18b)$$

and

$$I(p,\phi) = \int_o^p M(p,\phi)dp\ . \qquad (4.18c)$$

Since we have assumed T_R, N, M, and S to be known, it follows that the right-hand side of (4.18a) is known and therefore the problem now consists

in solving (4.18a) for $\bar{T}_z$ subject to the appropriate boundary conditions. For lack of information about the Southern Hemisphere we shall require symmetry in $\bar{T}_z$ about the equator thus providing the boundary condition

$$\frac{\partial T_z}{\partial \phi} = 0 \quad \text{at} \quad \phi = 0; \tag{4.19a}$$

the other boundary condition is provided by requiring

$$\bar{T}_z \text{ bounded at } \phi = \pi/2 \ . \tag{4.19b}$$

The solution $\bar{T}_z$ to (4.18a) can be obtained by expanding $G(p,\phi)$ as well as $\bar{T}_z$ itself in terms of the even Legendre polynomials P_n, that is,

$$\bar{T}_z(p,\phi) = \sum_{n=0}^{\infty} T_n(p) P_n(\sin \phi), \quad n \text{ even}, \tag{4.20a}$$

$$G(p,\phi) = \sum_{n=0}^{\infty} G_n(p) P_n(\sin \phi), \quad n \text{ even}. \tag{4.20b}$$

The choice of the even Legendre polynomials is appropriate here because they are the eigenfunctions of the differential operator on the left-hand side of (4.18a) and they satisfy the boundary conditions (4.19).

Substituting (4.20) into (4.18a) we obtain the following equation for the coefficients in the expansion of $\bar{T}_z$:

$$T_n(p) = -\frac{1}{q} \cdot \frac{m}{m+n(n+1)} \cdot G_n(p) \tag{4.21a}$$

where

$$m = m(p) = \frac{qa^2 f_o^2}{ARSp} \ . \tag{4.21b}$$

Formally the procedure to obtain $\bar{T}_z(p,\phi)$ consists in first computing the coefficients G_n in the expansion (4.20b) by means of the relation

$$G_n(p) = (2n+1) \int_0^{2\pi} G(p,\phi) P_n(\sin \phi) \cos \phi \, d\phi \qquad (4.22)$$

where $G(p,\phi)$ is known from observation and $P_n(\sin \phi)$ can be obtained from the recursion formula

$$nP_n(\sin \phi) + (n-1)P_{n-2}(\sin \phi) - (2n-1)\sin \phi \, P_{n-1}(\sin \phi) = 0$$

knowing that

$$P_o = 1$$

$$P_1 = \sin \phi \, .$$

Knowing the values of $G_n(p)$ we can find $T_n(p)$ by means of (4.21a) and finally $\bar{T}_z(p,\phi)$ by means of (4.20a). In the actual computations it was found sufficient to let the maximum value of n be 10 as the terms in the expansion (4.20a) decrease fairly rapidly in importance as n increases. To some extent this is due to the fact that the frictional mechanisn has introduced the factor n(n+1) as part of the denominator on the right-hand side of (4.21a). Thus the internal friction tends to damp preferentially those components of $\bar{T}_z$ in (4.20a) which have large values of n. It is also desirable to keep the maximum value of n relatively small since the function T_R in (4.18b) is available at intervals of 10 degrees of latitude only.

4.3 THE DATA

It is clear that to solve (4.18a) we need to know how the radiative equilibrium temperature T_R, the eddy heat transport N and the eddy momentum integral I vary with latitude at each pressure level p where we want to obtain $\bar{T}_z$. Of the three required functions, the eddy heat and momentum transports are by far the better known. The mean monthly values of the horizontal eddy momentum transport, averaged with respect to longitude, for the 12 months of 1963, were made available by Professor A. Wiin-Nielsen for the latitudes 20°N to 85°N at intervals of 2.5 degrees of latitude and for the pressure levels p = 10, 15, 20, 30, 50, 70, 85, and 100 cb except for January 1963 when the data at the levels p = 10, 15, and 100 cb were not available. At these three levels the momentum transport for January 1963 was computed using the assumption that the ratio of the missing momentum transport to the one at the closest level (also for January) where data are available is the same as the ratio of the momentum transports at the same two levels in February. The momentum transport values were then averaged over the year to obtain the distribution of M as given in Table A-1 of the Appendix.

It has been pointed out by Holopainen (1967) that the momentum transport values computed by Wiin-Nielsen, Brown, and Drake (1963, 1964) on the basis of data analyzed objectively at the National Meteorological Center have a tendency to be smaller in the low latitudes and larger in the middle and high latitudes than the ones obtained by himself and other investigators using data analyzed differently. The discrepancy can be expected to be present in the data of

Table A-1 since they were computed in the same manner and from the same type of data as those published by Wiin-Nielsen, Brown, and Drake (loc. cit.). It will become apparent from the results of the present study, on the other hand, that the effect of the eddy momentum transport on the temperature $\bar{T}_z$ is appreciably smaller (at least in the middle and high latitudes) than that of the eddy heat transport. The eddy heat transport values used in this study do not appear to have appreciable discrepancies when compared to those obtained by White (1954) so that at least the combined effect of the eddy heat and momentum transports on the solution $\bar{T}_z$ is probably not in error by a great deal.

To use the method of solution described in the previous section we require a knowledge of M from the equator to the pole. Since M was available only from 20°N to 85°N at intervals of 2.5°, it was necessary to generate the values between the equator and 20°N and the value at 87.5°N by means of some reasonable extrapolation procedure. The extrapolation to the equator was carried out on the hypotheses that M is symmetric about the equator and vanishes there. A simple polynomial of the form

$$M(p,\phi) = a_1(p)\phi^2 + a_2(p)\phi^4 \qquad (4.23)$$

was used, where a_1 and a_2 were determined by imposing the conditions that M and $\partial M/\partial\phi$ be continuous at 20°N. As for 87.5°N and 90°N it was assumed that M varies linearly from a value of zero at the pole to the given value at 85°N. In this way the value of M could be considered known from the equator to the pole at intervals of 2.5 degrees of latitude and at the pressure levels p = 10, 15, 20, 30, 50, 70, 85, and 100 cb.

The eddy heat transport was also made available by Professor Wiin-Nielsen in the form of mean monthly values for the twelve months of 1963 from 17.5°N to 87.5°N at intervals of 2.5 degrees of latitude. The values applied for the layers between the levels where the momentum transport had been computed. For the month of January the data were not available for the layers 10 to 15 cb, 15 to 20 cb, and 85 to 100 cb. The missing data were substituted with values obtained by extrapolating vertically in the same way as for the momentum transport. The 12 mean monthly distributions of the eddy heat transport were then averaged to yield the annual mean distribution, $N \cos \phi$, as shown in Table A-2 of the Appendix. The values of $N \cos \phi$ at the pressure levels p = 10, 15, 20, 30, 50, 70, 85, and 100 cb were obtained by means of a linear interpolation or extrapolation using the assumption that N vanishes at p = 0.

At all pressure levels the heat transport N and the horizontal divergence of the heat transport $\partial N/\partial \phi$ were taken to be zero at the equator and the values of $N \cos \phi$ from 2.5°N to 15°N were computed by means of the polynomial

$$N(p) \cos \phi = b_1(p)\phi^3 + b_2(p)\phi^5 \qquad (4.24)$$

in which b_1 and b_2 were evaluated by imposing the conditions that $N \cos \phi$ and $\partial(N \cos \phi)/\partial \phi$ be continuous at 17.5°N. An odd polynomial in ϕ was chosen to extrapolate $N \cos \phi$ in an effort to make each term on the right-hand side of (4.18b) symmetric about the equator. It was hoped that this procedure would minimize the number of terms required to obtain a good representation of $G(p,\phi)$ by means of (4.20b).

Of the three terms on the right-hand side of (4.18b), the one containing the equilibrium temperature is the only one which cannot be obtained in a straightforward manner from the standard meteorological observations. In

fact, it appears that no cross section of T_R extending from the low to the high latitudes and from the earth's surface to the lower stratosphere has been published, although some information is available for the stratosphere (see Manabe and Strickler (1964), p. 379). For lack of better information the values of T_R near the ground published by Milankovitch (1930) were used at p = 100 cb.

To obtain the value of T_R at the other pressure levels where N and M were available, it was assumed that in the absence of the large-scale motion the troposphere and lower part of the stratosphere would tend to be in a state of convective equilibrium rather than in a state of pure radiative equilibrium since the latter would be statically unstable (see Manabe and Strickler (loc. cit.)). It can be expected that the vertical temperature lapse rate of an atmosphere in convective equilibrium would be between the dry and moist adiabatic lapse rates and therefore not radically different from the average lapse rate in the real atmosphere. This suggests that setting the two equal to each other would constitute a reasonable approximation.

Wiin-Nielsen (1959b) has shown that the differential equation

$$-S \equiv \frac{dT}{dp} - \frac{R}{c_p}\frac{T}{p} = -\frac{a}{p}, \qquad (4.25)$$

where a is a constant determined from observations, yields a solution for T which closely approximates the average temperature in the lower atmosphere. It is found that the value a = 30°K gives a function S(p) which is in close agreement with the observed distribution of S published by Gates (1961), when the average of his January and July distributions is considered. Given

that $T = T_o$ at $p = p_o = 100$ cb the solution of (4.25) is

$$T = T_o \left(\frac{p}{p_o}\right)^{R/c_p} + \frac{c_p a}{R} \left[1 - \left(\frac{p}{p_o}\right)^{R/c_p}\right] . \qquad (4.26)$$

The empirical formula (4.26), with a = 30°K, was used to extrapolate the values of T_R obtained from Milankovitch (1930) from 100 to 20 cb. The values of T_R at 10 and 15 cb were assumed to be the same as those at 20 cb to simulate the lower stratosphere in the thermal equilibrium atmosphere. This distribution of T_R, which appears in Table A-3 of the Appendix, is undoubtedly oversimplified but it does not appear possible at the moment to improve upon it in a meaningful manner.

The constant A appearing in (4.18a) was evaluated (see (4.4b)) using $\tilde{T}$ = 250°K and K = 90 m^2 sec^{-1}. With a representative density of 0.5×10^{-3} t m^{-3}, this value of K corresponds to a value of $\mu = \rho K = 4.5 \times 10^{-2}$ t m^{-1} sec^{-1} which falls between Palmén's (1955) estimate of 2.25×10^{-2} t m^{-1} sec^{-1} and Riehl's (1951) estimate of 5.00×10^{-2} t m^{-1} sec^{-1}.

The static stability parameter S in (4.18) was evaluated as a function of pressure from Gates' (1961) observational study of the static stability by averaging his values of S for January and July. Some computations have shown that the formula (4.25), which was used to extrapolate T_R in the vertical, could have been used to evaluate S with very little change in the solution of (4.18).

4.4 THE COMPUTED TEMPERATURE DISTRIBUTION

The differential equation (4.18a) was solved for $\bar{T}_z$ by the method de-

scribed in Section 4.2. The equation is linear so that the contributions to the solution $\bar{T}_z$ by the three terms defining $G(p,\phi)$ are additive. In fact, the sum of their contributions gives the complete solution $\bar{T}_z$ since the homogeneous part of (4.18a) has no solution satisfying the boundary conditions.

To determine the role that the eddies play in maintaining the axisymmetric temperature field we shall compute $\bar{T}_z$ firstly under the conditions $T_R \equiv M \equiv 0$, $N \neq 0$, thus obtaining the effect of the eddy heat transport on $\bar{T}_z$, then under the conditions $T_R \equiv N \equiv 0$, $M \neq 0$, thereby obtaining the effect of the eddy momentum transport on $\bar{T}_z$, and thirdly under the condition $T_R \equiv 0$, $N \neq 0$, $M \neq 0$, to obtain the total contribution by the eddies to $\bar{T}_z$. After this study of the importance of the eddies we shall present the solution for the case $T_R \not\equiv 0$, $M \equiv N \equiv 0$ as well as the complete solution of (4.18) with $T_R \not\equiv 0$, $M \neq 0$, and $N \neq 0$.

The contribution to $\bar{T}_z$ by the horizontal eddy heat transport N appears in the form of a meridional-vertical cross section in Fig. 19. A positive (negative) values of temperature at a given point indicates that the eddy heat transport acts to raise (lower) the temperature at that point. The main features of the results, namely, the cooling and warming of the low and high latitudes, respectively, follow directly from the observed fact that on the average the eddies transport heat northward with a maximum in the middle latitudes. We note, in particular, that the computed effect of the eddy heat transport on the temperature field is strongest near 70 cb and at high latitudes.

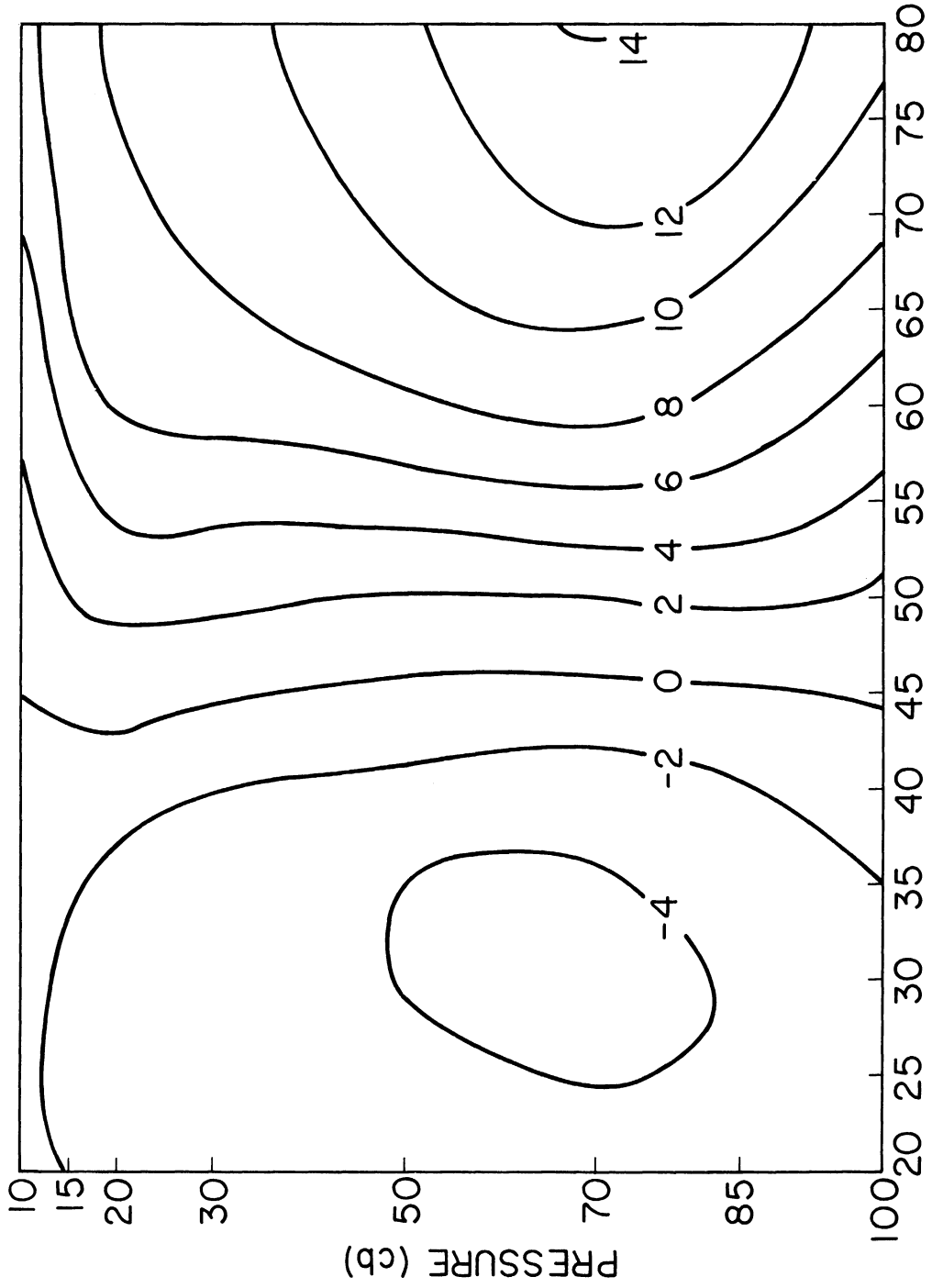

Fig. 19. The field of $\bar{T}_z$, in degrees Kelvin, as forced by the horizontal eddy heat transport.

We recall that in our formulation the diabatic heating is given by

$$\bar{H}_z = c_p q(T_R - \bar{T}_z) = q'(T_R - \bar{T}_z) .$$

In the above computations, however, we have set $T_R \equiv 0$ so that

$$\bar{H}_z = -q'\bar{T}_z$$

where q' is a positive constant. We can therefore obtain the diabatic heating rate $\bar{H}_z$ for the present case by multiplying the value of $\bar{T}_z$ in Fig. 18 by $-q' = -0.4 \times 10^{-3}$ kj t^{-1} deg^{-1} sec^{-1}. It is clear that in this case the low and high latitudes are regions of diabatic heating and cooling, respectively.

The contribution to $\bar{T}_z$ from the eddy momentum transport alone appears as a function of latitude and pressure in Fig. 20. The regions of positive (negative) temperature are regions where the eddy momentum transport acts to raise (lower) $\bar{T}_z$. To see how the eddy momentum transport can affect the axisymmetric temperature distribution, we first observe that the first equation of motion (4.9) contains both the eddy momentum transport M and the temperature so that a dependence of the latter on the former is not surprising. We can show, on the other hand, even for an inviscid atmosphere, for which (4.9) reduces to

$$\frac{1}{a\cos^2\phi}\frac{\partial(M\cos^2\phi)}{\partial\phi} = f_o\bar{v}_z , \qquad (4.27)$$

that the eddy momentum transport <u>can</u> have an effect on the axisymmetric temperature field. From (4.27) we see that by their transport of momentum the eddies force a mean meridional circulation with northward component $\bar{v}_z$. The

implied "vertical" component ω_z is easily obtained from the continuity equation (4.17) and finally from (4.16) with $N \equiv T_R \equiv 0$, that is,

$$S\bar{\omega}_z = q\bar{T}_z = -\bar{H}_z \qquad (4.28)$$

we can compute $\bar{T}_z$. In physical terms, (4.28) states that for a steady state to exist in the absence of the eddy heat transport there must be a balance between the adiabatic heating or cooling due to the vertical motion ($S\bar{\omega}_z$) and the diabatic cooling or heating ($q\bar{T}_z$).

From (4.28) and Fig. 20 we deduce that there is some diabatic cooling and downward motion ($\bar{\omega}_z > 0$) in the region between 20°N and about 46°N and near 80°N in the lower part of the atmosphere; in contrast, the polar front region, from about 46°N to about 75°N, is one of diabatic heating and upward motion.

Judging from Figs. 19 and 20 we can conclude that the eddy momentum transport has its maximum effect on the temperature field at a higher level than does the eddy heat transport. We note also that the effect of the eddy momentum transport on $\bar{T}_z$ is rather small near the pole in contrast to that of the eddy heat transport which is quite large. Perhaps the most important feature to be noticed from Figs. 19 and 20 is the tendency that the heat and momentum transports have, between 20°N and about 75°N, to oppose each other in the way in which they affect $\bar{T}_z$. Thus south of about 45°N the temperature values in Fig. 19 are positive whereas the reverse holds between 45°N and 75°N. The effect of the eddy momentum transport on $\bar{T}_z$, however, is smaller than that of the eddy heat transport over most of the domain.

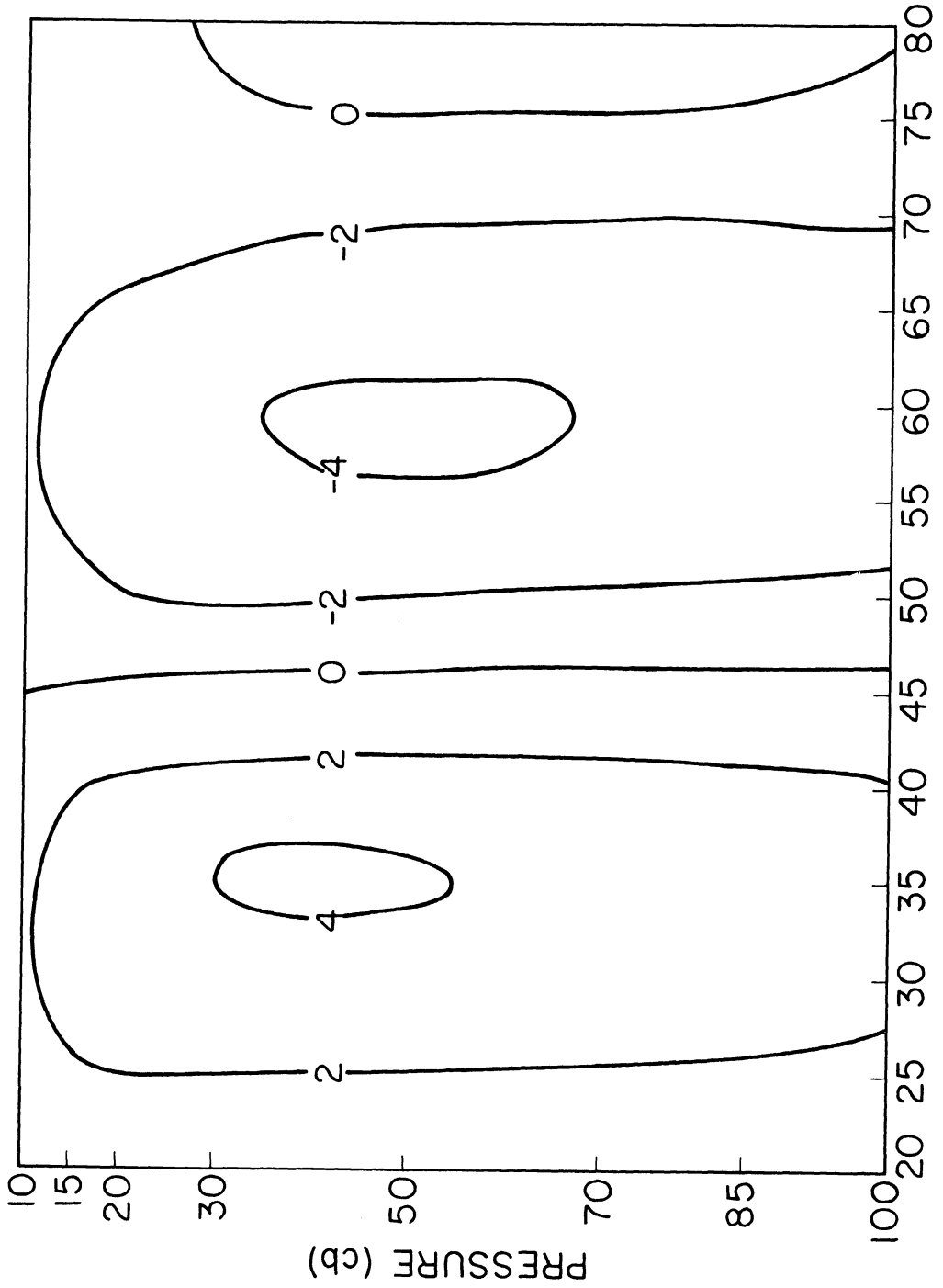

Fig. 20. The field of $\bar{T}_z$, in degrees Kelvin, as forced by the horizontal eddy momentum transport.

The effects of the heat and momentum transports on the temperature field, although opposite over most of the domain of interest, do not cancel each other completely but rather produce the combined effect found in Fig. 21. We see that the eddies cool the low latitudes and warm the high latitudes with the maximum effects being found near 70 cb.

The contribution to the solution $\bar{T}_z$ by the function T_R appears as the dotted curves in Fig. 22(a) for the pressure levels p = 10, 15, 20, and 30 cb and in Fig. 22(b) for p = 50, 70, 85, and 100 cb. The equilibrium temperature T_R appears in the figures as the dashed curve. The difference between the dashed and dotted curves is due to the presence of friction. We note from (4.16) that in the absence of the eddies the vertical motion is given by

$$\bar{\omega}_z = \frac{q}{S}(\bar{T}_z - T_R)$$

so that when $\bar{T}_z$ is greater than T_R we have downward motion and when $\bar{T}_z$ is less than T_R we have upward motion. It follows from Figs. 16 and 17 that in the case $T_R \not\equiv 0$, $M \equiv N \equiv 0$ we have a one cell circulation with upward motion in the low latitudes (where there is diabatic heating since $\bar{T}_z < \bar{T}_R$ and downward motion in the high latitudes (where there is diabatic cooling since $\bar{T}_z > \bar{T}_R$).

The solution to (4.18a), determined by the observed values of M and N for 1963 and the assumed distribution of T_R, appears as the solid lines in Figs. 22(a) and (b). Whereas the difference between the dashed and dotted curves is due to the presence of the one-cell mean meriodional circulation

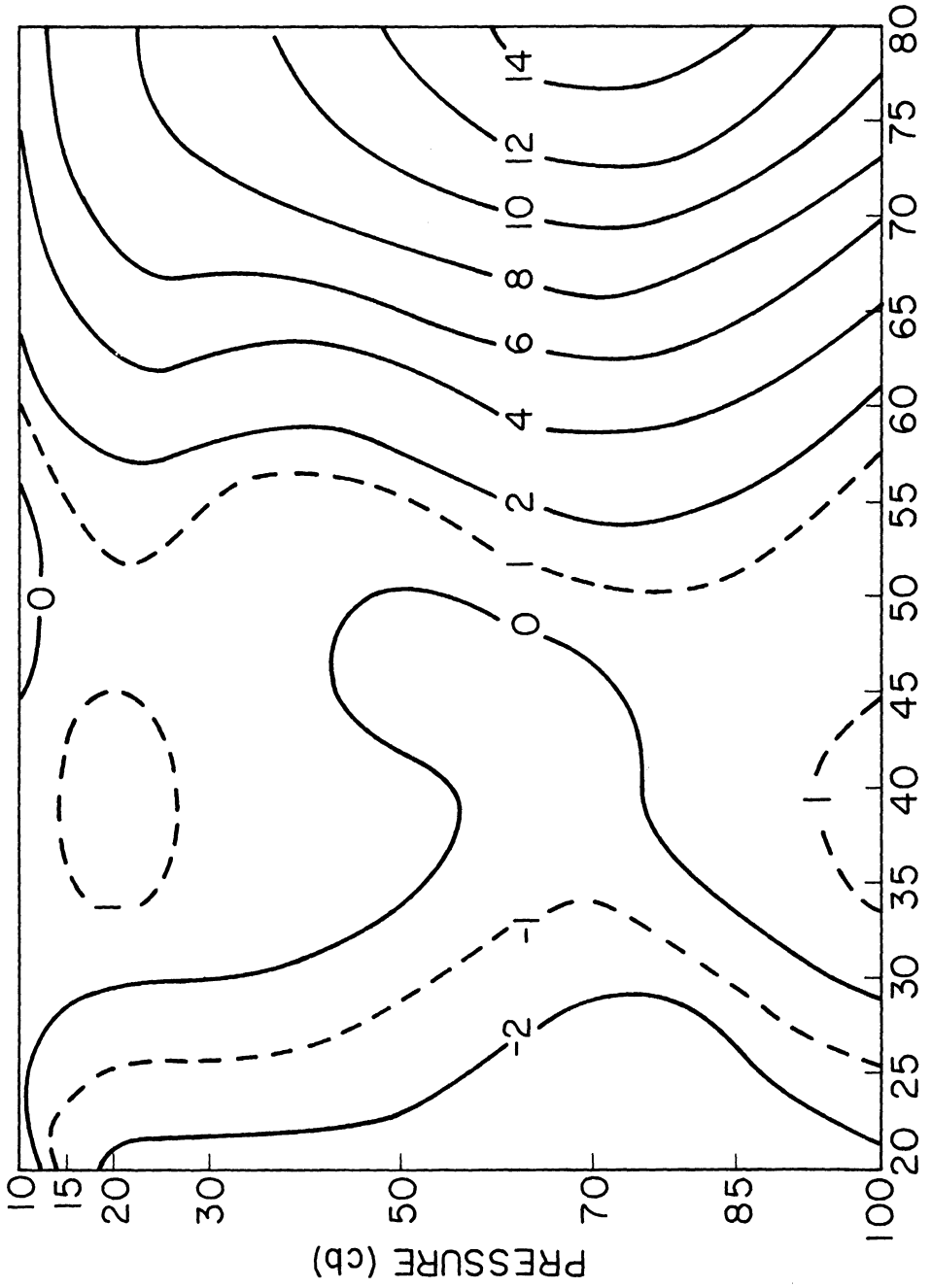

Fig. 21. The field of $\bar{T}_z$, in degrees Kelvin, as forced by the combined action of the eddy heat and momentum transports.

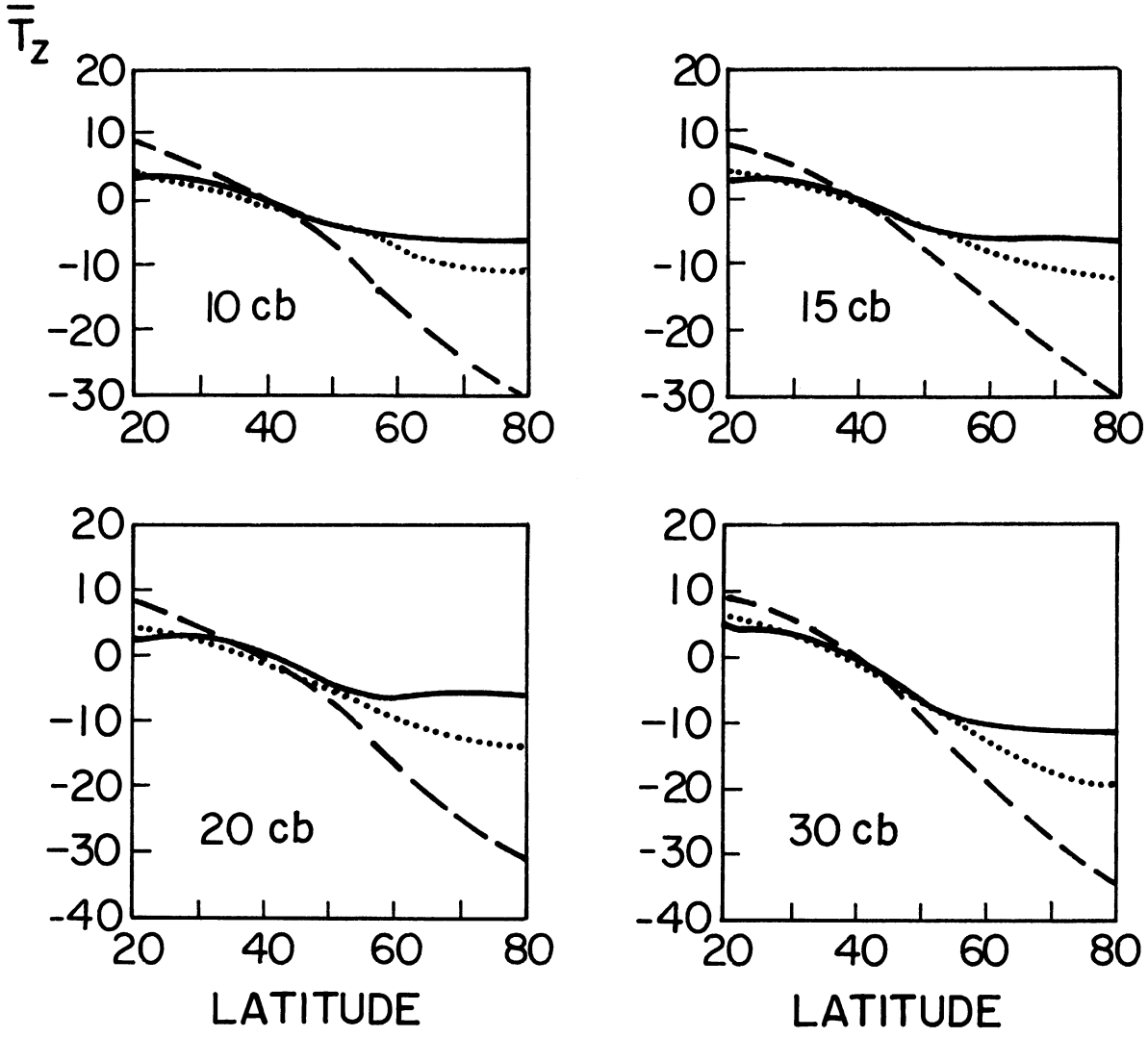

Fig. 22(a). The dotted curves show the solution $\bar{T}_z$ as forced by the assumed distribution of T_R (dashed curve) for the pressure levels p = 10, 15, 20 and 30 cb. The solid curves show the solution $\bar{T}_z$ as forced by the combined action of T_R together with the eddy heat and momentum transports. The temperatures are in degrees Kelvin and are deviations from their respective area average.

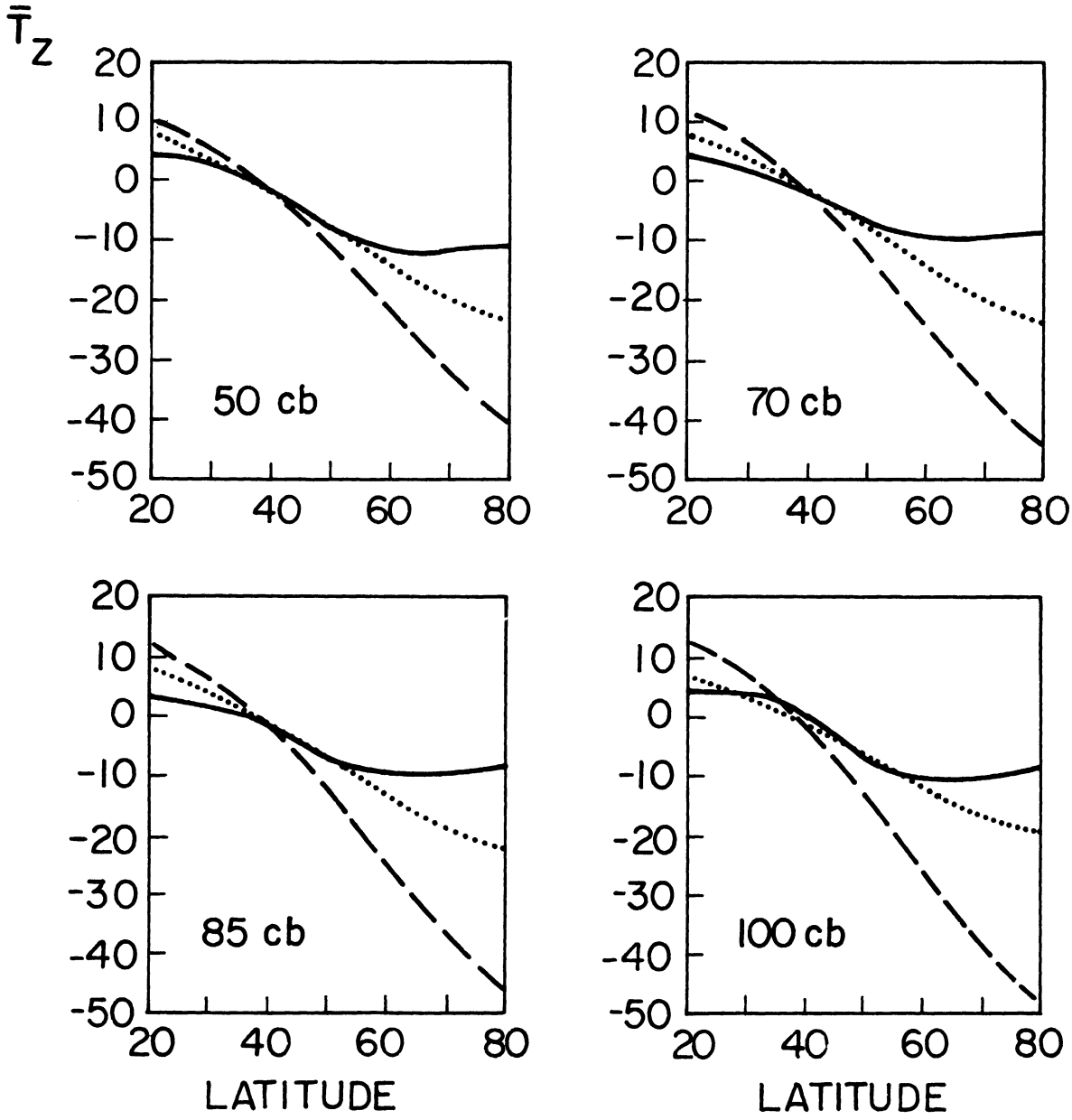

Fig. 22(b). Same as Fig. 22(a) but for the pressure levels p = 50, 70, 85, and 100 cb.

present in the absence of the eddies, the difference between the solid and dotted curves results from the presence of the eddies, whose effect on the temperature field was discussed earlier. It is clear from a comparison of the solid and dashed curves that at all levels shown the large scale eddies and friction mechanism force the temperature difference between 20°N and 80°N to be appreciably smaller than in the thermal equilibrium condition. For example, at 100 cb the computed temperature difference between 20°N and 80°N (solid curve) is 13°K, as compared to 62° in the equilibrium temperature (dashed curve).

The average observed temperature for the 12 month period starting in February 1963 appears in Fig. 23. This figure is presented in a different format from that of Figs. 22(a) and (b) because the lack of data south of 25°N made it impossible to compute and subtract from the data the average temperature over the northern hemisphere. If we focus our attention on the 100 cb level, we find that the observed temperature difference between 25°N and 80°N is larger than the computed one shown in Fig. 22(b). At first sight one might suppose that the computed temperature difference could be increased by lowering the value of the coefficient of eddy viscosity since in our formulation friction acts to smooth out the variations of the zonal wind with pressure or, equivalently, to reduce the meridional temperature gradient. Tests have shown, however, that reducing the value of the coefficient of eddy viscosity by a factor two increases the temperature difference between 25°N and 80°N by only about 2°K. Since the heat and momentum transports are taken from observations, it seems that an improvement in our results hinges upon a better specification of the equilibrium temperature.

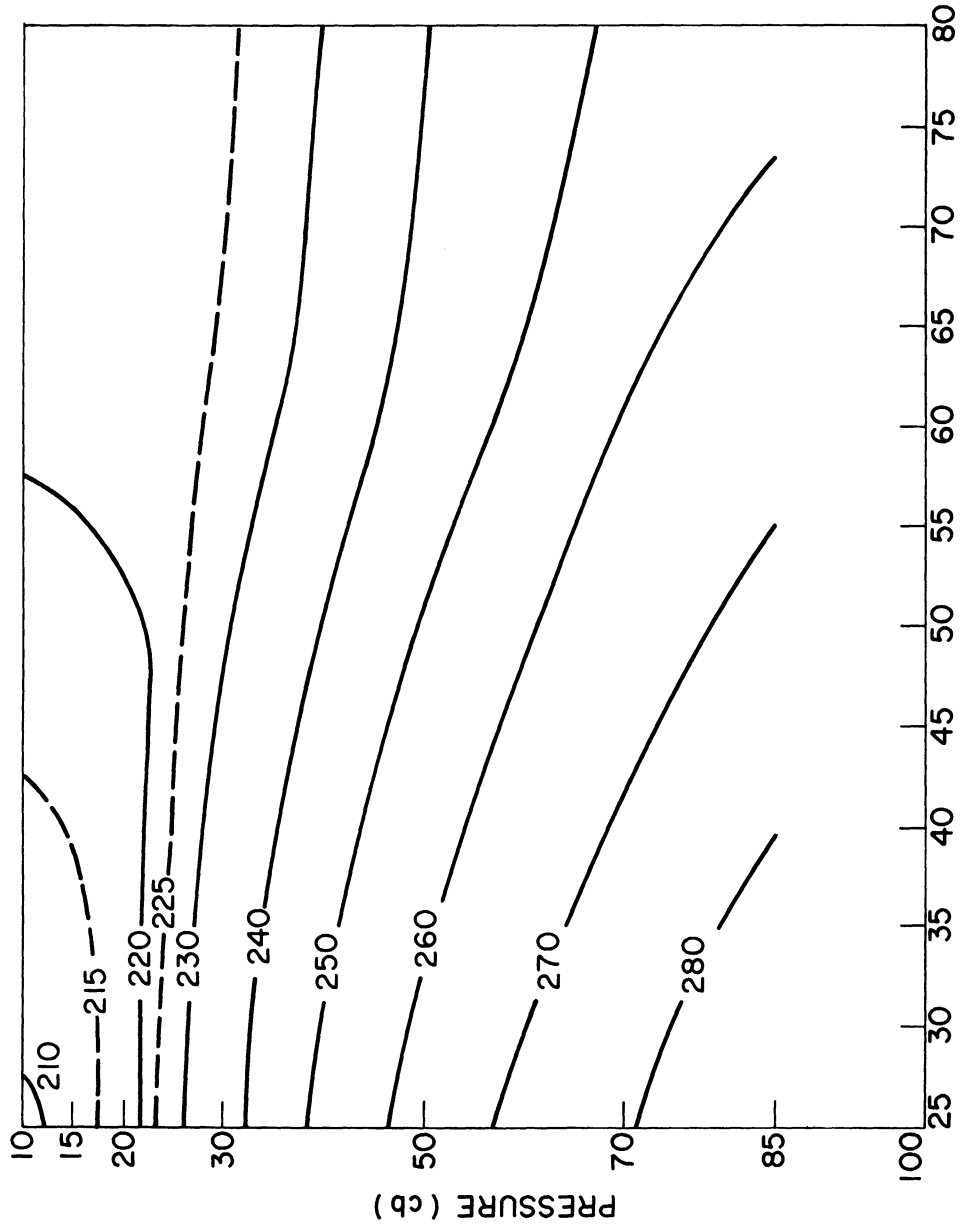

Fig. 23. The observed axisymmetric temperature field averaged over the one year period beginning in February 1963.

Although the solutions for $\bar{T}_z$ at the various pressure levels shown in Figs. 22(a) and (b) leave something to be desired, they do indicate how important the eddies and the friction mechanism used here can be in altering the axisymmetric temperature field.

4.5 THE COMPUTED MEAN MERIDIONAL CIRCULATION

Once $\bar{T}_z$ is obtained from (4.18a) for a given pressure level it is a simple matter to solve (4.16) for ω_z, the "vertical velocity" in the axisymmetric regime, since N, T_R, and S are taken to be known. The vertical-meridional cross section for ω_z appears in Fig. 24 for the case where the heat and momentum transports are included and T_R is as shown in Figs. 22(a) and (b). The direction of the arrows indicates whether the air is moving toward a higher or lower pressure. It may be mentioned for convenience here that at 70 cb a value of $\bar{\omega}_z = 10 \times 10^{-6}$ cb $\sec^{-1}$ corresponds to a vertical velocity of about 1 mm $\sec^{-1}$. We find some upward motion from 20°N to about 24°N, downward motion from 24°N to about 46°N changing into upward motion to about 65°N and finally some downward motion from 65°N to 80°N. This distribution is in good agreement with the results obtained by Vernekar (1967) in his extensive study of the mean meridional circulation.

In view of the continuity equation (4.17), $\bar{\omega}_z$ and $\bar{v}_z$ can be written in terms of a stream function $\psi(p,\phi)$ as

$$\bar{\omega}_z = -\frac{1}{\cos\phi}\frac{\partial\psi}{\partial\phi} \qquad (4.29a)$$

$$\bar{v}_z = \frac{a}{\cos\phi}\frac{\partial\psi}{\partial p}\,. \qquad (4.29b)$$

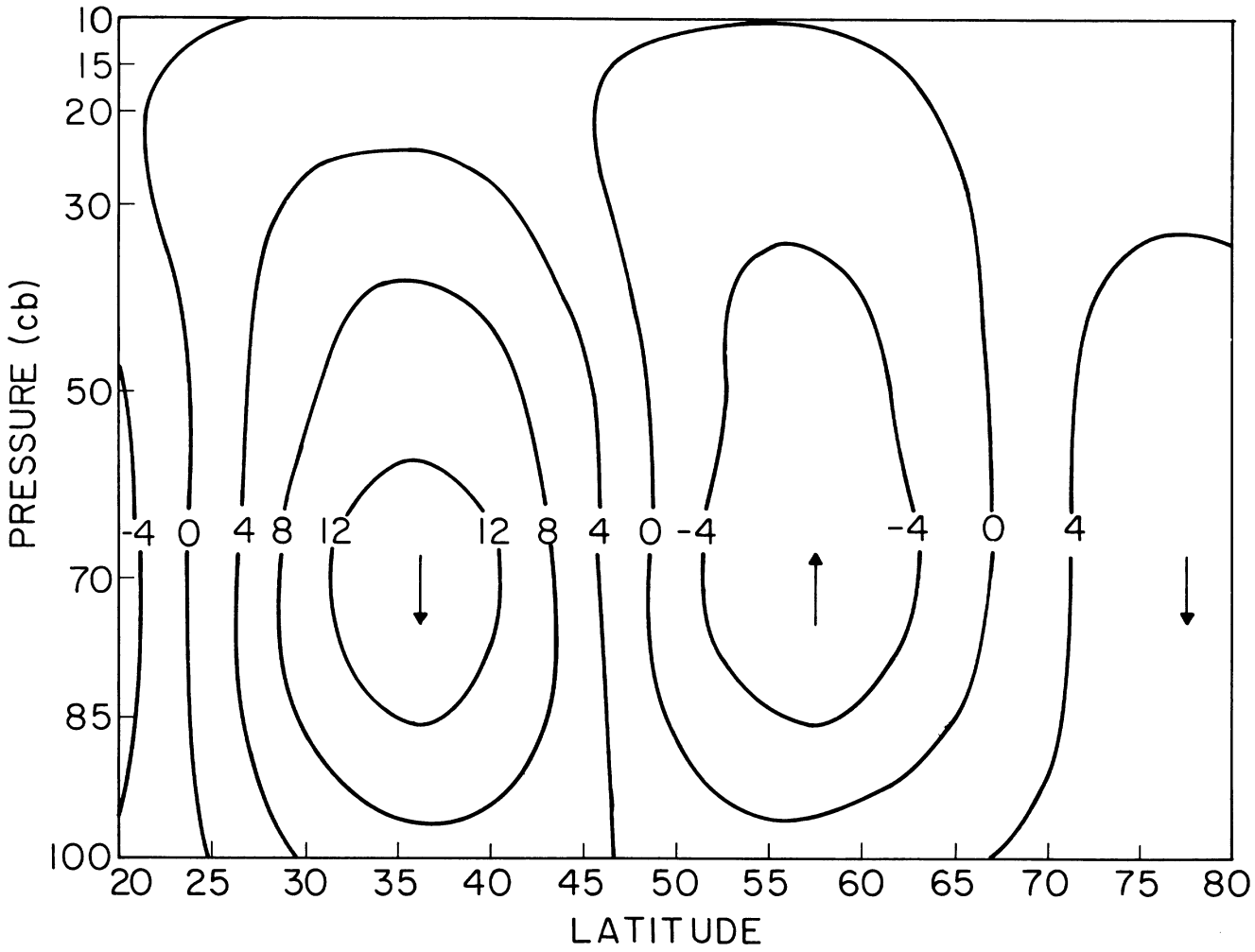

Fig. 24. The field of $\bar{\omega}_z$, in units of 10^{-6} cb sec^{-1}, resulting from the diabatic heating and the horizontal eddy transports of heat and momentum.

To find what boundary conditions $\psi(p,\phi)$ must obey, we first note from the first equation of motion (4.9) that the conditions $\partial\bar{T}_z/\partial\phi = \partial M/\partial\phi = 0$ at $\phi = 0$, which have already been used, imply that $\bar{v}_z(p,0) = 0$ so that

$$\psi(p,0) = \text{constant.} \tag{4.30a}$$

The usual boundary condition $\bar{\omega}_z(0,\phi) = 0$ then implies that

$$\psi(0,\phi) = \text{constant} \tag{4.30b}$$

and finally the condition that $\bar{v}_z(p,\pi/2)$ be finite implies, through (4.29b), that

$$\left.\frac{\partial\psi}{\partial p}\right|_{(p,\pi/2)} = 0 . \tag{4.30c}$$

From (4.30a,b,c) it follows that

$$\psi(p,0) = \psi(0,\phi) = \psi(p,\pi/2) = \text{constant.} \tag{4.31}$$

For convenience we shall take the constant in (4.31) to be zero.

The stream function $\psi(p,\phi)$ can be obtained by integrating (4.29a) so that

$$\psi(p,\phi) = -\int_0^{\phi} \bar{\omega}_z \cos\phi \, d\phi . \tag{4.32}$$

The boundary condition at $\phi = 0$ is automatically satisfied while the one at $\phi = \pi/2$ can be shown to be satisfied by using the equation of continuity (4.17) and the condition $v_z(p,0) = 0$.

The stream function $\psi(p,\phi)$ corresponding to the $\bar{\omega}_z$ field of Fig. 24 was computed from (4.32). The integral was evaluated numerically using finite

intervals of $\Delta\phi = 2.5$ degrees of latitude. The results are given in Fig. 25, where the arrows indicate schematically the direction of flow. The Hadley cell, centered at about 24°N, is clearly visible with its southerly flow at the high elevations and northerly flow near the ground. The middle latitude cell, centered at about 50°N and also well defined, shows the presence of a southerly current in the low levels with a return circulation aloft.

4.6 THE COMPUTED MEAN ZONAL WIND

To obtain the speed of the zonal current in the axisymmetric regime we integrate the thermal wind equation (4.8) so that $\bar{u}_z$ takes the form

$$\bar{u}_z(p,\phi) = \bar{u}_z(p_g,\phi) + \frac{R}{af_o}\frac{\partial}{\partial\phi}\int_{p_g}^{p}\frac{\bar{T}_z}{p}\,dp \qquad (4.33)$$

where p_g is the pressure at the ground. While the second term on the right-hand side of (4.33) can easily be evaluated using the distribution of $\bar{T}_z$ already computed, a method must now be found to evaluate $\bar{u}_z(p_g,\phi)$. To do this we note that the friction term F in (4.3) can be written as

$$F = g\frac{\partial\tau}{\partial p}, \qquad (4.34)$$

where τ is the zonal component of eddy stress, so that (4.5) becomes

$$\frac{1}{a\cos^2\phi}\frac{\partial(M\cos^2\phi)}{\partial\phi} = f_o\bar{v}_z + g\frac{\partial\tau_z}{\partial p}. \qquad (4.35)$$

If we neglect the presence of the continental elevations so that $\bar{\omega}_z = 0$ at the earth's surface, we find from the continuity equation (4.17) that

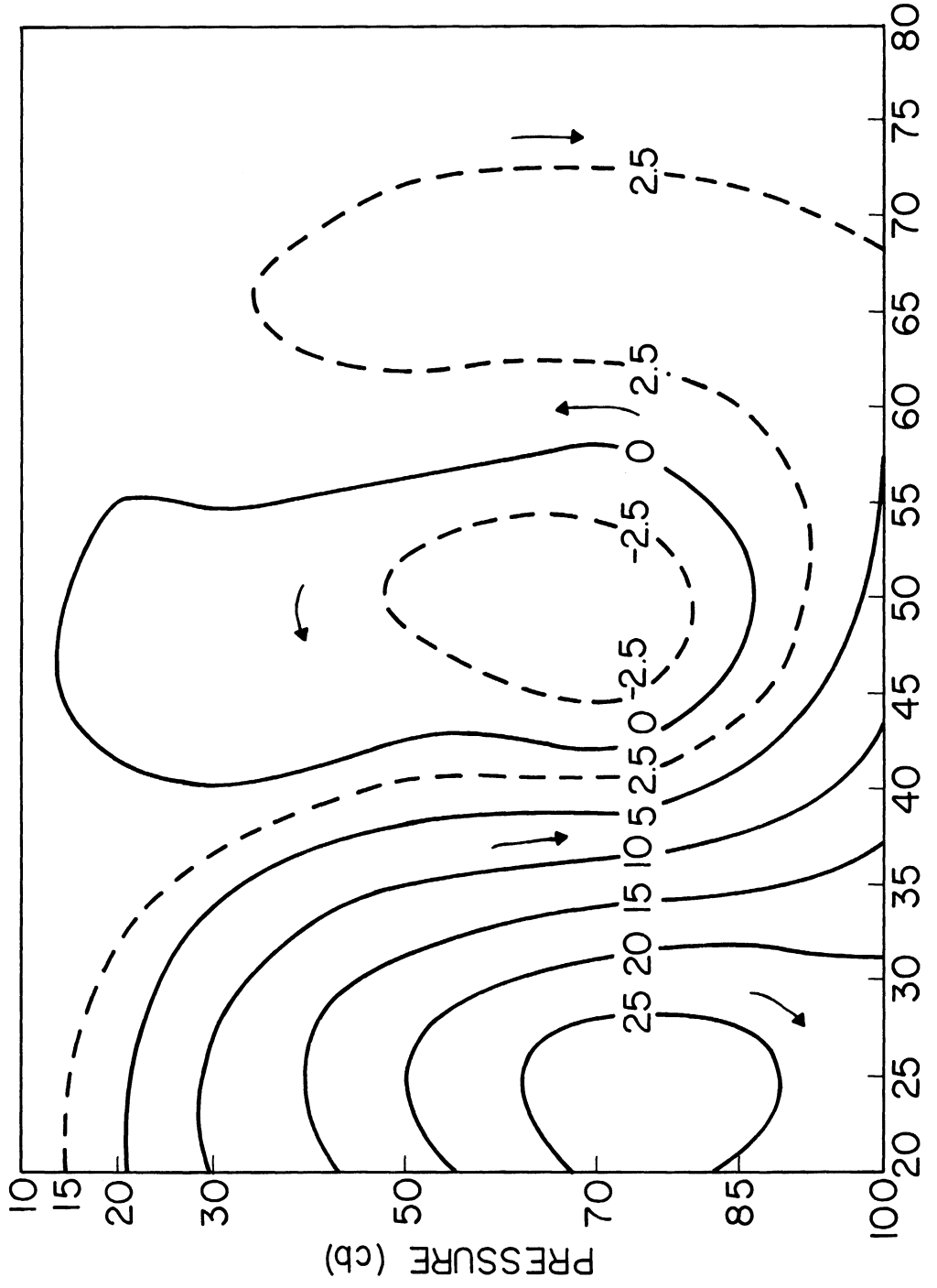

Fig. 25. The stream function ψ, in units of 10^{-7} cb sec^{-1}, corresponding to the $\bar{\omega}_z$ field of Fig. 23.

$$\int_{p_g}^{o} \bar{v}_z dp = 0$$

so that by integrating (4.35) from p = 0, where $\tau_z = 0$, to $p = p_g$ we obtain

$$\bar{\tau}_{z,g}(\phi) = \frac{1}{ga\cos^2\phi} \frac{\partial(I_g \cos^2\phi)}{\partial\phi} \qquad (4.36a)$$

where $\bar{\tau}_{z,g}$ is the value of τ_z at the ground and

$$I_g = \int_o^{p_g} M(p,\phi)dp \ . \qquad (4.36b)$$

If we now assume that the stress and wind speed at the ground obey the relation

$$\bar{\tau}_{z,g}(\phi) = - C_d \rho_g V u_z(p_g,\phi) \qquad (4.37)$$

where C_d is the drag coefficient, ρ_g the density at the ground and V a characteristic wind speed, we obtain the following equation for the wind speed at the ground:

$$u_z(p_g,\phi) = - \frac{1}{gaC_d\rho_g V} \frac{1}{\cos^2\phi} \frac{\partial(I_g \cos^2\phi)}{\partial\phi} \ . \qquad (4.38)$$

In the computations of $\bar{u}_z(p_g,\phi)$ we use the following values: $C_d = 3 \times 10^{-3}$, $\rho_g = 10^{-3}$ t m^{-3}, V = 10 m sec^{-1}, following Phillips (1956).

Since the eddy momentum transport is known from observations, the integral in (4.36) can be evaluated and the zonal wind at the surface can be determined from (4.38). The results can then be substituted in (4.33) to obtain the two-dimensional distribution of $u_z(p,\phi)$.

The contributions to the complete solution $\bar{u}_z(p,\phi)$ by the eddy heat transport, the eddy momentum transport and the equilibrium temperature distribution are additive so that it is a simple matter to investigate the importance of the eddies in determining the speed of the zonal flow. For this purpose we have computed the distribution of $\bar{u}_z(p,\phi)$ under the following special conditions:

(a) $N \neq 0$, $M \equiv T_R \equiv 0$

(b) $M \neq 0$, $N \equiv T_R \equiv 0$

(c) $N \neq 0$, $M \neq 0$, $T_R \equiv 0$

(d) $N \equiv M \equiv 0$, $T_R \neq 0$

(e) $N \neq 0$, $M \neq 0$, $T_R \neq 0$.

Those are the same cases for which $\bar{T}_z(p,\phi)$ has been computed previously.

The solution for case (a), giving the contribution by the eddy heat transport to the complete solution for $\bar{u}_z(p,\phi)$, appears in Fig. 26. This zonal wind distribution is that which is in geostrophic equilibrium with the temperature field of Fig. 19, with zero wind speed at the earth's surface since in the absence of the eddy momentum transport $\bar{u}_z(p_g,\phi) \equiv 0$ (see (4.38)). The results indicate that south of about 30°N the eddy heat transport tends to produce weak westerlies while north of 30°N the tendency is to produce easterlies which increase in speed with decreasing pressure.

If it were not for the eddy heat transport, then, the observed middle latitude westerlies would have still greater speeds. Although this fact has been known for some time, it appears that this is the first time that a quantitative presentation based on observations is given.

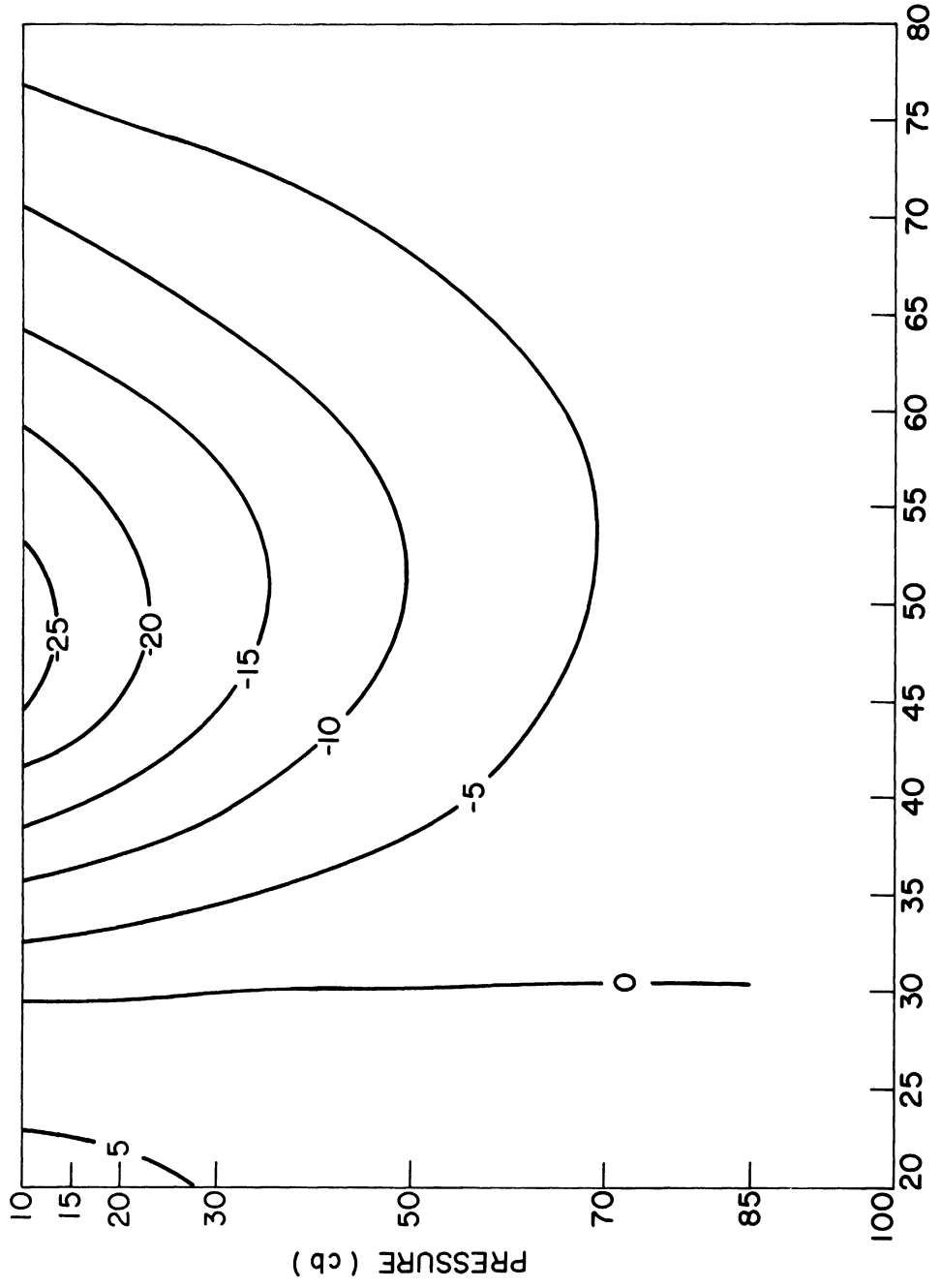

Fig. 26. The contribution by the horizontal eddy heat transport to the axisymmetric zonal wind $\bar{u}_z$, in m sec^{-1}.

The contribution by the eddy momentum transport to the distribution of the zonal mean wind can be found in Fig. 27. This distribution of $\bar{u}_z(p,\phi)$ is the one obtained for case (b) and is in geostrophic equilibrium with the temperature field of Fig. 20. Figure 27 shows that the eddies transport momentum in such a way as to produce westerlies from about 34°N to about 60°N and easterlies south of 34°N and north of 60°N. In each of the three regions the maximum influence of the eddy momentum transport is found at 10 cb, the highest level for which computations were made. This result deserves some comments in view of the fact that the eddy momentum transport for 1963 is found to have its relative maxima between 20 and 30 cb, not at 10 cb. Furthermore, Wiin-Nielsen (1967) has found that for the 12 month period starting in February 1963 the rate of kinetic energy conversion between the eddies and the zonal flow is a maximum near 20 cb. The question before us is the following: if the eddies transport more momentum and interact most strongly with the zonal current in the 20 to 30 cb region, why do we find, with the present formulation, that the speed of the zonal current is affected most by the eddy momentum transport at 10 cb? To answer this we must first remember that while the eddies are more effective at transporting and transferring their momentum to the zonal flow between 20 and 30 cb, they are also quite effective at creating a mean meridional circulation. The computations of the axisymmetric stream function show that the eddy momentum transport results in a three-cell mean meridional circulation with, in particular, the maximum northerly flow in the middle latitudes occurring between 20 and 30 cb. Through the action of the Coriolis force this circulation tends to create

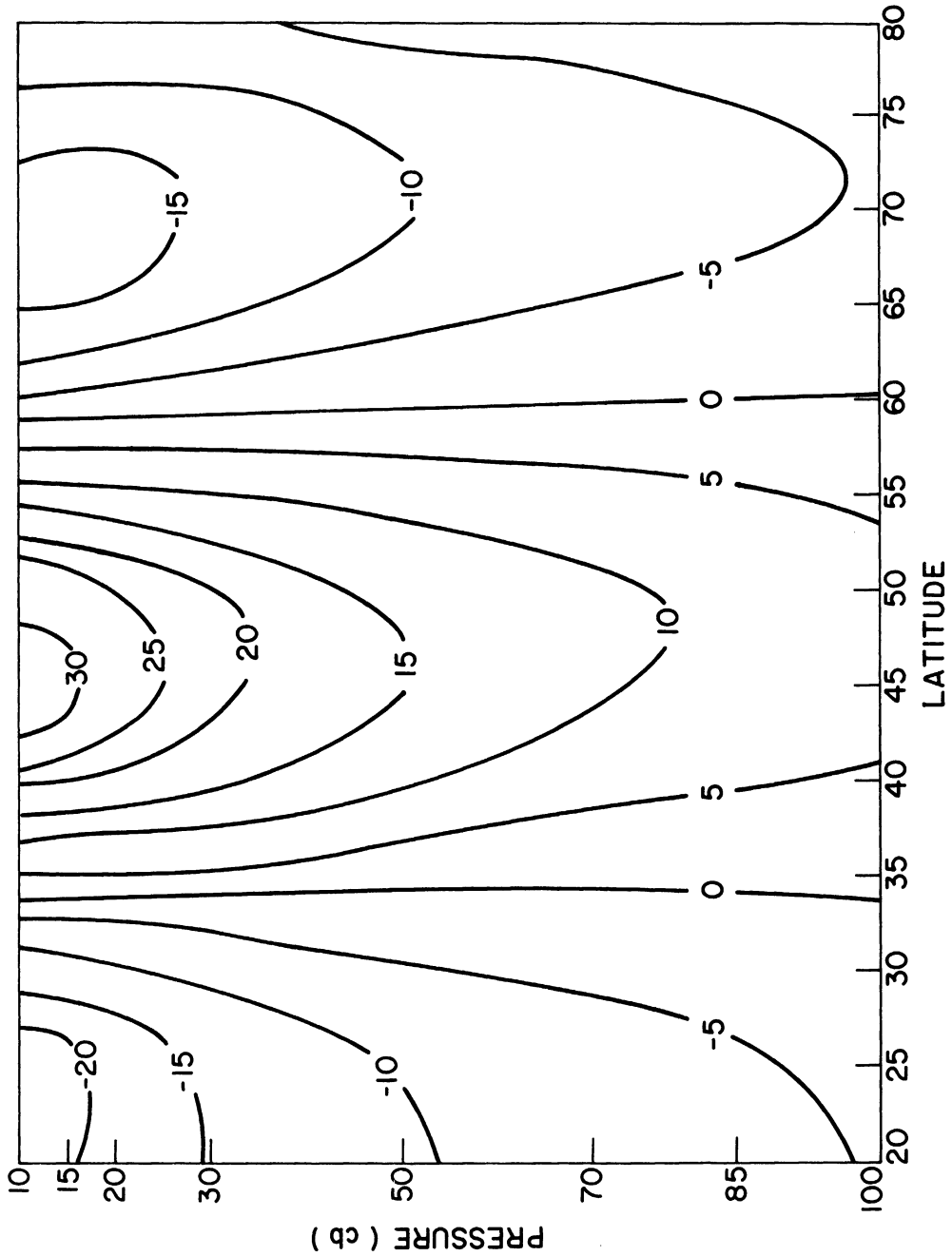

Fig. 27. The contribution by the horizontal eddy momentum transport to the axisymmetric zonal wind $\bar{u}_z$, in m sec^{-1}.

easterlies near the middle latitude tropopause in opposition to the other effect whereby the eddies tend to create a source of eastward momentum for the zonal current. A discussion of these two effects can be found in the article by Wiin-Nielsen and Vernekar (1967) but since their mean meridional circulation was produced by both the eddy momentum and the eddy heat transports in an inviscid, adiabatic atmosphere, their results are not directly comparable to ours. We should also note, in answering the above question, that the internal friction in the present study acts in such a way as to smooth the vertical distribution of $\bar{u}_z(p,\phi)$. Some test computations have shown, on the other hand, that even when the eddy coefficient of viscosity is reduced by a factor two the single maximum and the two minima in $\bar{u}_z(p,\phi)$ still occur at 10 cb.

If we add the values of $\bar{u}_z(p,\phi)$ in Figs. 26 and 27 we obtain the solution for case (c) mentioned above. The results, which indicate the combined effects of the heat and momentum transports on the zonal current, can be found in Fig. 28. Briefly, we note that the eddies tend to produce easterlies in the low and high latitudes and weak westerlies in the middle latitudes.

The solution for $\bar{u}_z(p,\phi)$ determined by the function T_R and the influence of internal friction appears in Fig. 29. This distribution of $\bar{u}_z$ is in geostrophic equilibrium with the temperature values given by the dotted curves in Figs. 22(a), and (b) and is identically zero at p = 100 cb since the effect of the eddies is not included. We note that in the absence of the eddies the zonal flow would consist of a broad westerly current with a maximum speed near 54°N. We note in particular that the wind speed increases with decreasing pressure at all latitudes as a consequence of the fact that the temperature

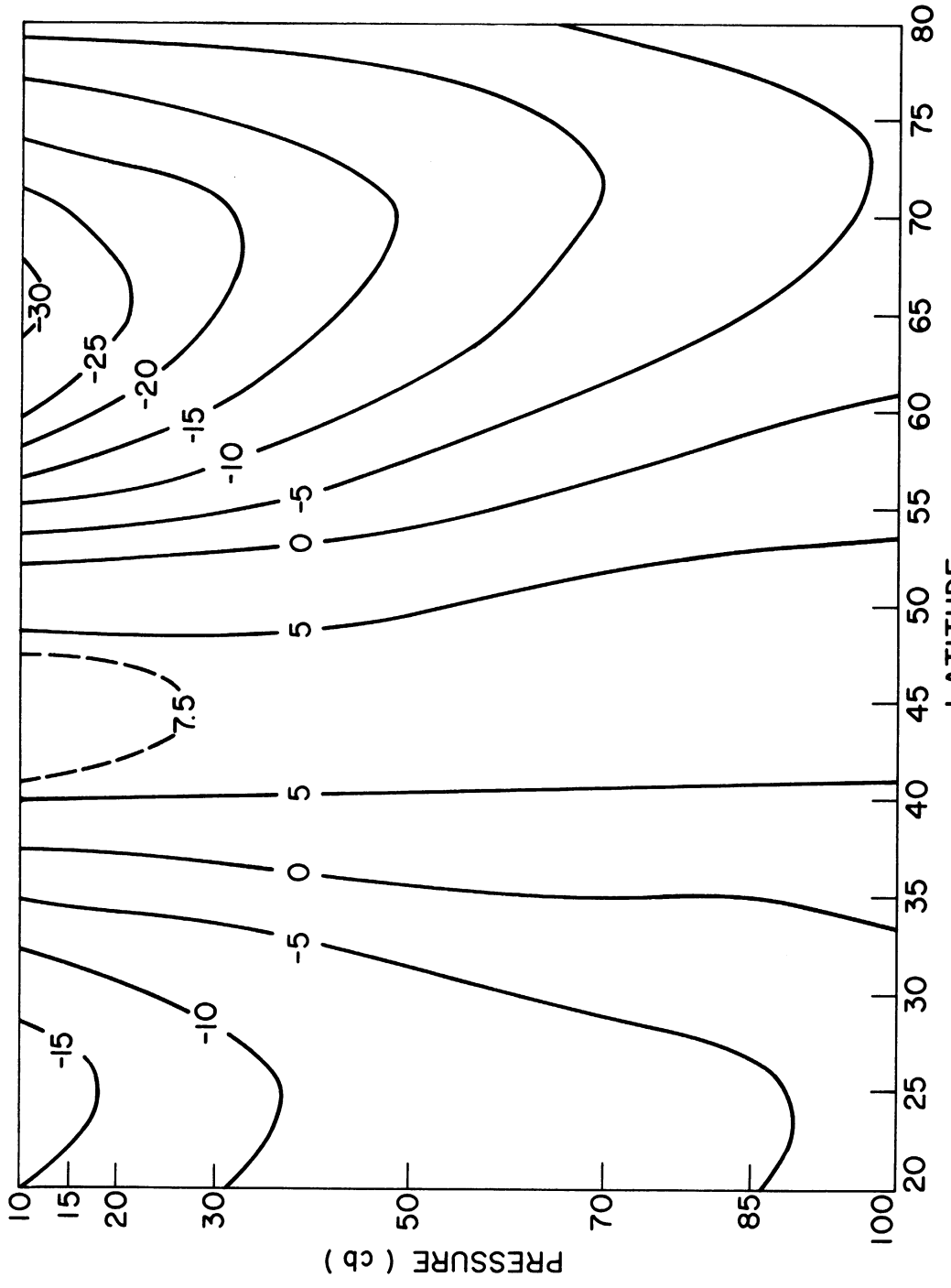

Fig. 28. The sum of the contributions shown in Figs. 26 and 27.

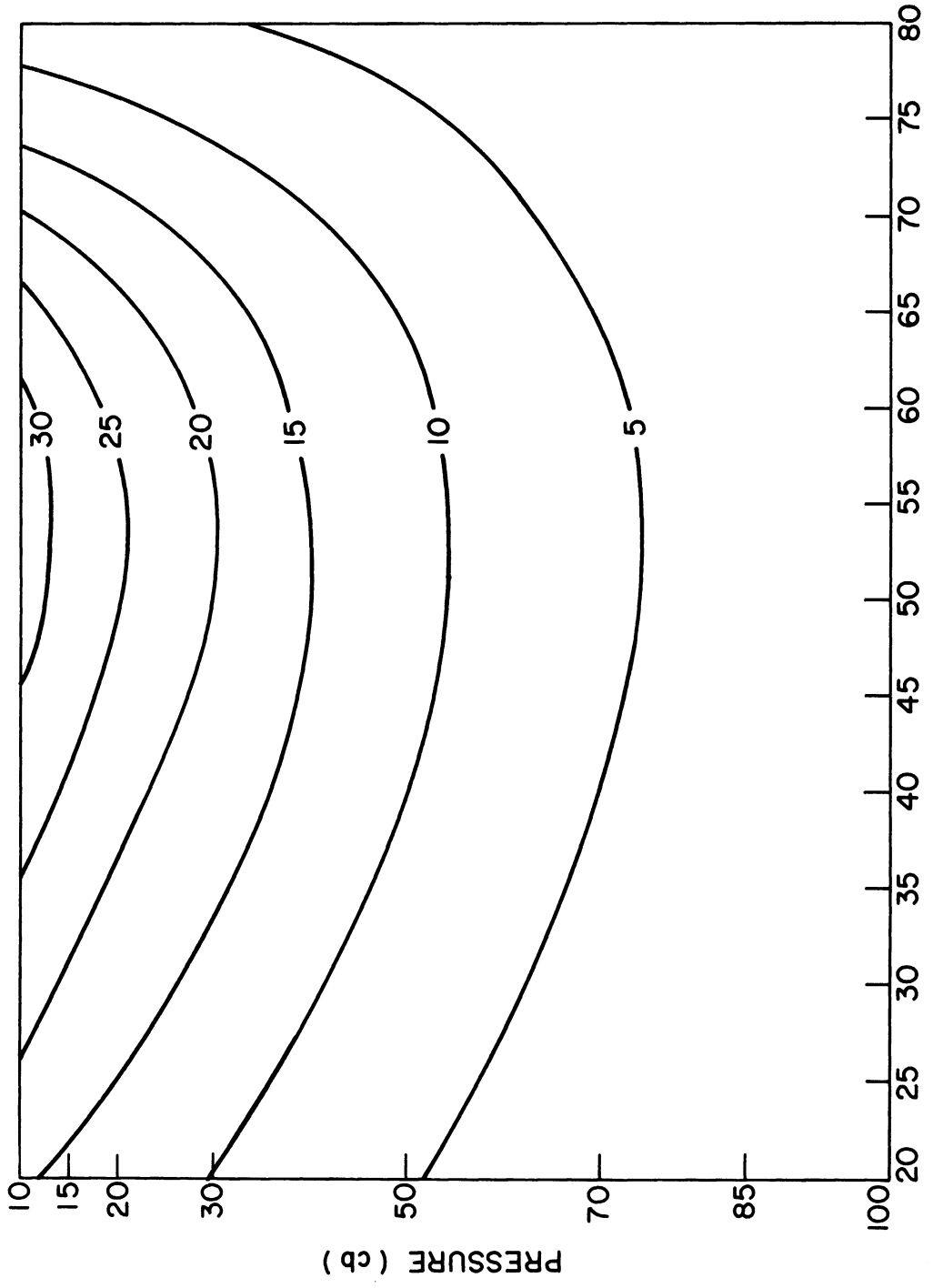

Fig. 29. The contribution by the function T_R to the axisymmetric zonal wind $\bar{u}_z$, in m sec^{-1}.

given by the dotted curves in Figs. 22(a) and (b) decreases from south to north at all levels. This temperature distribution was obtained using T_R as a forcing function which, in turn, was extrapolated vertically from surface data. Due to the vertical extrapolation of T_R, the values of T_z given by the dotted lines in Figs. 22(a) and (b) are probably less reliable at the upper levels than at the lower levels and hence the vertical wind shear at the upper levels in Fig. 29 should be considered with some caution. Nevertheless it is instructive to investigate how far we can go in trying to reproduce the observed mean zonal wind by adding the contributions shown in Figs. 28 and 29.

The result of adding the contributions to $\bar{u}_z$ by the eddies (Fig. 28) and by the function T_R (Fig. 29) appears in Fig. 30 and represents the complete solution for $\bar{u}_z$. We notice that the westerly current is concentrated in a band centered at about 46°N and flanked by weak easterlies in the low and high latitudes. Figure 30 should be compared with Fig. 31 which shows the observed geostrophic zonal wind averaged over the period February 1963 through January 1964. At the low levels the observed maximum speed is found near 45°N as in the computed distribution; at the high levels, on the other hand, the observed maximum speed is found further south than in the computed distribution. In the low and high latitudes we find weak easterlies in the computed zonal wind whereas weak westerlies are observed. Considering that Figs. 28 and 29 are used to obtain Fig. 30, we see that the westerlies forced by the function T_R (Fig. 29) are not sufficiently strong in the low and high latitudes to overcome the easterlies forced by the eddies (Fig. 28). Part of the dif-

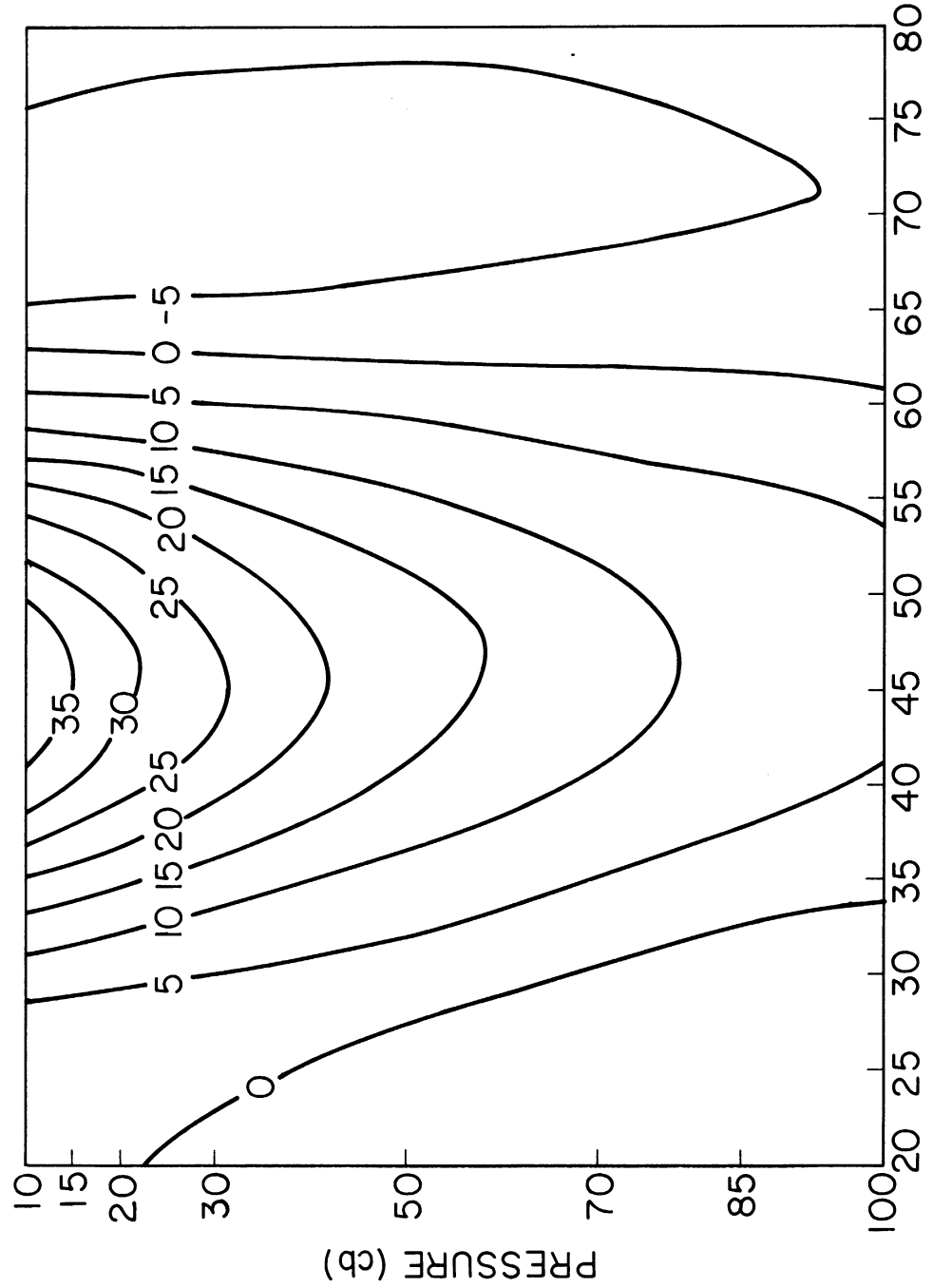

Fig. 30. The sum of the contributions by the eddy and momentum transports and by the assumed distribution of T_R to the axisymmetric zonal wind $\bar{u}_z$, in m sec^{-1}.

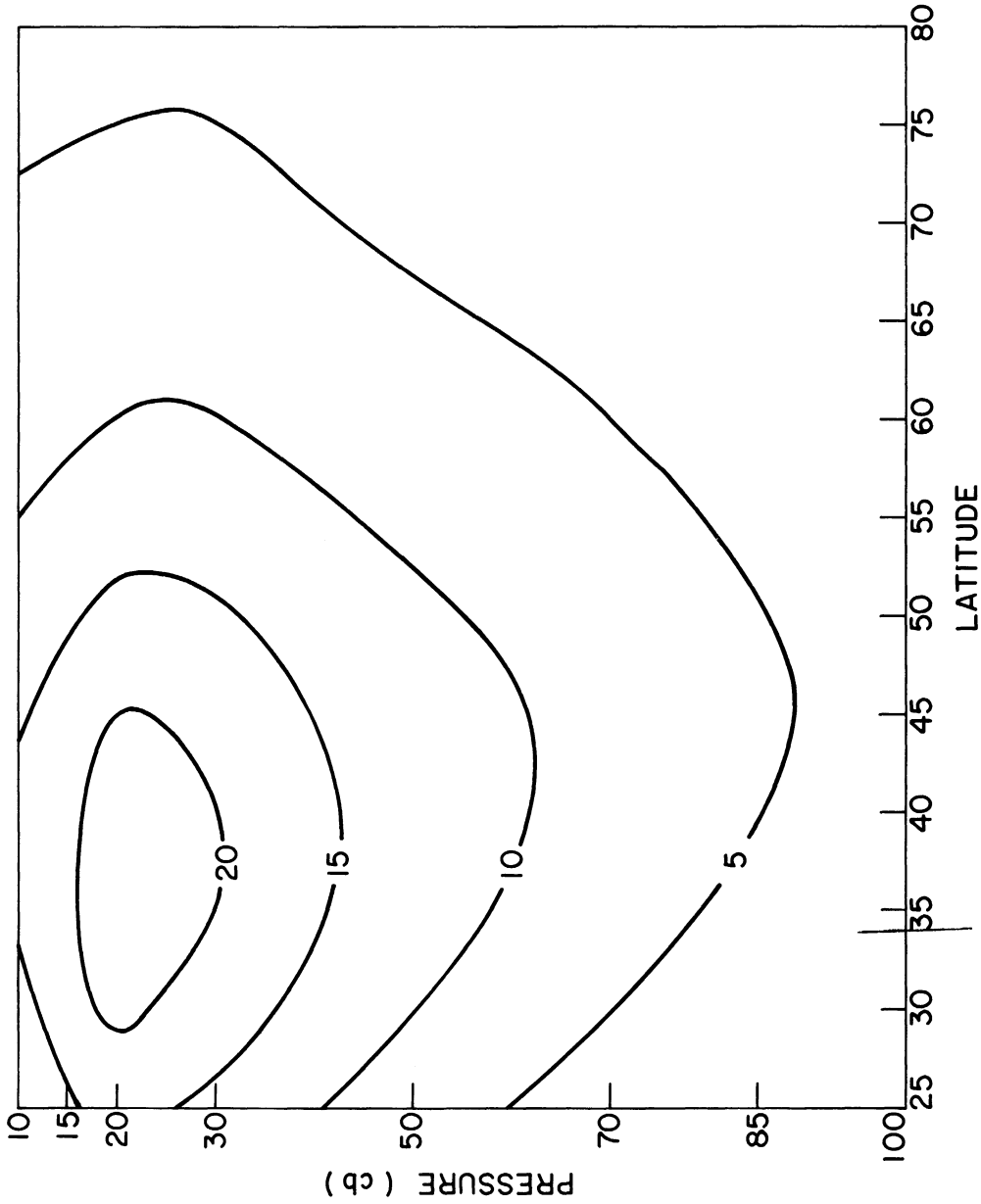

Fig. 31. The observed distribution of the geostrophic, axisymmetric zonal wind averaged over the one year period beginning in February 1963.

ference between Figs. 30 and 31 is probably due to the type of data used to compute the momentum transport (see Section 4.3) but some of it is undoubtedly due to the simplified distribution of T_R that has been used. It appears, for example, that if the function T_R decreased more quickly with latitude in the low troposphere of the low and high latitudes and increased slightly with latitude in the lower stratosphere, the solution for $\bar{u}_z(p,\phi)$ would be considerably improved. It seems, however, that little would be learned from using a different distribution of T_R and therefore the matter will not be pursued.

CHAPTER 5

CONCLUSION

5.1 SUMMARY OF THE RESULTS

By separating the time-averaged state of the atmosphere into the eddy and axisymmetric components, it has been possible to investigate the maintenance of each component against the dissipative forces. It was assumed that the more important mechanisms responsible for the maintenance of the standing waves could be reproduced by means of a linearized, steady state, two level model of the atmosphere in which the zonal current is perturbed by the earth's topography and by a steady distribution of heat sources and sinks. In the first treatment of the model it was further assumed that (a) a single effective meridional wavelength L_y can be assigned to all perturbation quantities, (b) the speed of the basic zonal current is independent of latitudes, and (c) the frictionally induced vertical motion at the top of the boundary layer is related to the vertical component of vorticity through a "friction coefficient" which is independent of longitude and latitude.

An investigation of the model was made with a basic state chosen to simulate winter condition and with L_y = 60 degrees of latitude. The results indicate that the model atmosphere tends to be most easily excited by those Fourier components of the topography and diabatic heating which have a large zonal wavelength. Furthermore, the components of the stream function with large zonal wavelengths are found to amplify with height whereas those with small zonal wavelengths are damped with height.

When the zonal variations in the standard pressure at the ground and in the diabatic heating for January 1962 are evaluated from the data published by Berkofsky and Bertoni (1955) and Brown (1964), respectively, the model atmosphere yields standing waves which exhibit a fair degree of similarity to the observed ones. When the forcing effects of the topography and of the diabatic heating are considered separately we find that the standing waves produced by the topography are in about the same position as those produced by the heat sources and sinks and that the former have somewhat larger amplitudes than the latter. The topographically induced standing waves appear to show no preferred slope with height in the sense that at some longitudes the waves slope slightly to the west with height while at others they are either vertical or slope slightly to the east with height. All the major troughs and ridges which are produced by the diabatic heating obtained from Brown (1964), on the other hand, slope to the west with height. Similarly when the composite response of the model to both the topography and diabatic heating is considered, we find that the major features in the response shift to the west with height, in general agreement with observations.

In an attempt to determine how a variation of the friction coefficient F with longitude would affect the standing eddies, the model equations were solved for the simple case where the friction coefficient has one value F_c (relatively large) over the continents and another value F_o (relatively small) over the oceans. Computations were made using $F_c/F_o = 2$ and $F_c/F_o = 6$, in each case choosing F_c and F_o in such a way that the zonal average of F was the same as that used in a control calculation with a constant value of F. For the case where $F_c/F_o = 6$ the computed heights of the 25 and 75 cb

surfaces were found to be quite different from those obtained with $F_c/F_o = 2$ which, in turn, were only slightly different from those obtained with $F_c/F_o = 1$. Judging from the observed variations of the angle between the surface wind and isobars with longitude it appears that the ratio $F_c/F_o = 2$ is more nearly valid than the ratio $F_c/F_o = 6$ so that assuming F to be constant is probably a fair approximation in the present context. It should be noted, on the other hand, that although only small changes are produced in the standing waves by using $F_c/F_o = 2$ instead of $F_c/F_o = 1$, the changes are such as to bring the computed standing waves and the observed ones into somewhat closer agreement.

In an effort to relax the restrictive assumption concerning the existence of a single effective meridional wavelength for the perturbation quantities, the model was generalized somewhat in order to allow several meridional modes in the forcing mechanisms (i.e., the topography and diabatic heating) and in the forced perturbations. Because the β-plane geometry was used it was necessary to assume the atmosphere to be bounded by solid vertical walls at the southern and northern boundaries, taken to be 30°N and 60°N, respectively. This assumption was found to be still restrictive but nevertheless the added degrees of freedom in the meridional plane made it possible for the computed standing waves to exhibit a tilt from the north-east to the south-west as is found most noticeably in the observed trough near the east coast of North America. The additional meridional modes had a second noticeable effect in that they caused the computed trough near the east coast of North America to be centered at 55°N, rather than 45°N, as in the previous formulation of the model, thereby coming into closer agreement with observations. The problem

was solved using finite differences in the meridional coordinate, a procedure which made it possible to remove the assumption that the speed of the zonal current is independent of the meridional coordinate. Some computations using the observed geostrophic zonal wind as the basic current yielded standing waves with smaller amplitudes than those obtained using constant values of $U_* = 15$ m sec^{-1} and $U_T = 5$ m sec^{-1} for half the sum and half the difference, respectively, of the speeds of the zonal current at 25 cb and 75 cb. The results served as a further indication that significant improvements in the model can only be achieved by using a spherical coordinate system.

The approach used in studying the maintenance of the standing eddies was then reversed in order to examine how the axisymmetric regime in the atmosphere is affected by the eddies, both transient and stationary. By using the quasi-geostrophic formulation with internal friction and assuming the axisymmetric diabatic heating to be Newtonian it was possible to show how the axisymmetric temperature field is affected by the eddy heat and momentum transports as well as by the assumed distribution of the convective-radiative equilibrium temperature. The results indicate that the eddy heat and momentum transports tend to oppose each other in the middle latitudes in the way they affect the temperature field. The combined effect of the two mechanisms is to heat the high latitudes and cool the low latitudes. One advantage of the formulation is that the effects of the eddies on the temperature field are given in degrees Kelvin rather than as heating rates as was the case in the study by Wiin-Nielsen and Vernekar (1967).

From the solution obtained for the temperature field it was possible to determine the velocity field. The mean meridional circulation thus obtained shows reasonable agreement with those obtained in previous investigations. A study was also made of the role played by the eddies in determining the geostrophic zonal wind. It was found that the eddy heat transport tends to produce easterlies north of 30°N, with the maximum effect being found at 10 cb, and weak westerlies south of 30°N also with the maximum effect in the upper levels. The computations indicated that the eddy momentum transport tends to produce westerlies from about 34°N to about 60°N so that in this latitude belt the eddy heat and momentum transports oppose each other in the way they affect the zonal current. To the south of 34°N and to the north of 60°N the effect of the eddy momentum transport was found to be such as to produce easterlies with maximum speeds at the top level (10 cb). The result of adding the effects of the eddy heat and momentum transports indicated that the eddies tend to produce easterlies in both the low and high latitudes and weak westerlies in the middle latitudes.

The final solution for the zonal wind was obtained by adding the zonal wind distribution produced by the eddies to the one that would exist if the atmosphere were in a state of convective-radiative equilibrium. In spite of some discrepancies between the observed and the computed zonal winds, the results did show the importance of both the eddy heat and momentum transports in modifying the distribution of the zonal wind. In particular, it was found that in the state of convective-radiative equilibrium the zonal wind distribution has a maximum speed which occurs too far to the north and shows

the presence of westerlies which are too strong in the low and high latitudes when compared with observations. It was shown that the eddies tend to shift the maximum westerly speed toward the south and to produce weak easterlies in the low and high latitudes. It is suspected that the differences between the computed and observed zonal winds are largely due to the poorly known and probably poorly specified convective-radiative equilibrium temperature, or to the type of eddy momentum transport used, or to a combination of both factors.

5.2 CONCLUDING REMARKS AND SUGGESTIONS FOR FUTURE WORK

The present investigation has been successful in showing that the two level model is a convenient tool for studying the maintenance of the standing eddies. It has become clear, however, that the β-plane approximation is rather restrictive and that to progress beyond the level of accuracy achieved in the present study proper attention must be given to the spherical geometry of the earth. It has become clear from the study by Sankar Rao (1965), on the other hand, that the spherical geometry introduces some new problems associated with the variation of the Coriolis parameter with latitude. Sankar Rao has simplified the problem by assuming, as we did in the β-plane geometry, that the variation of f could be neglected everywhere except in the so-called "β term" of the vorticity equation where a constant value of $df/d\phi$ (ϕ being the latitude) could be used. It appears from his discussion of the effect of rotation that this treatment of the Coriolis parameter is unsatisfactory when dealing with standing waves over a complete hemisphere and could

be responsible for the lack of agreement between his topographically forced waves and the observed standing waves. It would be of great importance, therefore, to investigate in more detail how the variation of the Coriolis parameter with latitude affects the response of the atmosphere to stationary forcing mechanisms.

After developing a model which properly takes into account the spherical geometry and the rotation of the earth, it would be instructive to determine the type of forced waves that it yields in response to the steady forcing by the topography, the time-averaged diabatic heating and the time-averaged effects due to the transient disturbances. Observational studies on the interaction between the standing and transient eddies by Murakami (1960) and Holopainen (1966) indicate that on the average over a period of one year or more there is a transfer of kinetic energy from the standing to the transient eddies. The rate of kinetic energy transfer appears to be sufficiently large to be of some importance in the energy budget of the standing waves and therefore should be included in future models of the stationary disturbances. The method suggested by Saltzman (1962) appears promising.

Our study of the maintenance of the axisymmetric regime could probably be improved by the use of a more realistic heating mechanism. In addition, the model should be generalized to permit the determination of the area average of the temperature at the various pressure levels. This would undoubtedly require the inclusion of the small-scale convective transports of heat and momentum in the vertical. It would also be necessary to abandon the convenient quasi-geostrophic formulation since in it we assume that the area average of the temperature is a known function of height.

APPENDIX A

TABULATION OF DATA

TABLE A-1

ANNUAL MEAN OF EDDY MOMENTUM TRANSPORT FOR 1963

Units: $m^2 sec^{-2}$

Latitude	Pressure (cb)							
	10	15	20	30	50	70	85	100
85.0	- 0.5	- 1.1	- 2.3	- 2.3	- 0.6	0.4	0.8	0.9
82.5	- 0.1	- 2.0	- 3.6	- 4.4	- 2.1	0.2	1.0	1.4
80.0	0.7	- 2.9	- 4.3	- 6.1	- 4.0	- 0.5	0.7	1.5
77.5	- 0.2	- 4.1	- 5.3	- 8.1	- 5.9	- 1.8	-0.2	1.3
75.0	- 1.4	- 5.6	- 7.7	-11.3	- 7.8	- 3.1	-0.8	0.8
72.5	- 3.4	- 7.2	-11.2	-15.4	- 9.9	- 4.2	-1.0	0.7
70.0	- 5.4	- 8.5	-14.5	-19.7	-12.1	- 4.9	-0.9	1.0
67.5	- 6.0	- 9.5	-16.5	-23.3	-13.7	- 5.3	-0.9	1.2
65.0	- 5.2	- 9.4	-16.6	-24.4	-13.8	- 5.4	-1.4	1.1
62.5	- 3.7	- 8.0	-14.4	-22.0	-12.5	- 5.2	-2.0	0.3
60.0	- 2.1	- 5.8	-10.9	-17.7	-10.5	- 4.8	-2.3	-0.9
57.5	- 0.7	- 3.9	- 6.9	-21.4	- 8.0	- 2.3	-2.1	-1.6
55.0	0.2	- 1.9	- 2.4	- 5.7	- 3.7	- 1.3	-0.8	-1.2
52.5	1.4	1.3	3.4	2.7	2.0	1.4	0.9	-0.4
50.0	2.8	6.3	11.8	13.5	8.1	4.3	2.5	2.0
47.5	5.6	13.0	22.6	25.2	13.4	6.6	3.6	2.9
45.0	9.6	23.4	33.7	34.8	17.3	8.1	4.8	4.6
42.5	15.7	31.0	44.7	41.8	19.6	9.2	6.2	7.0
40.0	22.7	42.6	55.5	47.1	21.2	10.1	7.5	8.8
37.5	28.5	52.5	64.2	50.8	22.1	10.7	8.1	9.2
35.0	31.5	57.2	68.2	52.3	22.6	10.7	7.8	8.2
32.5	31.4	55.8	65.4	50.1	22.2	10.0	6.6	6.4
30.0	28.4	48.8	57.1	44.5	20.1	8.5	5.2	4.8
27.5	23.7	38.5	45.8	37.1	13.4	6.5	3.7	3.3
25.0	18.4	27.8	33.2	28.1	11.7	4.2	2.0	1.5
22.5	12.6	18.4	20.0	18.6	6.8	1.6	0.2	-0.7
20.0	5.8	10.1	13.7	9.6	2.3	- 0.9	-1.7	-3.1

TABLE A-2

ANNUAL MEAN OF EDDY HEAT TRANSPORT FOR 1963

Units: 10^{9} kj cb^{-1} sec^{-1}

Latitude	Pressure (cb)						
	10-15	15-20	20-30	30-50	50-70	70-85	85-100
87.5	0.0	0.0	- 0.1	0.1	0.7	0.4	0.5
85.0	0.1	0.3	0.5	0.3	1.1	1.7	1.9
82.5	0.4	1.5	- 0.1	0.6	2.4	3.3	3.6
80.0	0.9	2.4	0.5	1.3	3.4	4.9	5.8
77.5	2.8	4.1	1.4	2.6	5.4	6.7	8.2
75.0	4.5	4.9	2.7	4.1	7.5	9.0	11.2
72.5	6.9	6.2	4.3	5.5	10.2	12.0	13.0
70.0	9.0	7.7	6.0	7.4	12.0	15.4	15.2
67.5	11.0	10.1	8.1	10.1	16.5	19.2	19.2
65.0	13.6	13.7	10.9	13.2	20.2	23.5	24.1
62.5	16.6	17.5	13.7	16.5	24.7	28.8	28.7
60.0	18.7	20.9	17.0	19.6	29.4	34.6	32.8
57.5	20.0	24.7	21.2	22.4	33.6	40.4	36.7
55.0	21.3	28.9	25.7	24.9	37.6	45.7	40.6
52.5	22.5	33.0	29.1	26.6	41.6	49.8	43.1
50.0	23.5	37.0	30.7	27.0	44.6	52.2	43.3
47.5	24.0	39.4	30.1	26.7	45.2	52.8	42.9
45.0	24.1	39.0	28.5	25.6	43.8	51.9	42.1
42.5	24.8	38.0	27.7	24.3	40.9	49.3	40.3
40.0	25.1	37.6	28.1	22.7	36.3	44.4	37.2
37.5	23.0	36.5	27.9	20.2	29.9	37.0	32.4
35.0	19.0	33.3	25.5	16.7	22.7	28.7	26.5
32.5	14.1	27.0	20.5	12.1	15.7	21.6	21.1
30.0	8.8	19.4	13.6	7.2	10.1	15.4	16.4
27.5	5.5	11.8	7.1	3.9	5.9	9.8	12.5
25.0	4.8	6.5	2.9	2.1	2.9	5.7	9.3
22.5	5.5	4.2	-0.9	1.2	1.0	2.5	6.3
20.0	6.4	1.0	-1.9	1.0	0.2	1.0	4.6
17.5	7.4	1.6	-1.0	1.6	0.4	0.9	4.2

TABLE A-3

THE ASSUMED DISTRIBUTION OF T_R

Unit: Degrees Centigrade

Latitude	Pressure (cb)					
	10, 15 and 20	30	50	70	85	100
90	-86.6	-76.6	-62.2	-51.5	-44.9	-39.0
80	-82.7	-72.2	-57.1	-45.9	-38.9	-32.8
70	-77.1	-65.9	-49.8	-37.9	-30.4	-23.9
60	-69.0	-56.8	-39.3	-26.3	-18.2	-11.1
50	-60.2	-47.0	-27.9	-13.8	- 5.0	2.8
40	-53.2	-39.1	-18.8	- 3.7	5.6	13.9
30	-48.0	-33.3	-12.0	3.8	13.6	22.2
20	-44.1	-28.9	- 7.0	9.3	19.4	28.3
10	-42.0	-26.5	- 4.2	12.3	22.6	31.7
0	-41.3	-25.7	- 3.3	13.3	23.7	32.8

BIBLIOGRAPHY

Adem, J., 1962: On the Theory of the General Circulation of the Atmosphere. Tellus, 14, No. 1, 102-115.

Berkofsky, L. and E. A. Bertoni, 1955: Mean Topographic Charts for the Entire Earth. Bull. Amer. Meteor. Soc., 36, No. 1, 350-354.

Blinova, E. N., 1943: Gidrodinamicheskaya Teoriya Voln Davleniya, Temperaturnikh Voln i Tsentrov Deistviya Atmosferi. Dokladi Akademiia Nauk SSSR, 39, No. 7, 284-287. (A Hydrodynamic Theory of Pressure and Temperature Waves and the Centers of Action of the Atmosphere)

Bolin, B., 1950: On the Influence of the Earth's Topography on the General Character of the Westerlies. Tellus, 2, No. 3, 184-195.

Brown, J. A., 1964: A Diagnostic Study of Tropospheric Diabatic Heating and the Generation of Available Potential Energy. Tellus, 16, No. 3, 371-387.

Charney, J., 1959: On the General Circulation of the Atmosphere. The Atmosphere and the Sea in Motion, B. Bolin ed., The Rockerfeller Institute Press, 178-193.

Charney, J. and A. Eliassen, 1949: A Numerical Method for Predicting the Perturbations of the Middle Latitude Westerlies. Tellus, 1, No. 1, 38-54.

Döös, B. R., 1962: The Influence of Exchange of Sensible Heat with the Earth's Surface on the Planetary Flow. Tellus, 14, No. 2, 133-147.

Gates, L. W., 1961: Static Stability Measures in the Atmosphere. J. Meteor., 18, No. 4, 526-533.

Gilchrist, B., 1954: The Seasonal Phase Changes of Thermally Produced Perturbations in the Westerlies. Proceedings of the Toronto Meteorological Conference, 1953. The American Meteorological Society and the Royal Meteorological Society, 129-131.

Haurwitz, B., 1940: The Motion of Atmospheric Disturbances on the Spherical Earth. J. Mar. Res., 3, Nos. 1-3, 254-267.

Houghton, H. G., 1954: On the Annual Heat Balance of the Northern Hemisphere. J. Meteor., 11, No. 1, 1-9.

Holopainen, E. O., 1966: A Diagnostic Study of the Maintenance of Stationary Disturbances in the Atmosphere. Technical Report 06372-3-T, Department of Meteorology and Oceanography, University of Michigan, 40 pp.

Holopainen, E. O., 1967: On the Mean Meridional Circulation and the Flux of Angular Momentum over the Northern Hemisphere. Tellus, 19, No. 1, 1-13.

Kasahara, A. and W. M. Washington, 1967: NCAR Global General Circulation Model of the Atmosphere. Mon. Wea. Rev., 95, No. 7, 389-402.

Leith, C. E., 1965: Numerical Simulation of the Earth's Atmosphere. Methods in Computational Physics, 4, Academic Press, New York, 1-28.

London, J., 1957: A Study of the Atmospheric Heat Balance. Final Report on contract AF 19(122)-165, (AFCRC-TR-57-287), Department of Meteorology, New York University, 99 pp.

Manabe, S., J. Smagorinsky and R. F. Strickler, 1965: Simulated Climatology of a General Circulation Model with a Hydrological Cycle. Mon. Wea. Rev., 93, No. 12, 769-798.

Manabe, S. and R. F. Strickler, 1964: Thermal Equilibrium of the Atmosphere with a Convective Adjustment. J. Atmos. Sci., 12, No. 4, 361-385.

Milankovitch, M., 1930: Mathematische Klimalehre und Astronomische Theorie der Klimaschwankungen. Handbuck der Klimatologie, 1, Section A, 1-176.

Mintz, Y., 1964: Very Long-Term Global Integration of the Primitive Equations of Atmospheric Motion. Proceedings of WMO-IUGG Symposium on Research and Development Aspects of Long Range Forecasting, Boulder, Colo., WMO Technical note, No. 66, 141-167.

Murakami, T., 1960: On the Maintenance of Kinetic Energy of the Large-Scale Stationary Disturbances in the Atmosphere. Scientific Report No. 2, AFCRL-TN-60-812, Planetary Circulations Project, Massachusetts Institute of Technology, 42 pp.

Murakami, T., 1963: The Topographic Effects in the Three-Level Model of the S-Coordinate. Pap. Meteor. Geophys., 14, Nos. 3-4, 144-150.

Oort, A. H., 1964: On the Energetics of the Mean and Eddy Circulations in the Lower Stratosphere. Tellus, 16, No. 3, 309-327.

Palmén, E., 1955: On the Mean Meridional Circulation in Low Latitudes of the Northern Hemisphere in Winter and the Associated Meridional and Vertical Flux of Angular Momentum. Societas Scientarium Fennica, Commentationas Physico-Mathematicae, 17, No. 8, 1-33.

Phillips, N. A., 1956: The General Circulation of the Atmosphere: a Numerical Experiment. Quart. J. Roy. Meteor. Soc., 82, No. 352, 123-164.

Phillips, N. A., 1958: Geostrophic Error in Predicting the Appalachian Storm of November 1950. Geophysica, 6, Nos. 3-4, 389-405.

Phillips, N. A., 1963: Geostrophic Motion. Rev. Geophys., 1, No. 2, 123-176.

Riehl, H. et al., 1951: The North-East Trade of the Pacific Ocean. Quart. J. Roy. Meteor. Soc., 77, No. 334, 598-626.

Robert, A. J., 1966: The Integration of a Low Order Spectral Form of the Primitive Meteorological Equations. J. Meteor. Soc. Japan, Series II, 44, No. 5, 237-245.

Rossby, C. G. and coll., 1939: Relation Between the Intensity of the Zonal Circulation of the Atmosphere and the Displacements of the Semipermanent Centers of Action. J. Mar. Res., 2, No. 1, 38-55.

Saltzman, B., 1961: Perturbation Equations for the Time-Average State of the Atmosphere Including the Effects of Transient Disturbances. Geofis. Pura e Appl., 48, No. 1, 143-150.

Saltzman, B., 1962: Empirical Forcing Functions for the Large-Scale Mean Disturbances in the Atmosphere. Geofis. Pura e Appl., 52, No. 2, 173-188.

Saltzman, B., 1964: On the Theory of the Axially-Symmetric, Time-Average, State of the Atmosphere. Pure and Appl. Geophys., 57, No. 1, 153-160.

Saltzman, B., 1965: On the Theory of the Winter-Average Perturbations in the Troposphere and Stratosphere. Mon. Wea. Rev., 93, No. 4, 195-211.

Saltzman, B., 1967: Steady State Solutions for the Axially-Symmetric Climatic Variables. Scientific Report No. 7045-249, Research on the Theory of Climate. Travellers Research Center, 1-38.

Saltzman, B. and M. Sankar Rao, 1963: A Diagnostic Study of the Mean State of the Atmosphere. J. Atmos. Sci, 20, No. 5, 438-447.

Sankar Rao, M., 1965a: Finite Difference Models for the Stationary Harmonics of Atmospheric Motion. Mon. Wea. Rev., 93, No. 4, 213-224.

Sankar Rao, M., 1965b: Continental Elevation Influence on the Stationary Harmonics of the Atmospheric Motion. Pure and Appl. Geophys., 60, No. 1, 141-159.

Sankar Rao, M., 1965c: On the Influence of the Vertical Distribution of Stationary Heat Sources and Sinks in the Atmosphere. Mon. Wea. Rev., 93, No. 7, 417-420.

Smagorinsky, J., 1953: The Dynamical Influence of Large-Scale Heat Sources and Sinks on the Quasi-Stationary Mean Motions of the Atmosphere. Quart. J. Roy. Meteor. Soc., 79, No. 341, 342-366.

Smagorinsky, J., 1963: General Circulation Experiments with the Primitive Equations: I. The Basic Experiment. Mon. Wea. Rev., 91, No. 3, 99-164.

Smagorinsky, J., S. Manabe and J. L. Holloway, 1965: Numerical Results from a Nine-Level General Circulation Model of the Atmosphere. Mon. Wea. Rev., 93, No. 12, 727-768.

Sutton, O. G., 1953: Micrometeorology: A Study of Physical Processes in the Lowest Layers of the Earth's Atmosphere. New York, McGraw-Hill, 333 pp.

Vernekar, A. D., 1967: On Mean Meridional Circulations in the Atmosphere. Mon. Wea. Rev., 95, No. 11, 705-721.

White, R. M., 1954: The Counter-Gradient Flux of Sensible Heat in the Lower Stratosphere. Tellus, 6, No. 2, 177-179.

Wiin-Nielsen, A., 1959a: On Certain Integral Constraints for the Time-Integration of Baroclinic Models. Tellus, 11, No. 1, 45-59.

Wiin-Nielsen, A., 1959b: On Barotropic and Baroclinic Models, with Special Emphasis on Ultra-Long Waves. Mon. Wea. Rev., 87, No. 5, 171-183.

Wiin-Nielsen, A., 1961: On the Distribution of Temperature Relative to Height in Stationary Planetary Waves. Tellus, 13, No. 2, 127-139.

Wiin-Nielsen, A., 1967: On the Annual and Spectral Distribution of Atmospheric Energy. Tellus, 19, No. 4, 540-559.

Wiin-Nielsen, A. and J. A. Brown, 1960: On Diagnostic Computations of Atmospheric Heat Sources and Sinks and the Generation of Available Potential Energy. Proceedings of the International Symposium on Numerical Weather Prediction in Tokyo, Meteor. Soc. Japan, 593-613.

Wiin-Nielsen, A., J. A. Brown and M. Drake, 1963: On Atmospheric Energy Conversions Between the Zonal Flow and the Eddies. Tellus, 15, No. 13, 261-279.

Wiin-Nielsen, A., 1964: Further Studies of Energy Exchange between the Zonal Flow and the Eddies. Tellus, 16, No. 2, 168-180.

Wiin-Nielsen, A. and A. D. Vernekar, 1967: On the Influence of the Mean Meridional Circulation on the Zonal Flow. Mon. Wea. Rev., 95, No. 11, 723-732.

Wiin-Nielsen, A., A. Vernekar and C. H. Yang, 1967: On the Development of Baroclinic Waves Influenced by Friction and Heating. Pure and Appl. Geophys., 68, No. 3, p. 131-161.

Williams, G. P. and D. R. Davies, 1965: A Mean Motion Model of the General Circulation. Quart. J. Roy. Meteor. Soc., 91, No. 390, 471-489.

Young, J. A. 1966: On the Relation Between Zonal Heating Asymmetries and Large-Scale Atmospheric Fluctuations in Space and Time. Department of Meteorology, Massachusetts Institute of Technology, 266 pp.